Master Thesis

Synthesis and characterization of acrylamide based polyelectrolytes

Conducted at the

Institute of Applied Synthetic Chemistry (TU Wien)

and

Institute for Chemical Technology of Organic Materials (JKU Linz)

under the supervision of

Univ.-Prof. Dipl.-Ing. Dr.techn. Robert Liska,

Dipl.-Ing. Dr. Klaus Bretterbauer

Univ.-Prof. Dipl.-Ing. Dr. Christian Paulik

by

Kristina Durstberger, BSc

Matrikelnr.: 01526478

Vienna, August, 2023

Kristina Durstberger, BSc

SWORN DECLARATION

I hereby declare under oath that the submitted Master's Thesis has been written solely by me without any third-party assistance, information other than provided sources or aids have not been used and those used have been fully documented. Sources for literal, paraphrased and cited quotes have been accurately credited.

Linz, 16.08.2023

Signature:

DANKSAGUNG

Zu Beginn möchte ich mich bei Prof. Dr. Christian Paulik und Dr. Klaus Bretterbauer bedanken, für die Möglichkeit meine Masterarbeit an der Johannes Kepler Universität am Institut für chemische Technologie organischer Stoffe durchführen zu können. Vielen Dank Klaus für deine Unterstützung und die wöchentlichen Meetings, in denen ich viel neues lernen konnte.

Besonderer Dank gilt auch Prof. Dr. Robert Liska. Danke, dass Sie in meinem ersten Wahlpraktikum mein Interesse an der Polymerchemie geweckt haben, weshalb ich mich für dieses Themengebiet entschieden habe.

Ich möchte mich außerdem beim gesamten CTO Team für die herzliche Aufnahme und die unvergessliche Zeit bei euch bedanken. Danke Mani, Marco, Felix und Dario für die vielen Tipps im Labor, für den fachlichen Input, fürs Korrekturlesen und vor allem Danke für die gemeinsame Zeit mit euch!

Nicht zu vergessen sind die allerbesten Studienkollegen und Freunde Kathi, Seli, Jelena, Johanna und Jakob. Gemeinsam mit euch ist die Zeit während des Bachelor- und Masterstudiums unvergesslich geworden. Ich blicke immer mit Freude an unsere gemeinsamen Prüfungsvorbereitungen und Laborpraktika zurück.

Zu guter Letzt bedanke ich mich bei meiner Familie. Danke an meine Eltern und Großeltern, ohne die dieses Studium nicht möglich gewesen wäre. Danke Michael für deine Unterstützung, dein Verständnis und die zahlreichen Wienwochenenden in den letzten Jahren.

KURZFASSUNG

Polyelektrolyte sind Polymere mit ionischen oder ionisierbaren Seitenketten. Sie werden als Flockungsmittel in der Abwasserbehandlung eingesetzt und gewinnen immer mehr an Bedeutung in der Batterieentwicklung als Festkörperelektrolyt. Das Ziel dieser Arbeit war die Herstellung von flexiblen und selbst ordnenden Polyelektrolyten auf Acrylamid Basis.

Dazu wurden zuerst geeignete Monomere wie 6-Acrylamidohexansäure und 6-(6-Acrylamidohexanamido)hexansäure synthetisiert. Das Ausgangsmolekül der Monomersynthese war stets die 6-Aminohexansäure. Für die Synthese der 6-(6-Acrylamidohexanamido)hexansäure, wurde die Amidbindung zwischen der 6-Acrylamidohexansäure und Methyl 6-aminohexanoat hydrochlorid einerseits klassisch über das Säurechlorid, andererseits mit Hilfe von *N*,*N*′-Dicyclohexylcarbodiimid (DCC) als Kupplungsreagenz geknüpft.

Die anschließende Polymerisation dieser Moleküle erfolgte mit *N*,*N*-Dimethylacrylamid (DMAA) als Comonomer. Die Polymerisation wurde vor allem in Benzol mit Azo-bis-(isobutylonitril) (AIBN) durchgeführt. Es wurden jedoch auch Lösungsmittel wie Wasser, Methanol und Dimethylformamid (DMF) getestet, um die Polymerisation zu optimieren und das bedenkliche Benzol zu vermeiden. Neben DMAA als Comonomer wurde auch 2-Hydroxyethylmethacrylat (HEMA) verwendet, sowie Homopolymere hergestellt. Die gewünschten Polyelektrolyte wurden anschließend durch Verseifung der hergestellten Polyamide erhalten.

Auf Grund der langen aliphatischen Kette sowie den beiden Amidbindungen, konnten bei den resultierenden Polymeren spezielle Eigenschaften wie beispielsweise ein vom Lösungsmittel und Gegenion abhängiges Quellverhalten beobachtet werden. Als Vergleich dazu wurde Poly(DMAA-co-methyl 6-acrylamidohexanoat) hergestellt, bei welchen dieses Quellverhalten nicht beobachtet werden konnte.

Die Polymere wurden mittels Kernspinresonanzspektroskopie (NMR) und Infrarotspektroskopie (IR) charakterisiert und mittels Thermogravimetrischer Analyse (TGA) und Dynamischer Differenzkalorimetrie (DSC) analysiert.

ABSTRACT

Polyelectrolytes are polymers with ionic or ionizable side chains. They are used as flocculants in wastewater treatment and are becoming increasingly important in battery development as solid-state electrolytes. This thesis aimed to prepare flexible and self-ordering polyelectrolytes based on acrylamide.

Therefore suitable monomers such as 6-acrylamidohexanoic acid and 6-(6-acrylamidohexanamido)hexanoic acid were synthesized. The starting molecule of monomer synthesis was always 6-aminohexanoic acid. For the synthesis of 6-(6-acrylamidohexanamido)hexanoic acid, the amide bond between 6-acrylamidohexanoic acid and methyl 6-aminohexanoate hydrochloride was linked classically *via* the acid chloride on the one hand, and with the help of *N*,*N*′-dicyclohexylcarbodiimide (DCC) as coupling agent on the other hand.

Subsequent polymerization of these molecules was carried out with *N*,*N*-dimethylacrylamide (DMAA) as comonomer. The polymerization was mainly carried out in benzene with azo-bis-(isobutylonitrile) (AIBN). However, solvents such as water, methanol and dimethylformamide (DMF) were also tested to optimize the polymerization and to avoid the harmful benzene. In addition to DMAA as comonomer, 2-hydroxyethyl methacrylate (HEMA) was also used, and homopolymers were prepared. The desired polyelectrolytes were then obtained by saponification of the prepared polyamides.

Due to the long aliphatic chain as well as the two amide bonds, special properties such as solvent- and counterion-dependent swelling behavior were observed in the resulting polymers. As a comparison, poly(DMAA-co-methyl 6-acrylamidohexanoate) was prepared, in which this swelling behavior could not be observed.

The polymers were characterized by nuclear magnetic resonance spectroscopy (NMR) and infrared spectroscopy (IR) and analyzed with thermogravimetric analysis (TGA) and differential scanning calorimetry (DSC).

TABLE OF CONTENTS

INTRODUCTION

Nowadays, due to climate change, more and more areas are looking for more environmentally friendly alternatives. For example, renewable energies in electricity and heat generation play an important role in reducing CO_2 emissions [1]. Road transport is also responsible for 19 % of global CO_2 emissions [2]. Therefore, a ban on diesel and petrol cars should be introduced in the future to reduce greenhouse gas emissions. [3]. In recent years, electric cars therefore also gained more and more importance. The electric motor was patented already in 1837 and is used in many common products such as washing machines, escalators, fans [4] and many other areas. In addition to its high energy efficiency, a major advantage of an electric motor is that it is almost noiseless and wear-resistant [5]. The first mass-produced electric car came from Tesla in 2006 [6]. Since then, they have been gaining more and more importance. One of the most important components of an electric car is also the battery.

The first battery was developed by Volta in 1800. Since then, various battery systems have been developed, which allowed us to use, for example, mobile phones and laptops [7]. The further development of batteries has become increasingly important in recent years due to electric cars. However, the biggest problem with these cars is still the battery. In order to make electric cars more popular, batteries should be developed to have a high storage capacity and are fast to recharge. Another important factor, however, is the cost and recycling of the batteries [8]. Nowadays, so-called lithium-ion batteries are most commonly used (Figure 1) [9]. The battery consists of a positive electrode (e.g. metal oxide like $LiCoO_2$), a negative electrode (Li graphite) and an electrolyte (lithium salt in an organic solvent). During discharge, the Li ions migrate from the negative electrode to the positive electrode. When the battery is charged, the Li ions migrate in the opposite direction, as from the positive to the negative electrode. Advantages of such batteries are that Li-ion batteries have no memory effect and a low self-discharge rate [9]. However, disadvantages of this battery are that lithium is expensive, there is a limitation in the life cycle rate and often cobalt is used, which is harmful to the environment [8,9].

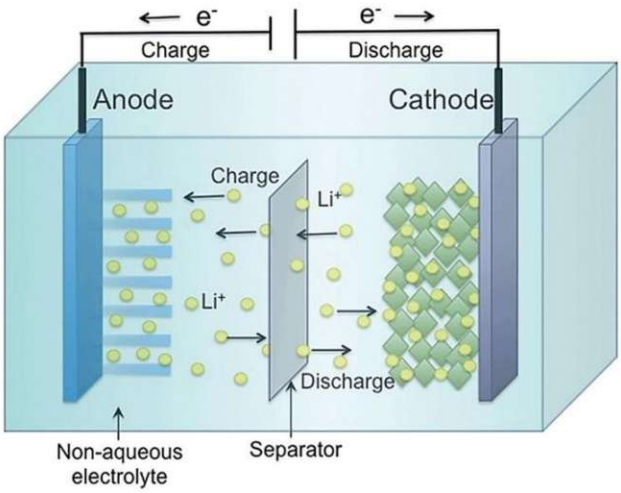

Figure 1: During discharge, electrons move from the anode to the cathode. During charging, the electrons move in the opposite direction (from the cathode to the anode). For example, Li graphite is used as the anode material and $LiCoO_2$ as the cathode material. Between the electrodes, there is an organic solvent (electrolyte). The anode and cathode are separated by a separator to prevent a short circuit [10].

Newer batteries, which are already in use, such as the lithium iron phosphate battery or sodium ion battery, have significantly less power, which is of course not desirable for use in electric cars [8]. The greatest hopes currently lie in the further development of so-called solid-state batteries [8]. The idea is to produce batteries with solid electrolytes, such as the lithium-ion polymer battery [11]. The normally liquid electrolyte is replaced by a solid polymer-based electrolyte. The advantages are the flexibility of the polymer, which means that a wide variety of shapes can be produced. In addition, the use of the solid electrolyte is safer, since leakage of the electrolyte can be prevented. Another advantage is that Li-ion polymer batteries are also lighter, since no metal coat is used. Applications include radio-controlled cars and aircrafts or e-cigarettes. However, since Li-ion polymer batteries are currently more expensive than Li-ion batteries and also have a lower energy density and fewer life cycles, they cannot be used in many areas [11].

Higher theoretical energy densities than with the lithium-ion battery can be achieved with the Li-metal battery [12]. Unfortunately, the growth of lithium dendrites in these batteries poses a safety risk (Figure 2) [13]. The dendrites are formed at the anode during the charging process by deposition of lithium. Since they are very sharp, they can get through the separator and thus grow to the cathode. If the dendrite comes into contact with the cathode, this causes a short circuit [13].

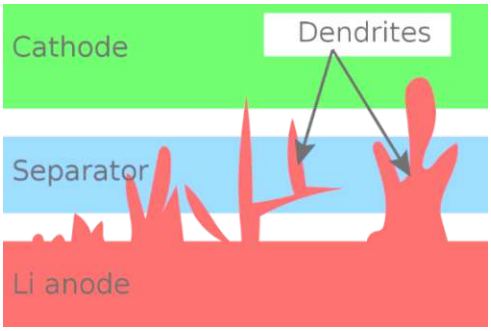

Figure 2: Dendrites are formed at the anode by depositions. Since they are very sharp at their ends, they can break through the separator. This poses the risk of contact being made between the anode and cathode, thus causing a short circuit [14].

By using solid-state electrolytes, this dendrite growth can be prevented and the safety of lithium metal batteries can be drastically increased [7]. The electrolyte here often consists of a conductive polymer [15]. However, the problem with solid state batteries is currently still the lower conductivity than with liquid electrolytes and the electrochemical stability [7,15]. Another way to prevent dendrite growth is to use a polymer-based solid electrolyte interphase (SEI) [16]. This ionically conductive interphase is between the anode and the electrolyte and protects the lithium metal. The use of polymers is particularly advantageous, since the SEI film should be elastic due to the volume expansion of the anode [16].

So, new batteries with high energy density are still being developed, and the lithium metal battery is very promising. However, to enable the use of such batteries, safety must still be improved by preventing the growth of lithium dendrites [7].

These ionic polymers, which are used as solid electrolytes in batteries, also have other potential applications. The use of such polymers as so-called smart polymers is very promising.

Smart polymers respond to different stimuli such as pH change, temperature, electric and magnetic fields by changing their physical or chemical properties [17] (Figure 3). As a result, they can be used in a variety of areas, such as actuators in robotics [18], in medical fields (tissue engineering [19], drug delivery systems [20]) or as smart textiles [21].

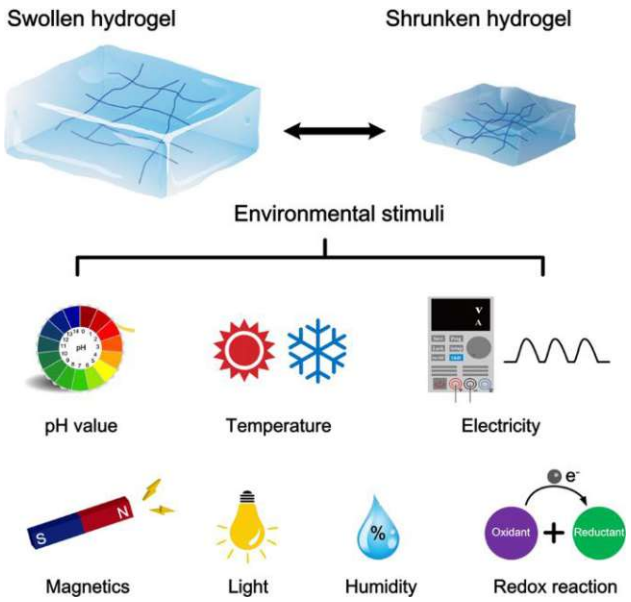

Figure 3: The material reacts to various environmental influences by changing physical or chemical properties. Here, swelling or shrinkage of the sample occurs due to influences such as pH value, temperature, electricity, magnetics and others. Such materials are called smart materials [22].

Actuators and sensors play an important role in current research. Actuators respond to electrical signals by mechanical movement or change of a physical quantity such as temperature or pressure, for example [23]. When used as actuators, polymer materials have the advantage that they have a lower density and can be shaped in various ways [24]. If polymers respond to an electrical signal by changing their shape or size, they are referred to as electroactive polymers (EAPs). A distinction is made between electrical EAPs (e.g. ferroelectric polymers) and ionic EAPs (e.g. conducting polymers, ionic polymer gels) [24]. The materials used in this work belong to the class of ionic EAPs. The application of a voltage causes ionic motion in these polymers, which leads to a movement of the material [25]. Actuators based on ionic EAPs usually consist of two electrodes with an ion exchange membrane between them. This membrane is often made of Nafion. When a voltage is applied to the electrodes, the counterions in the Nafion polymer migrate to the opposite electrode, causing the actuator to bend [25]. Due to the fact that actuators based on ionic EAPs behave like biological muscles, they are also often used as artificial muscles [26] and thus play an important role in the development of robots [27] or in the field of muscle tissue engineering [28].

In addition, these materials are also used, for example, in lab-on-a-chip systems [29]. This can affect the movement of fluids in the channels, as the EAP changes shape or size when a voltage is applied, thereby changing the volume of the microfluidic channel [29].

The counterpart to actuators are sensors, which convert a physical parameter back into an electrical signal [23]. Ionic EAPs are also used here. They function like the actuators, but in the opposite direction. If the polymer film is bent, the ions move and a measurable voltage difference

occurs [26,30]. EAPs-based sensors are used, for example, in the medical field as sensors for hand prostheses [31] or sensors for blood pressure and pulse [32].

Another important possible field of application is the use of ionic polymers as self-healing hydrogels. Hydrogels are materials that are insoluble in water. When hydrogels are exposed to water, they swell, which leads to an increase in volume (Figure 4). An example of a well-known hydrogel is gelatin. However, hydrogels can also be produced from synthetic polymers [33]. Hydrogels are used, for example, in medical devices [34], biosensors [35] and tissue engineering [36]. If the solvent in which the hydrogels swell is not water but another organic solvent, they are also known as organogels. [37].

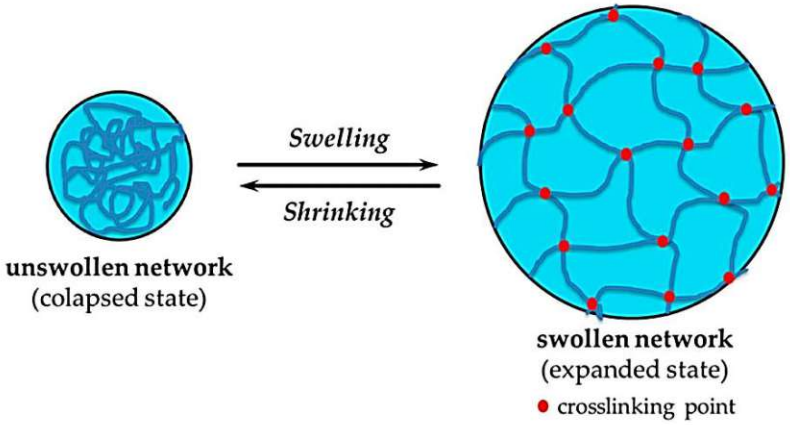

Figure 4: The unswollen polymer increases its volume in water or another solvent. However, the swollen network can also shrink again by releasing solvent [38].

Self-healing hydrogels are, for example, polymer networks with flexible side chains that can form hydrogen bonds [36]. These bonds can be formed beyond the hydrogel interface, resulting in the effect of "self-healing". Self-healing hydrogels are very important, especially in the medical field, because they can act like organic tissue. Damage can be repaired and the original state can be restored [36].

All the applications described above (batteries, actuators, sensors and self-healing hydrogels) have polyelectrolytes as their basic material. Therefore, molecules belonging to the group of polyelectrolytes were prepared in the scope of this work. This allows, for example, the development of batteries or the use as actuators and sensors in lab-on-a-chip systems.

Polyelectrolytes are polymers with ionic or ionizable side chains [39]. There are natural, modified natural and synthetic polyelectrolytes and a distinction is made between polyanions (Figure 5a), polycations (Figure 5b) and polyampholytes (Figure 5c) [40].

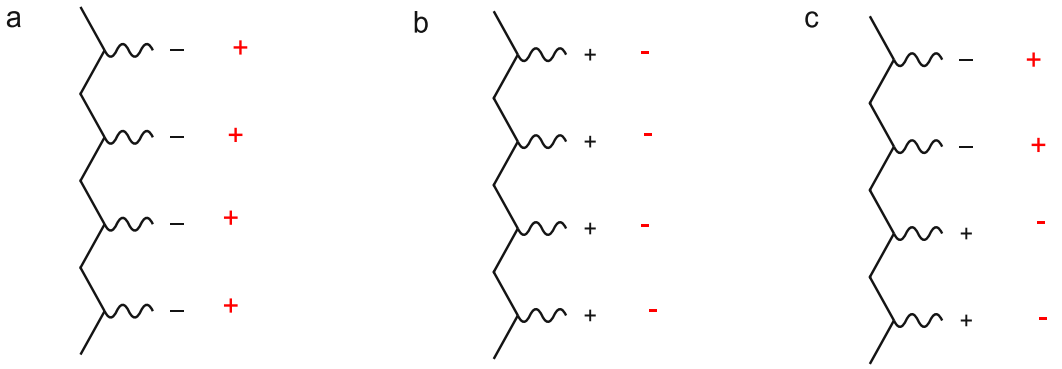

Figure 5: Polyelectrolytes can be distinguished between anionic (a), cationic (b) and ampholyte (c) polyelectrolytes. The corresponding counterions are marked in red in the figure.

A distinction can also be made between strong and weak polyelectrolytes [40]. The counterions of strong polyelectrolytes are completely dissociated over a wide range of pH values. For weak polyelectrolytes, the degree of dissociation depends on the pH value [41]. The pH value thus determines the distribution of the charge density in the polyelectrolyte and thus also has an important influence, for example, in the production of so-called polyelectrolyte multilayers [41].

Due to the high charge density in combination with the macromolecular character, unique properties can be achieved and thus they can be used in many different fields [40]. Polyelectrolytes are used as coagulants and flocculants in wastewater treatment. The water-soluble polymers result in faster and better filtration and sedimentation [42]. As polyelectrolyte multilayers, they are used, for example, as separation membranes [43] or self-healing coatings [44]. The fields of solid-state batteries [15] and smart materials [17], which have become increasingly important in recent years, are also areas of application for polyelectrolytes.

The molecules synthesized in this thesis can also be classified as brush polymers due to their long side chains.

Polymer brushes are polymers that resemble a brush due to their structure. They are polymers with a long chain, which is bound to a surface at one end. The long chain stretches away from this surface [45].

These polymers are produced with the aid of grafting reactions. A distinction is made between “grafting from”, “grafting to” and “grafting through” (Figure 6) [46]. In “grafting from”, the radical site is located on the main chain. In “grafting to”, the polymer backbone and the side chains are synthesized individually. Then, chemical reactions occur *via* functional groups between the backbone and side chain. In “grafting through”, macromonomers are homo- or copolymerized [46,47]. The latter method allows a high control over the length of the brushes and was therefore used in this thesis. Macromonomers were both homo- and copolymerized. With the help of the grafting through method, the highest grafting density can be achieved. Thus, there is one side chain per backbone unit in the final polymer [48].

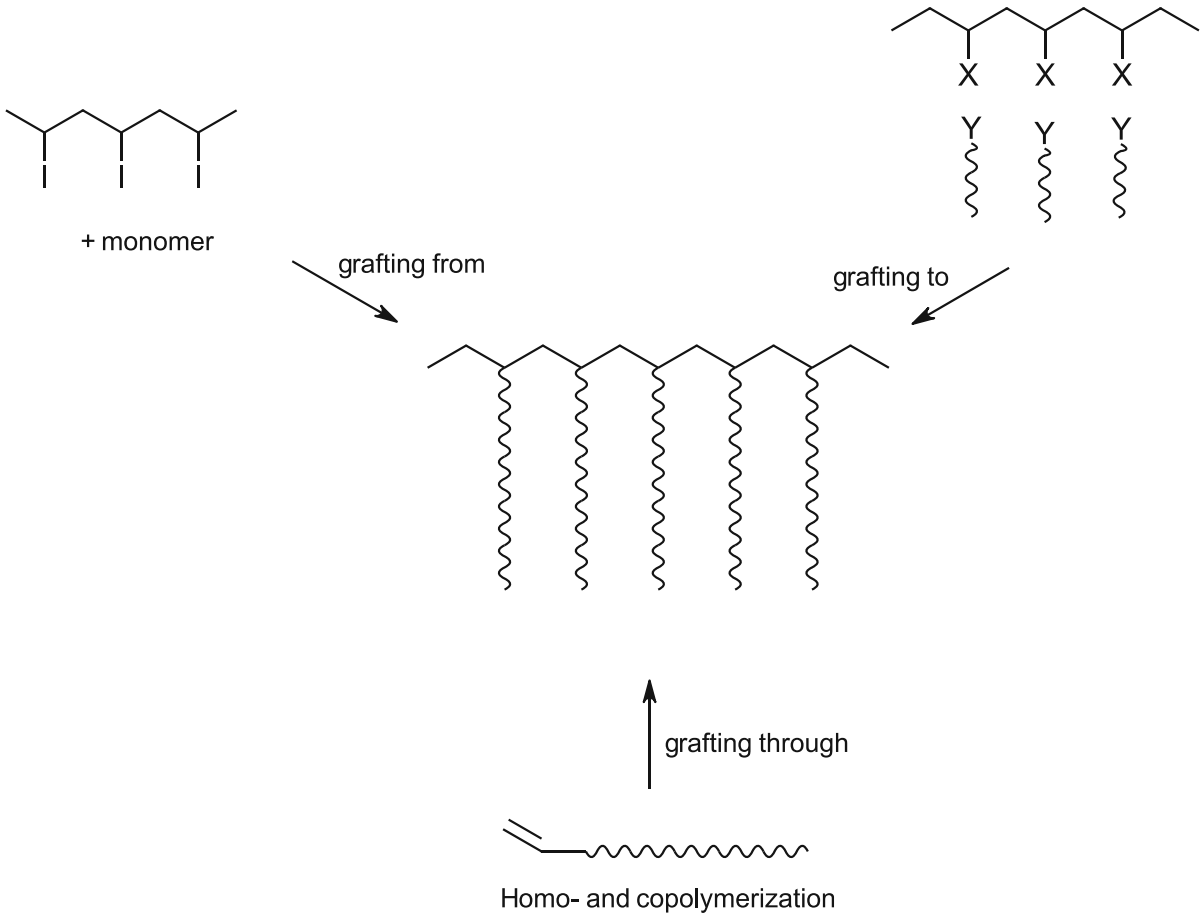

Figure 6: Brush polymers can be synthesized *via* “grafting from”, “grafting to” or “grafting trough”.

The basic reaction of these described molecules is polymerization. In this process, macromolecules (polymers) are synthesized from small molecules.

Polymers can be divided into two large groups, biopolymers (e.g. DNA) and synthetic polymers [49]. Both consist of small repeating units (monomers), which together form a large molecule [49,50].

Synthetic polymers can be made using chain-growth reactions or step-growth reactions (Figure 7). In a step-growth polymerization, two molecules, with reactive functional groups at their ends, are combined, resulting in a condensation reaction. In chain-growth polymerization, a monomer is added to the reactive end (radical, anionic or cationic) of a growing chain [49,50]. In this thesis free radical polymerization was used.

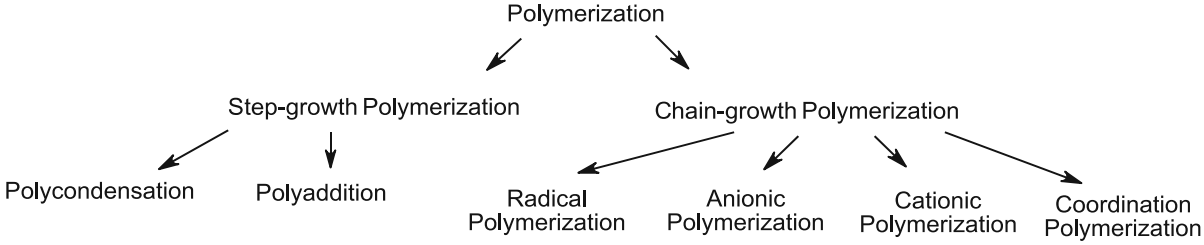

Figure 7: Classification of polymerization types.

In this work, monomers with a double bond were prepared, allowing the corresponding macromolecules to be synthesized by free radical polymerization.

In free radical polymerization, the chain-growth reaction takes place with the aid of radicals. This requires an initiator which can decompose into two radicals, such as peroxides or azo compounds [49]. The monomers usually have a vinyl group. Radical polymerization consists of the steps initiation, propagation, chain transfer and termination [51].

Initiation

Initially, a primary radical is formed by the decomposition of the initiator. The initiator radical can now react with the double bond of the monomer. A new radical molecule is formed (Figure 8) [46].

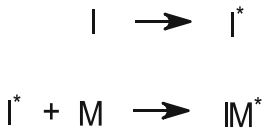

Figure 8: First step of a radical polymerization. An initiator molecule I decompose into the radical I*. The radical species IM* is formed by reaction with a monomer molecule.

Usually, peroxides (e.g. dibenzoyl peroxide) or azo compounds (e.g. AIBN) are used, in which homolytic cleavage of the covalent bond occurs even at low heating [50]. Other possibilities for initiation include photoinitiation and redox initiation [50].

One of the most commonly used azo initiators is AIBN. Decomposition starts at about 60 °C [52]. The half-life at 63 °C is 10 h [53] decreasing to 1 h at 80 °C [54]. A homolytic bond cleavage releases N_2 and two radicals are formed (Figure 9) [46,52]. Since the subsequent polymerization is a chain reaction, only small amounts of AIBN are needed as initiator. AIBN is readily soluble in benzene [54]. However, for polymerization in water, another initiator, e.g. ammonium persulfate (APS) [55], must be used due to the insolubility of AIBN.

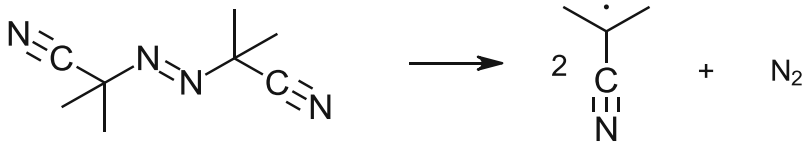

Figure 9: Decomposition of the initiator AIBN. This produces two radical molecules and N_2.

Propagation

During propagation, monomer units are constantly added to the growing radical polymer chain (Figure 10). The stability of the new radical with the additional monomer unit does not change,

since it is structurally the same as the radical before it. With increasing initiator concentration or increasing temperature, the polymer chain length decreases [51].

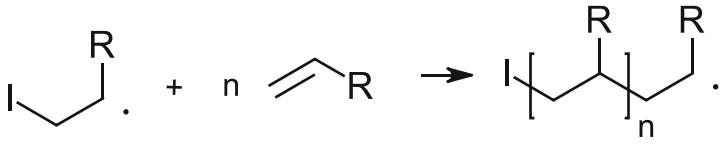

Figure 10: Propagation step of radical polymerization. A radical molecule reacts with another monomer.

Chain-transfer reaction

Free radical polymerization can also lead to chain transfer reactions (Figure 11). Here, the termination of the growing polymer chain occurs. There are inter- and intramolecular chain transfer reactions. An intermolecular transfer reaction leads to long-chain branching and intramolecular reactions lead to short-chain branching [51].

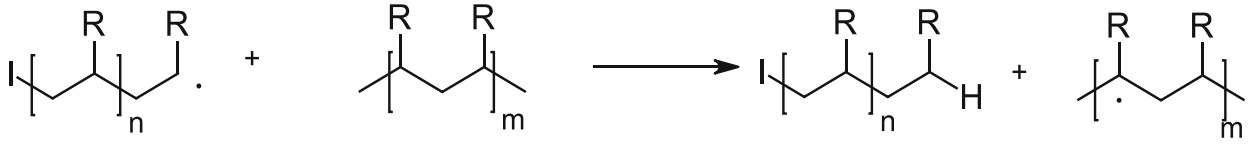

Figure 11: The chain transfer reaction transfers a radical to another molecule. This results in long- and short-chain branching.

Termination

Termination refers to reactions in which no further growth of the polymer chain occurs. The reason for this can be a recombination or disproportionation (Figure 12). Furthermore, the addition of e.g. O_2 can lead to inhibition [46].

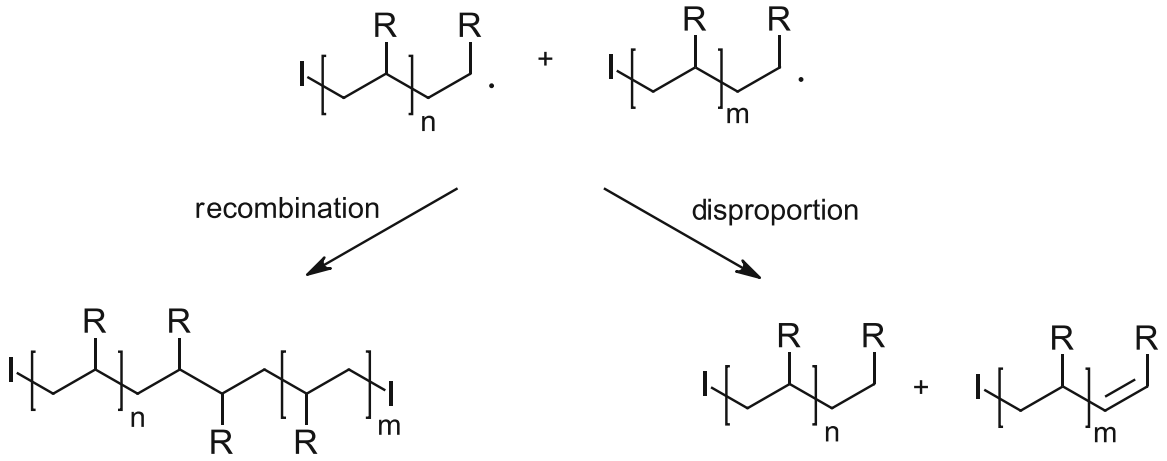

Figure 12: The termination of free radical polymerization occurs by recombination or disproportionation.

There is also a distinction between homo and copolymers. While homopolymers contain only one type of monomer, copolymers contain two or more different types of monomer. In copolymers, the individual monomer units can be arranged in different orders, resulting in a classification into random and alternating copolymers, block copolymers and graft copolymers (Figure 13) [56].

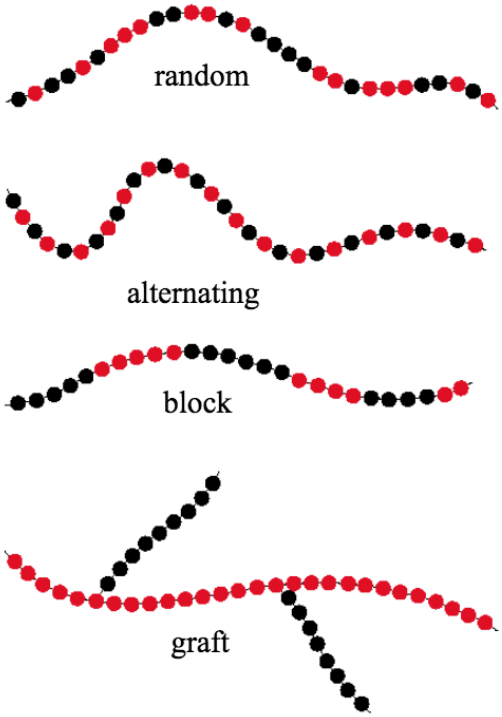

Figure 13: Classification of copolymers into random and alternating copolymers, block copolymers and graft copolymers. One monomer is represented by red colored dots and the other monomer by black colored dots [57].

The advantage of copolymers is that unique properties can be achieved through copolymerization. Important representatives of such copolymers are, for example, acrylonitrile-butadiene-styrene copolymer or styrene-acrylonitrile copolymer. [56].

In this work, both homopolymers and copolymers were prepared. This allowed the properties to be specifically improved.

OBJECTIVE

This master thesis is about the synthesis, characterization and testing of polyelectrolytes. Polyelectrolytes have ionic or ionizable side chains and are therefore used, for example, in the field of solid-state batteries and smart materials. Battery development has become an important area of research in recent years. Therefore, the aim of this work was to develop and optimize a monomer synthesis with regard to high order and flexibility in the final polymer, with the aim of obtaining sufficiently high yields and pure products on a multigram scale.

Previous work has already been done, and in the context of a masters thesis by Leibetseder [58], 11-acrylamidoundecanoate (Figure 14) was prepared and (co-)polymerized.

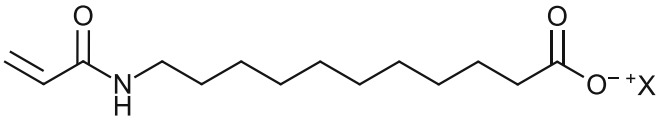

Figure 14: The structure of 11-acrylamidoundecanoate.

The aim of this thesis was to synthesize structurally similar molecules as a comparison to 11-acrylamidoundecanoate, whereby the acrylamide group is an essential component for the subsequent radical polymerization. The idea was to synthesize molecules containing the 6-acrylamidohexanoic acid and to attach two 6-acrylamidohexanoic acid units to each other by different functional groups in order to obtain the desired monomer. In first considerations, the influence of an aromatic group should be investigated by synthesizing 6-(4-(6-acrylamidohexanamido)benzamido)hexanoate (Figure 15). Due to the additional amide bonds as well as the aromatic group, 6-(4-(6-acrylamidohexanamido)benzamido)hexanoate has a higher order due to additional hydrogen bonds and pi-stacking. In addition, the molecule remains flexible due to the aliphatic chain. Furthermore, 6-(6-acrylamidohexanamido)hexanoate was selected as monomer (Figure 16). Here, the flexible part in the molecule is again about the same length as in 11-acrylamidoundecanoate, but the aliphatic chain is interrupted by one amide bond, which allows higher self-ordering through hydrogen bonds.

The prepared monomers should then be (co-) polymerized, characterized by NMR and IR, and analyzed by TGA and DSC. Finally, the behavior of the prepared polyelectrolytes should be investigated in an electric field.

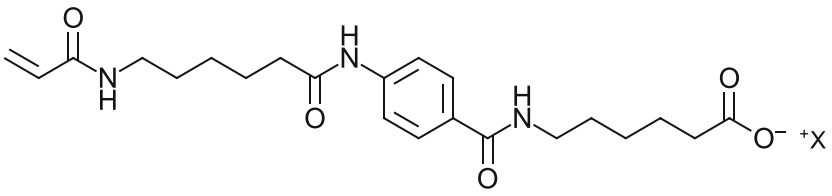

Figure 15: The structure of 6-(4-(6-acrylamidohexanamido)benzamido)hexanoate.

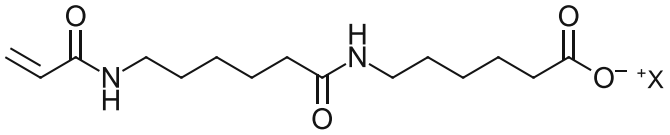

Figure 16: The structure of 6-(6-acrylamidohexanamido)hexanoate.

STATE OF THE ART

1. New types of batteries based on polymers

A major problem with lithium metal anode batteries is Li dendrite growth, which shortens battery life [59]. In addition, this growth can also cause short circuits or even fires, which endangers the safety [13]. To prevent this dendrite growth, additives are used in the electrolyte or protective layers, for example [59]. To circumvent this problem, solid state batteries with comb polymer layers can be used as described by Zhang *et al.* [59]. Here, polyetheramine is grafted onto reduced graphene oxide. In experiments it was found that the ether groups can distribute the lithium atoms evenly [59].

Zeng *et al.* [60] also attempts to prevent dendrite growth by using artificial polymer-based SEI films. Conventional SEI films have the disadvantage of being brittle and also non-uniform, resulting in inhomogeneous Li ion flux and inhomogeneous deposition. Polymer-based SEI films have the advantage over inorganic materials in that there is no breakage of the SEI film due to its high elasticity and flexibility. Zeng *et al.* [60] uses bottlebrush polymers instead of linear polymers for the artificial SEI film, since linear polymers do not prevent dendrite growth. Bottlebrush polymers have a linear polymer backbone with densely grafted polymer side chains. Due to the steric repulsion of the side chain, bottlebrush polymers also have the special property that there are no entanglements [61].

The bottlebrush polymers used in Zeng *et al.* [60] are prepared by grafting poly(lithium p-styrenesulfonate) onto cellulose nanofibrils. The SO_3- groups in the side chain of the polymers offer some advantages. On the one hand, transport channels for the lithium ions are formed and on the other hand, electrostatic repulsion also occurs between the SO_3- group and the negatively charged dendrites formed [60].

2. Polymer based actuators and sensors

Another important field of application for polyelectrolytes is the use of actuators and sensors. These are referred to as electroactive polymers. Kruusamäe *et al.* [62] describes how such polymers are exposed to an electrical stimulus and thus deform mechanically, which is why they can be used well as actuators. One example is the bending actuator which bends when voltage is applied [62].

Browe *et al.* [28] describe the use of electroactive polymers as artificial muscles. The hydrogel produced for this purpose consists of poly(ethylene glycol) diacrylate (PEGA) and poly(acrylic acid) (PAA). Hydrogels with PAA show reversible movement behavior when voltage is applied. Therefore, a polymer network was prepared with PEGA and PAA by free radical polymerization (Figure 17) [28].

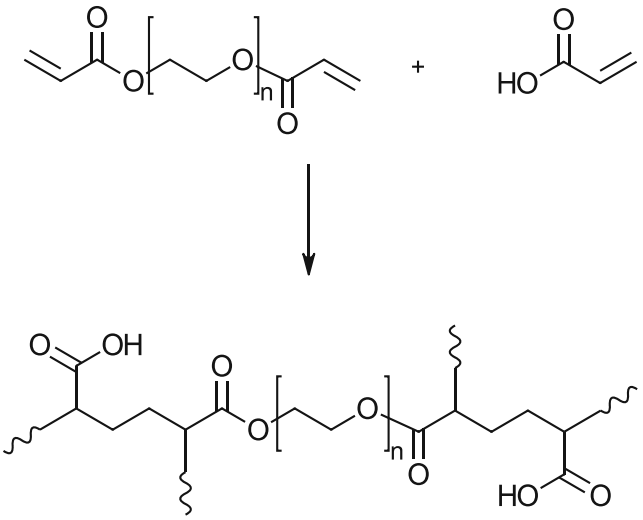

Figure 17: Synthesized polymer network based on PEGA and PAA.

The hydrogels were placed in a phosphate buffer saline (PBS) solution to allow swelling. The behavior of the samples was then tested in an electric field. For actuation testing, a strip of the hydrogel was placed in a PBS solution between two platinum electrodes (Figure 18). A DC voltage of 20 V was then applied. The sample bends in the direction of the negative electrode (Figure 19).

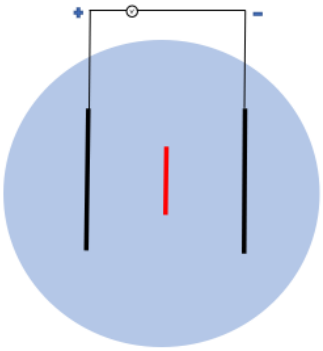

Figure 18: Design of the experiment before a voltage was applied. The polymer is placed in an PBS solution (light blue) that it can swell. The swollen polymer (red) is between two electrodes (black).

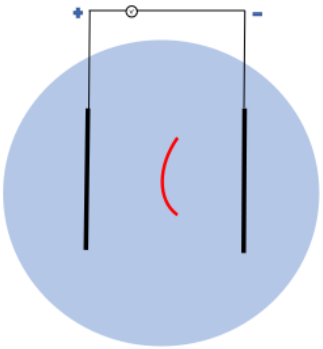

Figure 19: After applying a DC voltage of 20 V, the swollen polymer (red) changes its shape. The polymer bends to the negative electrode.

It was also found that the greater the proportion of acrylic acid, the stronger the movement. The best results were obtained with a PEGA:PAA ratio of 1:8 [28].

3. Self-healing hydrogels based on 6-acrylamidohexanoic acid

The poly(6-acrylamidohexanoic acid) produced in this work was investigated in a paper by Phadke *et al.* [36] due to its fast self-healing properties. The aim here was to prepare a hydrogel network with flexible side chains. Poly(6-acrylamidohexanoic acid) was therefore chosen because of the presence of both hydrophilic and hydrophobic interactions, which is a prerequisite for this self-healing. The flexible part of the side chain must not be too much to avoid steric hindrance, but they must be long enough for the network to be deformable. The functional groups at the end can form hydrogen bonds, which is the reason for the so-called self-healing of these hydrogels. Polymer hydrogels based on 6-acrylamidohexanoic acid have an optimal ratio of hydrophilic and hydrophobic interactions [36]. Hydrogen bonds between the functional groups (amide and carboxy groups) can be formed across a hydrogel interface (Figure 20). Two connected hydrogels can also be separated again by a higher pH value (Figure 21) or reconnected at lower pH values. This process is reversible and the healed hydrogels are resilient and can withstand deformation.

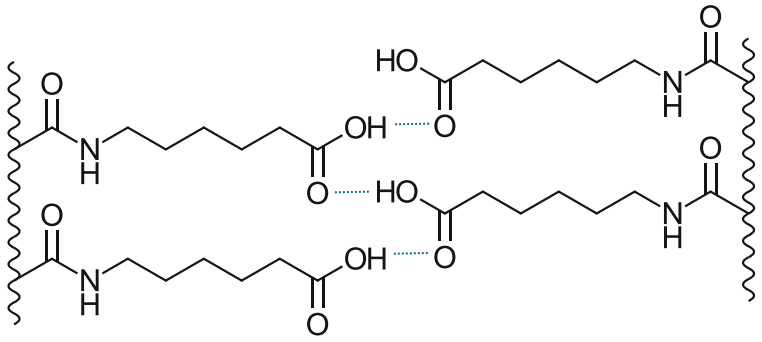

Figure 20: Hydrogen bonds are formed between two interfaces, which allows the material to self-heal.

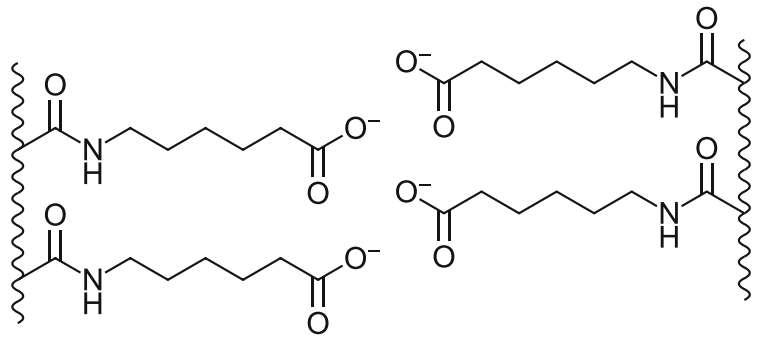

Figure 21: At higher pH values, no hydrogen bonds can be formed due to the dissociation of the carboxylic acid.

The self-healing properties depend strongly on the degree of crosslinking [36]. In addition, the length of the side chain plays an important role, which is why hydrogels based on other molecules were also investigated for comparison. A higher degree of crosslinking means poorer self-healing behavior. In addition, a poorer self-healing process was observed for hydrogels with shorter side

chains. If the aliphatic chains are too long, steric hindrance can occur and the side chains aggregate and finally collapse due to the hydrophobic interactions. This reduces the accessibility of the amide groups and makes the formation of hydrogen bonds more difficult [36].

Such hydrogels are used, for example, as tissue adhesives. Phadke *et al.* [36] investigated the possibility of using poly(6-acrylamidohexanoic acid) hydrogels as tissue adhesives on gastric mucosa in rabbits. Due to the low pH in such an environment, perfect conditions for the self-healing of the hydrogels are given [36]. Due to the enteric properties of 6-acrylamidohexanoic acid, Zhang *et al.* [63] also describe the possibility of using this material for devices that remain in the stomach. The advantage over other materials is that if the material enters the intestinal tract, no intestinal obstruction can occur due to the pH-neutral environment in the intestine, in which the hydrogen bonds of the material are broken [63]. In vivo tests in pigs have already shown the success of the use of these materials for applications in the stomach [63].

4. Polymers based on 11-acrylamidohexanoic acid

An earlier master's thesis dealt with polyelectrolytes that already had a flexible content due to the defined length of the aliphatic chain.

Leibetseder [58] developed a way of synthesizing monomer 11-acrylamidoundecanoic acid from 11-aminoundecanoic acid (Figure 22). This molecule was chosen because of the carboxy group, which can be protonated or deprotonated depending on the pH value. In addition, it is a flexible molecule due to the aliphatic chain with 11 carbon atoms. This flexible chain allows the charge to move more freely and thus new properties can be introduced into the final polymer.

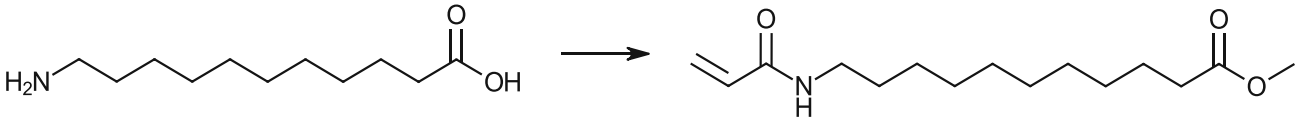

Figure 22: The starting molecule was 11-aminoundecanoic acid. An acrylic group was added *via* the reaction with acryloyl chloride. The carboxylic acid was protected with an ester group.

The amino group was converted into an acrylamide group with the aid of acryloyl chloride. The carboxylic acid was esterified to increase solubility in organic solvents and to facilitate subsequent polymerization. On the one hand, the *tert*-butyl ester and, on the other hand, the methyl ester were prepared. Experiments showed, however, that the contacting by means of *tert*-butyl ester was very time-consuming and afforded only moderate yields. Therefore, the contactor was preferably the methyl ester. The esterification was acid catalyzed by HCl or H_2SO_4 in methanol. Other compounds, such as 4-aminobenzoic acid, were also methyl esterified using HCl in order to test the simplicity of the synthesis on other substrates (Figure 23).

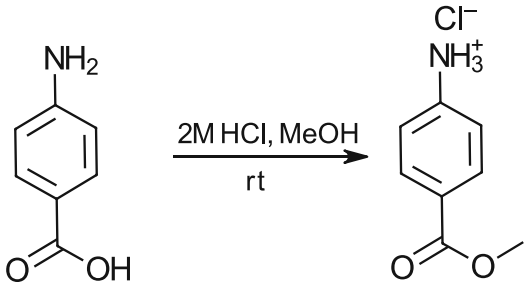

Figure 23: Protection of 4-aminobezoic acid *via* the methyl ester.

In addition, an attempt was made not to esterify 11-acrylamidoundecanoic acid and to react it directly with acryloyl chloride and then polymerize it. However, the problem with this synthesis was that the resulting monomer was only soluble in DMSO, making classical solution polymerization difficult. Attempts were made to polymerize the monomer in water with APS/TEMED, but this was not successful. Therefore, this synthesis route, without methyl esterification of the starting product, was discarded. The monomer prepared in this way could now be polymerized. For this purpose, polymerization was carried out both in solution and in bulk. An exciting effect was observed during bulk polymerization. The polymer shows a swelling behavior in DCM. However, this effect was not investigated in detail since only small amounts (<0.5 g) were bulk polymerized. The main mode of polymerization in this work was solution polymerization in benzene with 1 w% AIBN. However, other solvents such as toluene, ethanol, and a mixture of 1:1 MeOH/chlorobenzene were tested, and polymerization in benzene worked best. The polymer was then deprotected to give the poly(11-acrylamidoundecanoic acid) (Figure 24).

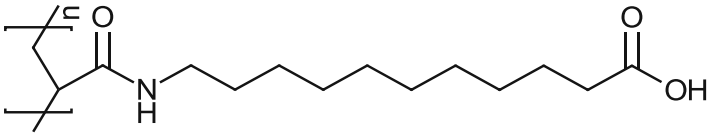

Figure 24: Structure of the target molecule poly(11-acrylamidoundecanoic acid) synthesized in the master thesis of Leibetseder [58].

This work left some questions unanswered, both in monomer synthesis and polymerization.

RESULTS AND DISCUSSION

The polymers prepared in this thesis belong to the class of amide functionalized polyacrylamides. The polymer backbone is built up *via* the acrylamide and the amide function is located in the brushes of the polymer.

In principle, polyamides are produced by polycondensation reactions. In this process, an amine and a carbonic acid react [56]. Due to the many hydrogen bonds that polyamides can form, these materials have special properties, such as high mechanical stability. Therefore, they are often used as fibers [64]. The associated monomers are e.g. based on 6-aminohexanoic acid. A well-known representative of polyamides based on 6-aminohexanoic acid is, for example, polyamide-6 (Perlon). However, this is produced from ε-caprolactam *via* ring-opening polymerization and 6-aminohexanoic acid is only an intermediate product [52].

Within this thesis, a radical polymerization was carried out. For this, the monomers must contain a double bond. The reaction of 6-aminohexanoic acid with acryloyl chloride can introduce a double bond, making radical polymerization easy to carry out.

1. Brush polymers with aromatic based C12 side chains

At the beginning of this thesis, the idea was to prepare a molecule that shows a comparable molecular dimension to 11-acrylamidoundecanoic acid (**1)** (Figure 25) including additional functional groups that enhance self-ordering properties.

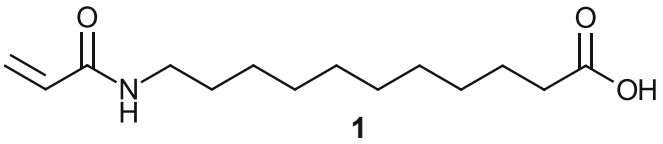

1

Figure 25: Structure of 11-acrylamidoundecanoic acid (**1**).

In first considerations, the influence of an aromatic group should be investigated by synthesizing methyl-6-(4-(6-acrylamidohexanamido)benzamido)hexanoate (**2**). The aromatic compound leads to π- π stacking, which is expected to result in a higher order of the final polymer. In the following the retrosynthetic considerations for the preparation of monomer **2** are discussed (Figure 26).

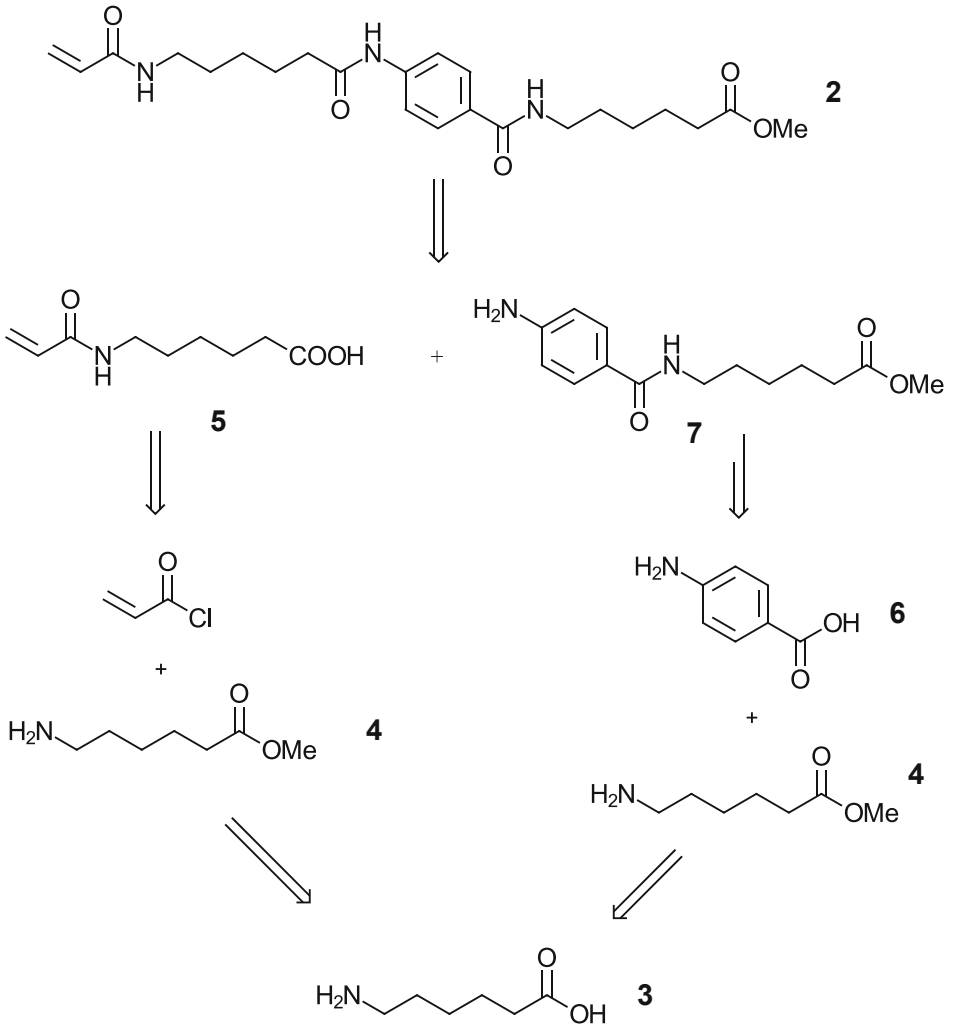

Figure 26: Retrosynthesis of methyl 6-(4-(6-acrylamidohexanamido)benzamido)hexanoate (**2**).

For the syntheses, the use of protecting groups (for the carboxylic acid and the amide) and activating groups (for the carboxylic acid) was essential.

The carboxylic acid can be both, protected and activated, so that a nucleophilic attack at a certain position is prevented or preferred. If the carboxylic acid is protected, however, it is also important to be able to remove the protective group again without problems after the reaction [65].

In this work, the protection and activation of the carboxylic acid were important for monomer synthesis. The simplest way to protect the functional group is to convert the carboxylic acid into a methyl ester [66]. From Leibetseder [58] it is known that the methyl ester shows good stability for further molecular transformations and is easily cleaved at the stage of the polymer. Thus, route was also chosen in this work. Additionally, the methyl ester does not require much steric space and does not complicate the NMR spectra, since only one signal of the methyl group is obtained [66].

Methylation can be carried out using thionyl chloride and methanol. Deprotection of the methyl ester group is achieved by base-catalyzed hydrolysis in an aqueous methanolic solution. Attention must be paid to the stability of the remaining molecule under the basic conditions, as otherwise

unwanted decomposition reactions may occur [66]. Therefore, the phenyl ring is inserted into the targeted molecule *via* amide bonds that are expected to withstand the ester cleavage reaction and additionally possess the ability for self-ordering through hydrogen bonds.

The amide bond can be formed by activating the carboxylic acid. The activation of can be done, for example, by converting the carboxylic acid to the corresponding acyl chloride [65]. The acyl chloride can be prepared using chlorinating reagents such as thionyl chloride [67] or oxalyl chloride [68]. This then reacts readily with the amine to give the corresponding amide.

In addition, protection of the amino group of aminobenzoic acid **6** has also been considered to prevent undesirable reactions of the amino group. One possibility to protect an amine is the trifluoroacetyl group (Figure 27). This group is stable under acidic conditions and easily removed under alkaline conditions [66].

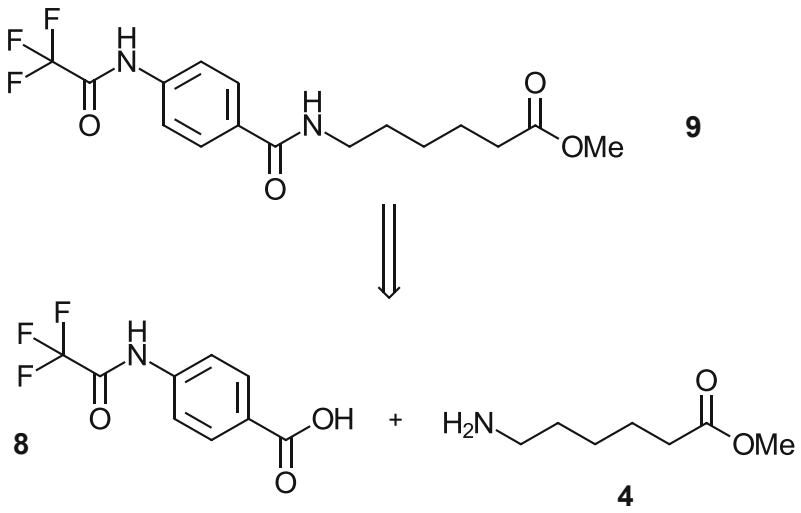

Figure 27: Retrosynthetic considerations for methyl 6-[(2,2,2- trifluoro-acetylamino)benzylamino]hexanoate (**9**). In contrast to Figure 26, the monomer component **7** can also be prepared with the aid of a protecting group. After the synthesis of **9**, the protecting group can be removed again under basic conditions and molecule **7** is obtained.

A protecting group for amines that is also stable under acidic conditions is the 9-fluorenylmethoxycarbonyl (FMOC) group [66]. The advantage of these two protecting groups is that a carboxy group, which is also present, can easily react with thionyl chloride to form acid chloride without the protecting group of the amine being split off [66].

1.1. Monomer synthesis

1.1.1 Synthesis of methyl 6-aminohexanoate hydrochloride (4)

To obtain the desired monomer **2**, methyl 6-aminohexanoate hydrochloride (**4**) first had to be prepared. Methylester **4** was synthesized in accordance to Gurjar *et al.* [69] (Figure 28). First, 2 eq $SOCl_2$ and MeOH were mixed and cooled with an ice bath. Then 1 eq carboxylic acid **3** was added and the solution was stirred at room temperature. After removing the solvent under reduced pressure, 90 % of a white powder were obtained.

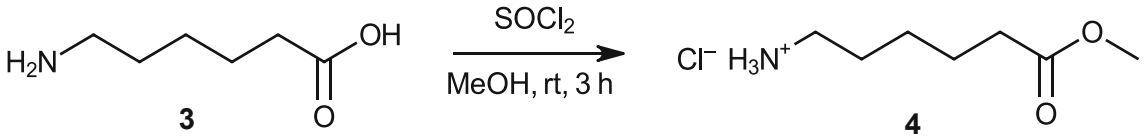

Figure 28 Synthesis of methyl 6-aminohexanoate hydrochloride (**4**).

The product was characterized by ^{1}H-NMR and IR. In the ^{1}H-NMR spectrum (Figure 29), the signal of the methyl ester at 3.59 ppm is clearly visible. In addition, the signal of the carboxylic acid at about 12 ppm has disappeared as expected. Thus, the spectrum shows all expected signals and proofs a successful esterification. In addition, the melting point was determined using an Optimelt device. The product was first dried well and then a melting range of 121-123°C could be determined, which agrees with the melting point in the literature (117-124 °C) [70]. The product was used for subsequent syntheses without further purification.

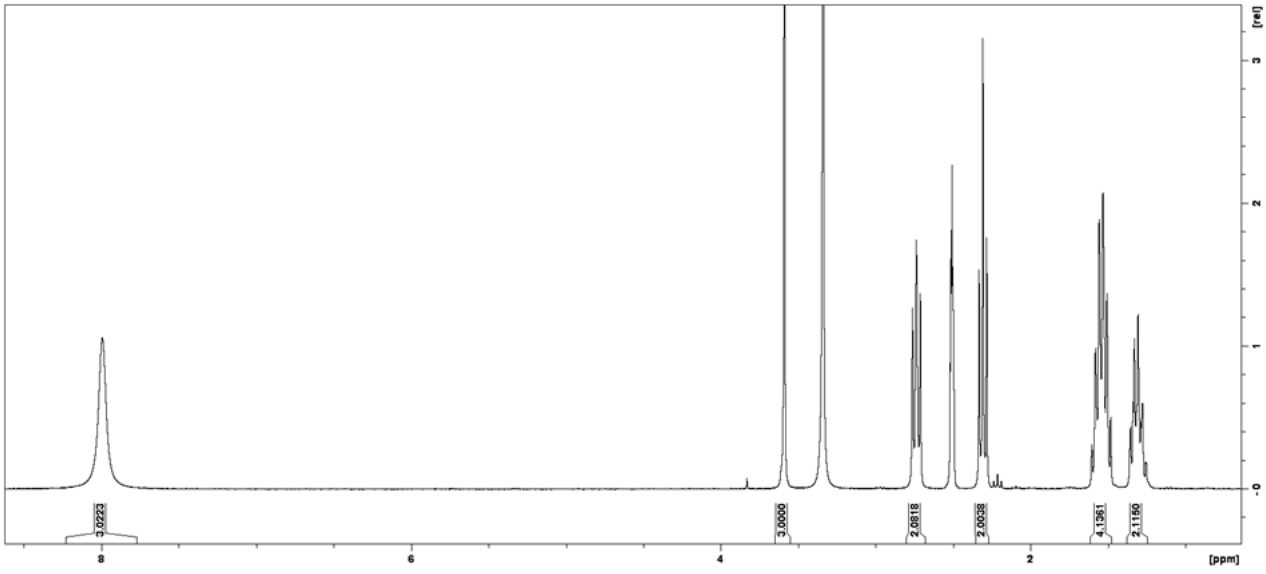

Figure 29: ^{1}H-NMR (300 MHz, DMSO-d_6 = 2.50 ppm, H_2O = 3.33 ppm) of **4**. The spectrum shows characteristic signals of the compound. The signal at 3.59 ppm shows that the methyl ester was successfully formed.

1.1.2 Synthesis of methyl 6-(4-aminobenzamido)hexanoate (7)

To synthesize target molecule **2**, intermediate **7** must be prepared next. The amide bond was prepared as described in Bruice [71]. For this purpose, 1 eq aminobenzoic acid **6** was reacted with 2 eq $SOCl_2$ to give the corresponding acid chloride.

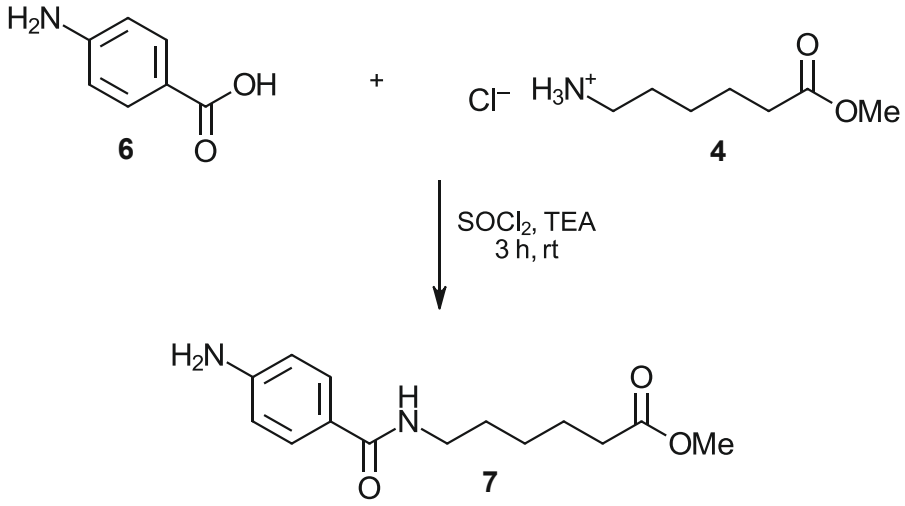

Figure 30. Synthesis of methyl 6-(4-aminobenzamido)hexanoate (**7**).

Subsequently, the amide bond could be linked, with 2 eq of amine **4**, before being treated with 2 eq TEA, to give product **7** (Figure 30). The product was purified by extraction with brine and then characterized by ^{1}H-NMR and IR. A yield of 29 % was obtained. The ^{1}H-NMR shows that no complete conversion occurred and a mixture of reactant **4** and **6**, an unidentified by-product and the product was obtained.

The reason for the incomplete conversion was found in the first step of the synthesis, the formation of the acid chloride. Attempts to optimize this reaction showed the dimerization of **6** under harsh conditions. The protection of the aromatic amine by the formation of the hydrochloride did not work as desired. Milder conditions did not achieve an acceptable conversion and caused by the required prolonged reaction time still formed the dimer.

Hereinafter, the synthesis was tried under protection of the amino-functionality in aminobenzoic acid **6**. A comparison should be made whether better conversions can be obtained by the protective group.

1.1.3 Synthesis of 4-(2,2,2-trifluoro-acetylamino) benzoic acid (8)

Now, an attempt was made to prepare amide **7** with the aid of an additional protecting group on the amino group of benzoic acid **6**. The first step in this multistep synthesis was to protect benzoic acid **6** with a protecting group on the amino group (Figure 31). The synthesis was carried out following Steiner *et al.* [72].

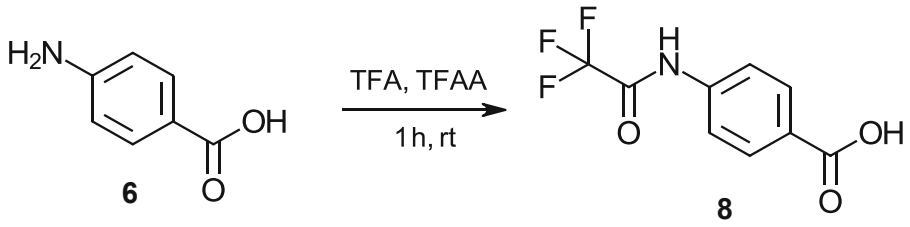

Figure 31: Synthesis of 4-(2,2,2-trifluoro-acetylamino) benzoic acid (**8**).

Therefore, 1 eq of starting material **6** was reacted in trifluoroacetic acid (TFA) with 1 eq trifluoroacetic anhydride (TFAA) to the protected benzoic acid **8**. The product was obtained by precipitation in cold water. After drying in vacuo, a yield of 63 % was obtained and a ^{1}H-NMR of the product was recorded.

Educt **6** and product **8** differ in the ^{1}H-NMR spectrum only by the number of H atoms on the nitrogen. To fully characterize the structure of product **8**, for example, a ^{13}C- or ^{19}F-NMR spectrum should have been made. Nevertheless, work was continued with this intermediate **8** to prepare amide **9** in the next step.

1.1.4 Synthesis of methyl 6-((2,2,2- trifluoro-acetylamino) benzylamino) hexanoate (9)

The previously synthesized protected amine **8** can now react with hydrochloride **4** to methyl 6-((2,2,2- trifluoro-acetylamino)benzylamino) hexanoate (**9**) *via* a common amide synthesis as described in Bruice [71] (Figure 32).

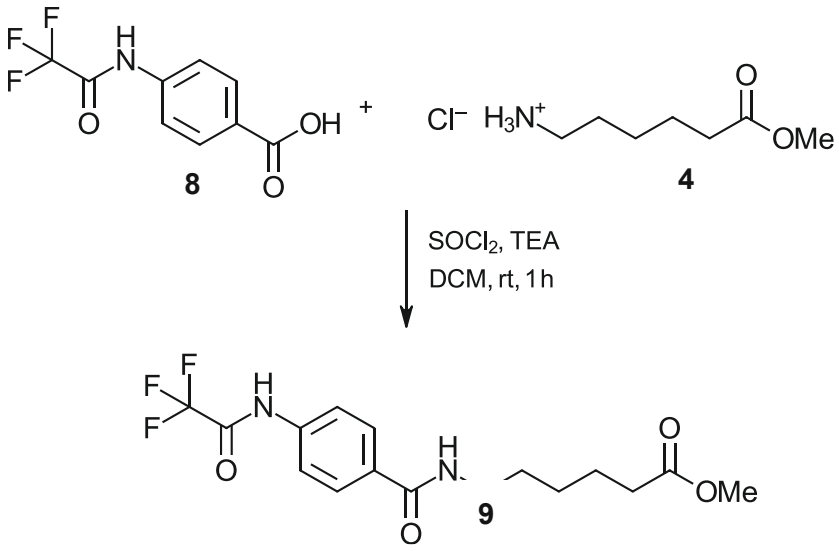

Figure 32: Synthesis of methyl 6-((2,2,2- trifluoro-acetylamino)benzylamino) hexanoate (**9**).

This is done in a two-step synthesis. First, the acid chloride of **8** is prepared to activate the carbonyl group (Figure 33). Here it is important that the amino group of **8** is previously protected by a protecting group that is stable under the conditions of $SOCl_2$, which is the case with the TFA protecting group.

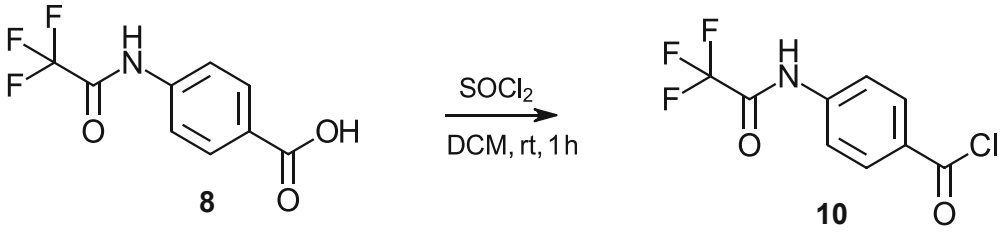

Figure 33: Synthesis of 4-(2,2,2-trifluoro-acetylamino) benzoyl chloride (10).

To prepare acid chloride **10**, 1.5 eq of $SOCl_2$ is added to a solution of 1 eq carboxylic acid **8** in DCM under cooling. The solvent is then removed under reduced pressure, thus removing any remaining $SOCl_2$. The pungent odor of $SOCl_2$ should now no longer be detected in product **10**. Subsequently, the amide bond between acid chloride **10** with hydrochloride **4** (1 eq) can be formed with the aid of 3 eq TEA in DCM to product **9**. The reaction solution was then extracted using HCl and the remaining solvent was removed. Product **9** was obtained in a yield of 46 % and characterized by ^{1}H-NMR.

Figure 34 shows the ^{1}H-NMR spectrum of carboxylic acid **8** (blue), hydrochloride **4** (green) and product **9** (red).

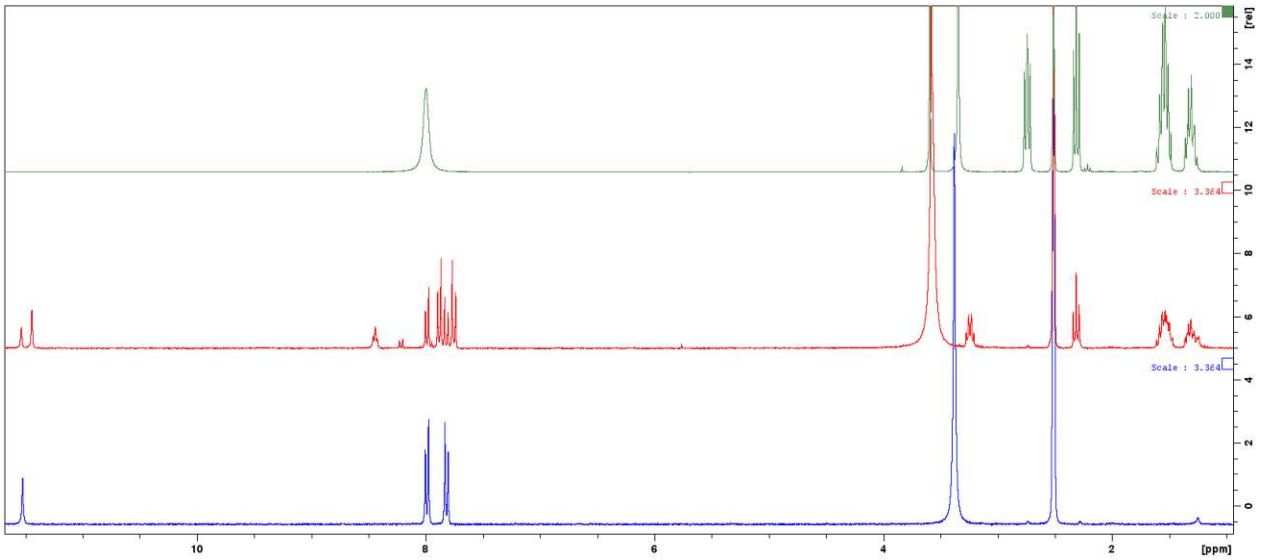

Figure 34: ^{1}H-NMR spectra (300 MHz, DMSO-d_6 = 2.50 ppm, H_2O = 3.33 ppm) of carboxylic acid **8** (blue), hydrochloride **4** (green) and product **9** (red). The amide signals at 11.53 ppm and 11.44 ppm for product **9** (red) show different intensities because there is an overlap of the amide signal of reactant **8** (blue). In addition, the signals 7.98 ppm and 7.81 ppm show that there is still unreacted reactant **8** (blue) in the product. In addition, the signals of hydrochloride **4** can also be found in the range of 1.63-1.21 ppm in the product. Based on the signal intensities, the quantity of each substance in the final product can be calculated. There are about 27 % carboxylic acid **8**, 26 % hydrochloride **4** and 47 % product **9** in the final mixture.

The ^{1}H-NMR spectrum shows that a mixture of reactants and product was obtained. The amide signal (11.52 ppm) as well as the signals of the aromatic H atoms (7.98 ppm and 7.81 ppm) of reactant **8** can also be found in the NMR spectrum of the product. At 3.57 ppm and in the range of 1.63-1.21 ppm, there is also superposition of signals from the product and hydrochloride **4**. Based on the ^{1}H-NMR spectrum, it can therefore be said that 47 % conversion has occurred.

Summarizing the above-discussed three-step synthesis of intermediate **9** a low overall yield of 13 % was obtained. With regard to the following synthesis steps to obtain the final product **2** the attempts to synthesize monomer **2** were stopped at that point.
In addition, the amide linkage can be done using coupling reagents instead of the acid chloride which can also lead to a more successful synthesis. However, parallel to these attempts, work was also already being done on the synthesis of 6-(6-acrylamidohexanamido)hexanoic acid (**11)** and the formation *via* a strategy using coupling reagents was not further followed. The synthesis of **11** seemed more promising at that time, so it was decided to continue working on this molecule and to optimize the syntheses. The development of the synthesis of monomer **2** was terminated with this last step, since the goal was to develop a simple monomer synthesis, with the requirement not to be too complex and to obtain product in multigram scale. In addition, molecule 2 would be probably unsuitable as a monomer, due to its likely high melting point and difficult solubility. Therefore, it makes more sense to focus on aliphatic monomers with amide groups.

Optimizing both monomer syntheses would not have been possible in terms of time. Therefore, it was attempted to focus on one monomer and to optimize the synthesis route up to the final polymer.

2. Brush polymers with amide based C6 side chains

In contrast to acrylamide **1** with 11 aliphatic carbons, 6-acrylamidohexanoic acid **5** and methyl 6-acrylamidohexanoate **12** with only 6 carbons were also prepared in order to investigate the influence of the length of the aliphatic chain. These monomers with 6 aliphatic carbon atoms are actually intermediates in the synthesis of monomer **11**, but they were also considered to be interesting independent monomers, which is why they are described here.

2.1 Monomer synthesis

2.1.1 Synthesis of 6-acrylamidohexanoic acid (5)

This synthesis is based on the nucleophilic attack of the amine on the carbonyl group of acryloyl chloride. The synthesis was carried out according to D'Souza *et al.* [73] (Figure 35).

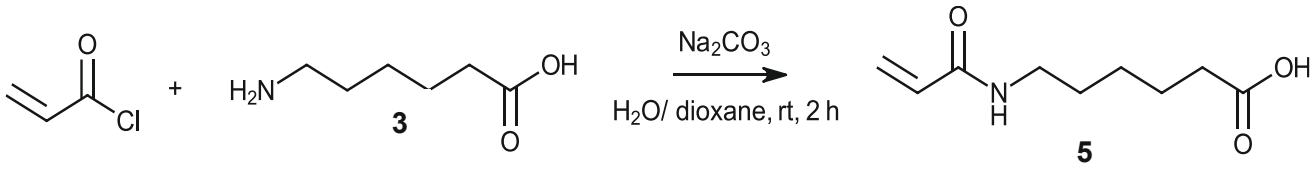

Figure 35: Synthesis of 6-acrylamidohexanoic acid (**5**).

Therefore, 1 eq of amine **3** was reacted with 2 eq of sodium carbonate in water. Then 1 eq acryloyl chloride in dioxane was added to obtain product **5**. The major difficulty in this synthesis was the following workup, more precisely the complete separation of acrylic acid. Most of it could be removed by putting the sample in a vacuum drying oven for 48 h at 45 °C. Due to the pungent smell of acrylic acid, it can be quickly determined whether residues are still present in the product. The ^{1}H-NMR (Figure 36) shows that most of the acrylic acid was removed in the vacuum drying oven. There was a residue of 1 wt% acrylic acid still left in the product.

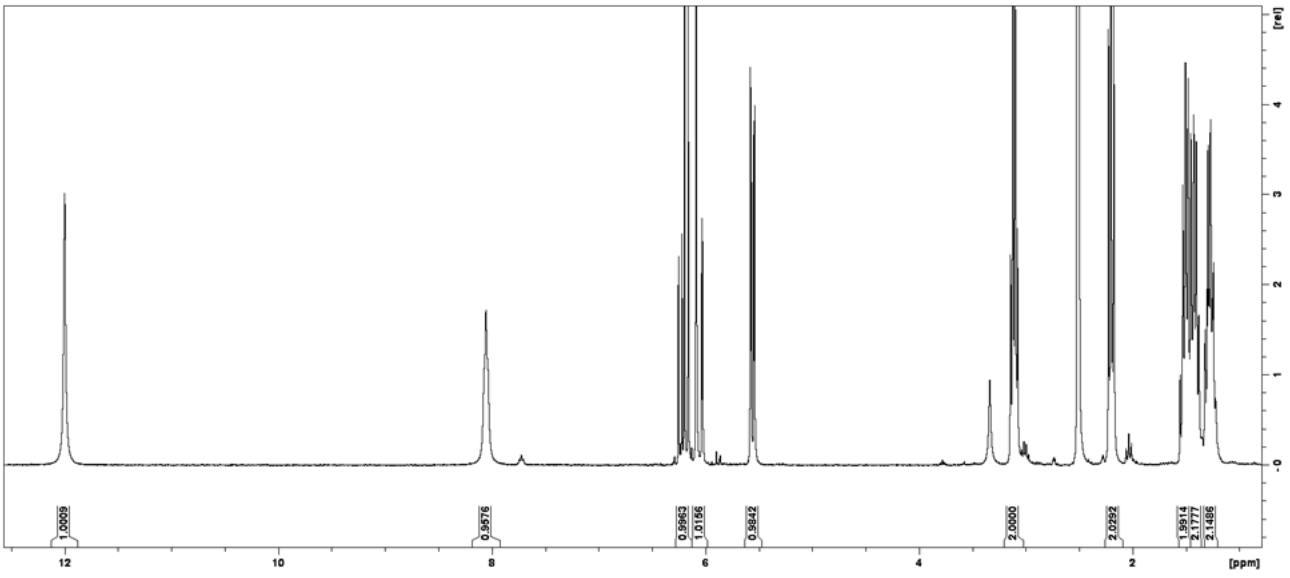

Figure 36: ^{1}H-NMR spectrum (300 MHz, DMSO-d_6 = 2.50 ppm, H_2O = 3.33 ppm) of **5**. The spectrum shows all characteristic signals of the product. There are also some weak signals which are caused by residual acrylic acid. Most of this could be removed by drying in a vacuum drying oven at 45 °C.

Particularly in the range of 6.3-5.8 ppm, acrylic acid can still be detected (Figure 37). Although there was still a small amount of acrylic acid in the product, it was used for polymerization without further purification.

In addition, it was later determined by HPLC that the dimer of amide **5** is also formed during the synthesis, which is why additional signals appear in the NMR spectrum.

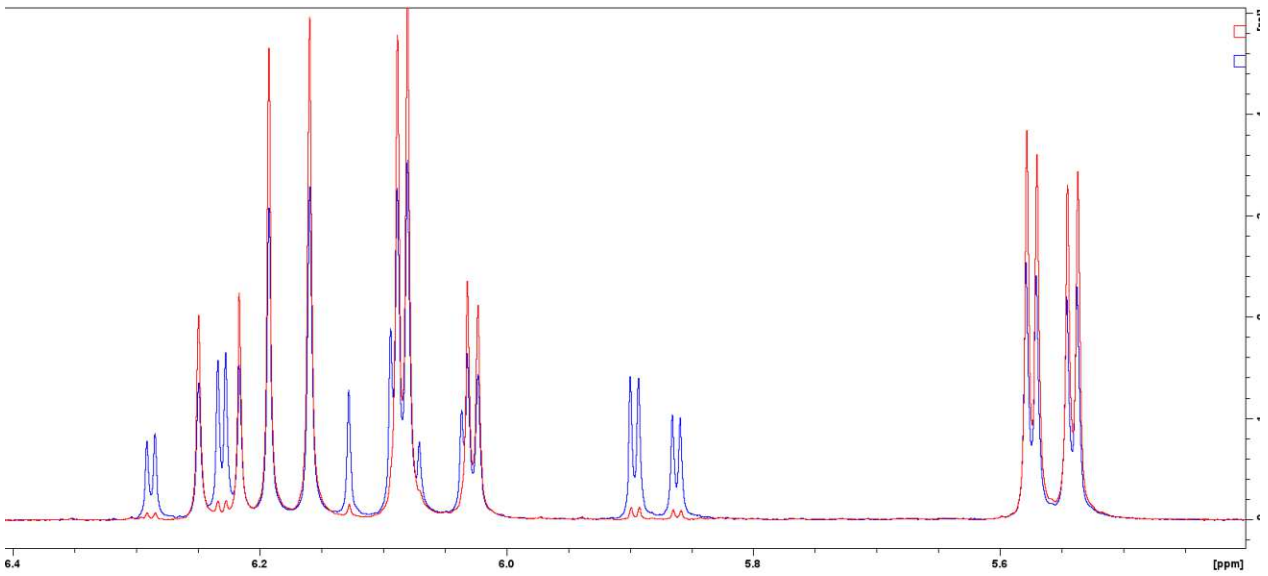

Figure 37: Comparison of product **5** before and after 48 h at 45 °C in a vacuum drying oven. ^{1}H-NMR spectrum of **5** before drying (blue): Signals can be clearly seen in the range of 6.3-5.8 ppm, which can be assigned to acrylic acid. ^{1}H-NMR spectrum of the final product after drying (red): The peaks caused by acrylic acid are clearly smaller here. There is still a residue of 1 wt% (2 mol%) acrylic acid in the product (normalized to the CH_2-group next to the amide bond at 3.10 ppm).

Product **5** was identified *via* IR and ^{1}H-NMR. The IR spectrum shows characteristic signals for the compound (Figure 38). The broad signal between 3460-2280 cm^{-1} is caused by an OH-stretching vibration and thus indicates a carboxylic acid. The sharp signal at 3286 cm^{-1} is assigned to the

amide. The CH_2-stretching and CH-stretching vibration signal are at 2940 cm^{-1} and 2850 cm^{-1}. The CO-stretching vibration leads to a signal at 1690 cm^{-1}.

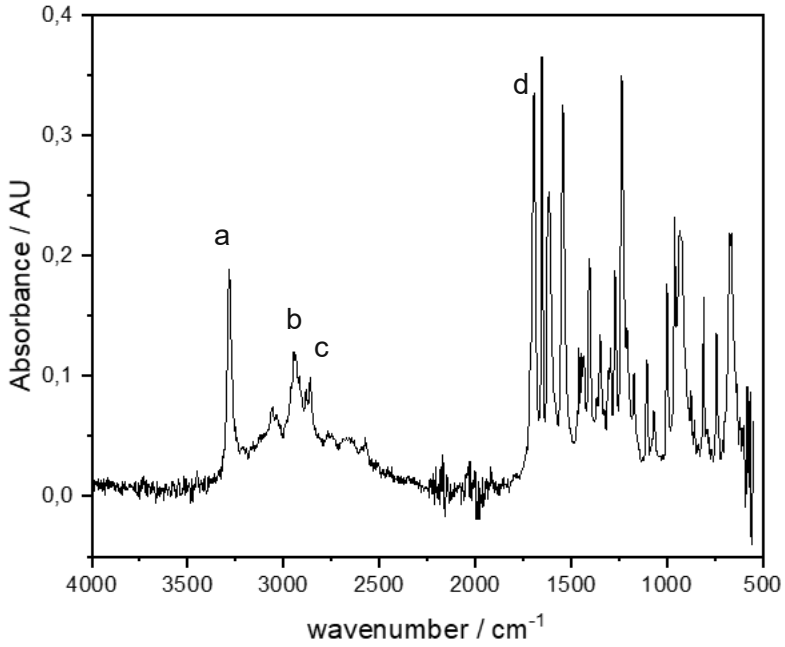

Figure 38: FTIR-ATR spectrum of 6-acrylamidohexanoic acid (**5**). 3460-2280 cm^{-1}(OH-stretching, carboxylic acid), (a) 3286 cm^{-1} (amide), (b) 2940 cm^{-1} (CH_2-stretching, alkene), (c) 2850 cm^{-1} (CH-stretching), (d) 1690 cm^{-1} (C=O-stretching), 1651 cm^{-1} (secondary amide).

2.1.2 Synthesis of methyl-6-acrylamidohexanoate (12)

The synthesis was carried out according to D`Souza *et al.* [73] (Figure 39).

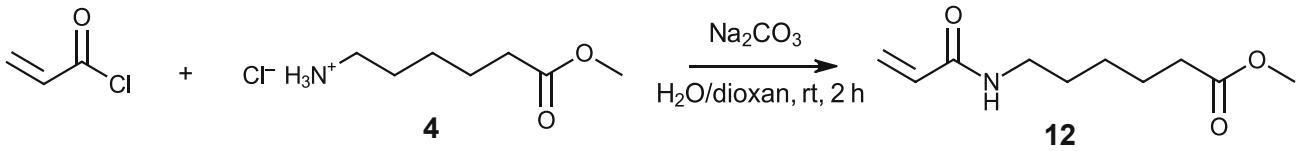

Figure 39: Synthesis of methyl-6-acrylamidohexanoate (**12**).

Na_2CO_3 (2 eq) releases the amine of **4** (1 eq) and a nucleophilic attack of the amine of **4** on the carbonyl group of the acryloyl chloride (1 eq) occurs. Released HCl is bound by Na_2CO_3. Monomer **12** was characterized by ^{1}H-NMR. Consequently, the corresponding homopolymer as well as copolymers (with DMAA and HEMA) were synthesized.

2.2 Polymerization

Based on the previously prepared monomers **5** and **12**, various homo- and copolymers could now be synthesized.

2.2.1 Synthesis of poly(6-acrylamidohexanoicacid) (13)

The homopolymer of **5** was prepared to compare its properties with those of the copolymers.

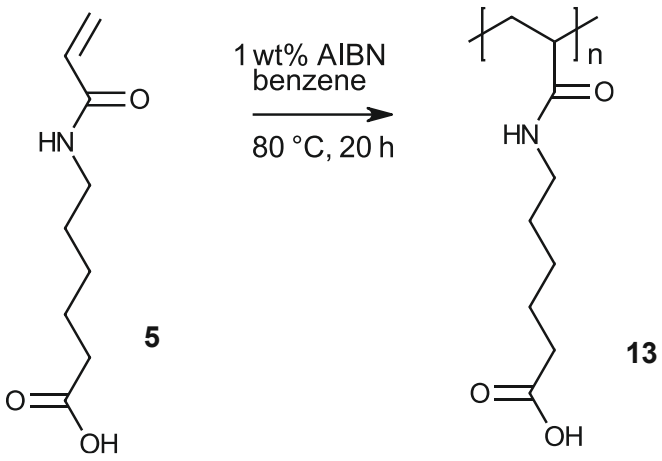

Figure 40: Synthesis of poly(6-acrylamidohexanoicacid) (**13**).

Therefore, acrylamide **5** was polymerized in benzene with 1 wt% AIBN (Figure 40). The obtained homopolymer **13** was very hard and brittle and was characterized via ^{1}H-NMR and IR spectroscopy. The missing protons of the acrylic group in the ^{1}H-NMR spectrum of **13** indicates a high conversion in the polymerization.

2.2.2 Synthesis of poly(6-acrylamidohexanoicacid) copolymers (14, 15)

The copolymers of **5** were also prepared. *N,N*-Dimethylacrylamide (DMAA) and hydroxyethylmethacrylate (HEMA) were used as comonomers to influence the properties of the final polymer. Due to its properties such as, adhesion to glass and metal surfaces [74], DMAA is a popular comonomer, therefore it was also used here. In comparison, HEMA was also used, as it has already been used in the past as a comonomer for hydrogels in biomedicine due to its swelling properties in water [75].

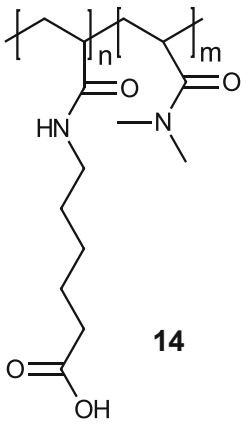

14

Figure 41: Structure of poly(6-acrylamidohexanoicacid-co-DMAA) (**14**).

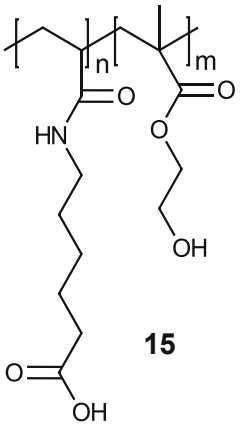

15

Figure 42: Structure of poly(6-acrylamidohexanoicacid-co-HEMA) (**15**).

Copolymerization of acrylamide **5** was carried out with DMAA (Figure 41, polymer **14**) as well as with HEMA (Figure 42, polymer **15**) for comparison. Therefore, 1 eq of monomer **5** and 1 eq of the comonomer were polymerized in benzene with 1 wt% AIBN. Homopolymer **13** is very hard and brittle, but by using comonomers, a white, softer powder is obtained as product. By using DMAA as comonomer, the polymer loses brittleness . The DMAA homopolymer constitutes a very tough and sticky polymer. Therefore, the polymer also becomes softer and less brittle by using 50 mol% DMAA as comonomer.

Figure 43 shows the IR spectra of homopolymer **13**, DMAA-copolymer **14** and HEMA-copolymer **15**. The black und blue graph show the amide signal at 3640 cm^{-1} (Figure 43, a). The green graph generally has lower intensities across the spectrum, therefore this signal is not apparent here. The broad signal at 3590-3100 cm^{-1} (Figure 43, b) is caused by the OH-stretching vibration from the HEMA-copolymer (blue graph), All three graphs show the CH_2-stretching (2980 cm^{-1}, Figure 43, c), CH-stretching (2890 cm^{-1}, Figure 43, d) and the C=O -stretching vibration signal (1720 cm^{-1}, Figure 43, e).

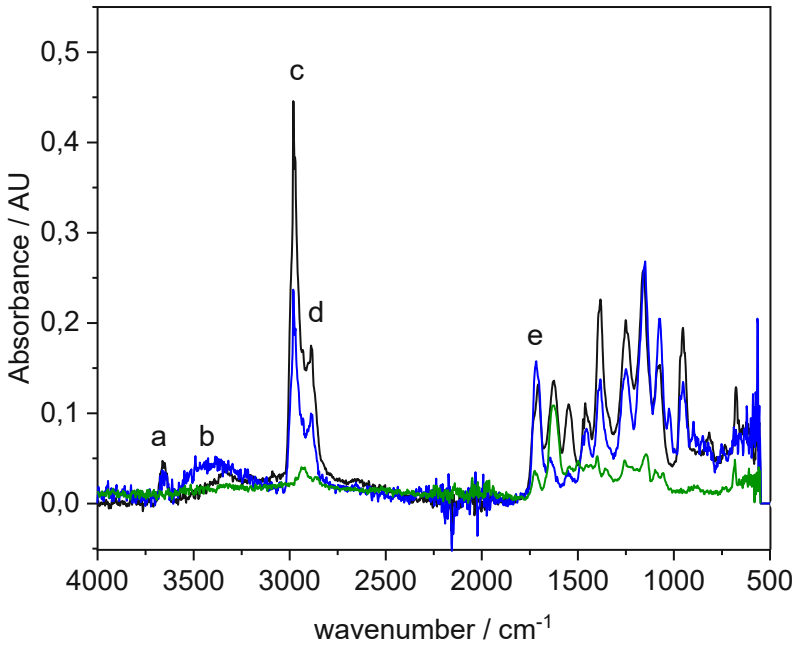

Figure 43: IR spectra of homopolymer **13** (black), DMAA-copolymer **14** (green) and HEMA-copolymer **15** (blue). (a) 3640 cm^{-1} (amide), (b) 3590-3100 cm^{-1} (OH-stretching), (c) 2980 cm^{-1} (CH_2-stretching), (d) 2890 cm^{-1} (CH-stretching, alkane), (e) 1720 cm^{-1} (C=O-stretching).

2.2.3 Synthesis of the lithium-salts of poly(6-acrylamidohexanoicacid) copolymers (16, 17)

Finally, the lithium-salts (Figure 44, Figure 45) were produced in accordance with Leibetseder [58].

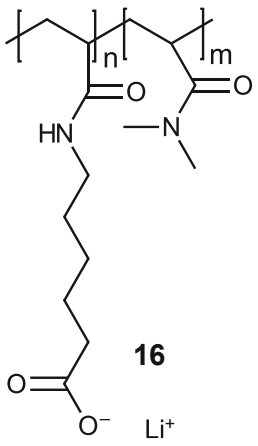

16

Figure 44: Structure of poly(DMAA-co- lithium 6-acrylamidohexanoate) (**16**).

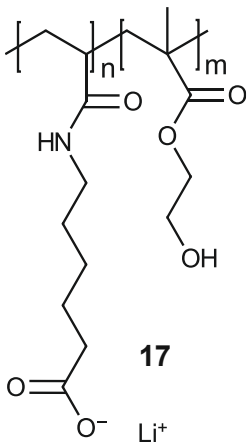

17

Figure 45: Structure of poly(HEMA-co- lithium 6-acrylamidohexanoate) (**17**).

Therefore, 1 eq of the lithium salt of polyacid **14** and **15** was prepared by the reaction with 1 eq of a methanolic lithium hydroxide solution. Polymer **16** (Figure 44) was characterized via ^{1}H-NMR in D_2O and **17** (Figure 45) in CD_3OD. The spectrum of HEMA-copolymer **17** differs from DMAA-copolymer **16** by the additional peaks caused by HEMA at 4.06 ppm, 3.80 ppm. and in the area 1.72-0.85 ppm. The DMAA-copolymer has additional peaks in the area 3.25-2.81 ppm. Both polymers were hard, brittle and insoluble in DMSO.

2.2.4. Synthesis of methyl-6-acrylamidohexanoate copolymers (18, 19)

The corresponding methyl esters **18** (Figure 46) and **19** (Figure 47) were also prepared to compare the properties of these polymers with those of the salts (Polymer **16** and **17**) and carboxylic acids (Polymer **14** and **15**).

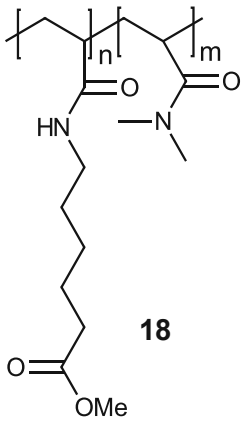

Figure 46: Structure of poly(DMAA-co-methyl-6-acrylamidohexanoate) (**18**).

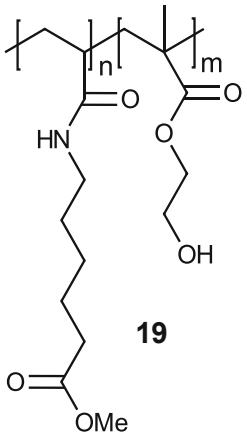

Figure 47: Structure of poly(HEMA-co-methyl-6-acrylamidohexanoate) (**19**).

For polymerization, benzene was always used as solvent and 1 wt% AIBN as initiator. HEMA was used as comonomer in addition to DMAA to investigate the influence of different comonomers. The main difference between the two copolymers was solubility. The HEMA copolymer **19** is less soluble than the DMAA copolymer **18**. DMAA copolymer **18** is a sticky polymer that is highly soluble in acetone, DCM, DMSO, and benzene, but not in water. HEMA copolymer **19** is a yellow sticky polymer, insoluble in DMSO, DCM and benzene.

The TGA thermogram shows that the decomposition of methyl ester **18** starts at about 350°C. The polymer was also characterized *via* ^{1}H-NMR (Figure 48). Compared to monomer **5**, the protons of the acrylic group are no longer visible in the NMR spectrum of polymer **18**, indicating a high conversion in the synthesis of the polymer.

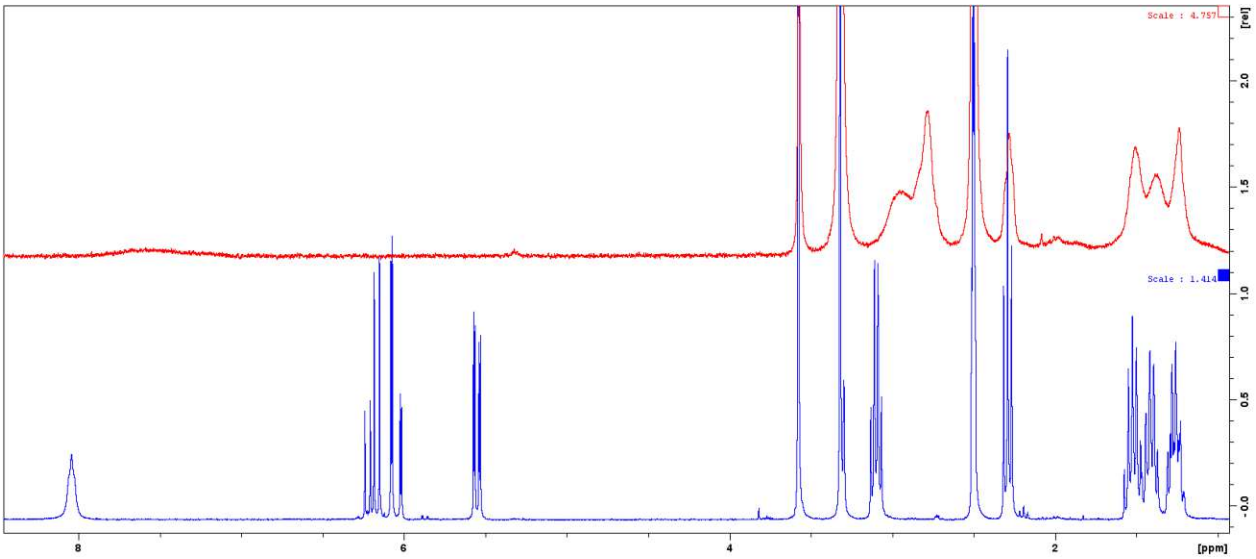

Figure 48: ^{1}H-NMR (300 MHz, DMSO-d_6 = 2.50 ppm, H_2O = 3.33 ppm) of monomer **5** (blue) and the corresponding copolymer **18** (red). The missing protons of the acrylic group in the spectrum of the polymer indicates a high conversion in the polymerization.

The next step is to produce comparable polymers with 12 carbon atoms in the side chain instead of 6 carbon atoms. The additional amide bond to be introduced in the longer side chains is also special. Similar polymers as described above are to be prepared by using the same comonomers and counterions.

3. Brush polymers with amide based C12 side chains

Already at the beginning of this thesis it was decided to prepare monomer **11**, since it has the same number of aliphatic carbons compared to monomer **1**, but has an additional amide bond, which may have an influence on the polymer order. First retrosynthetic considerations suggested synthesizing this molecule *via* acrylamide **5** and the hydrochloride **4** (Figure 49).

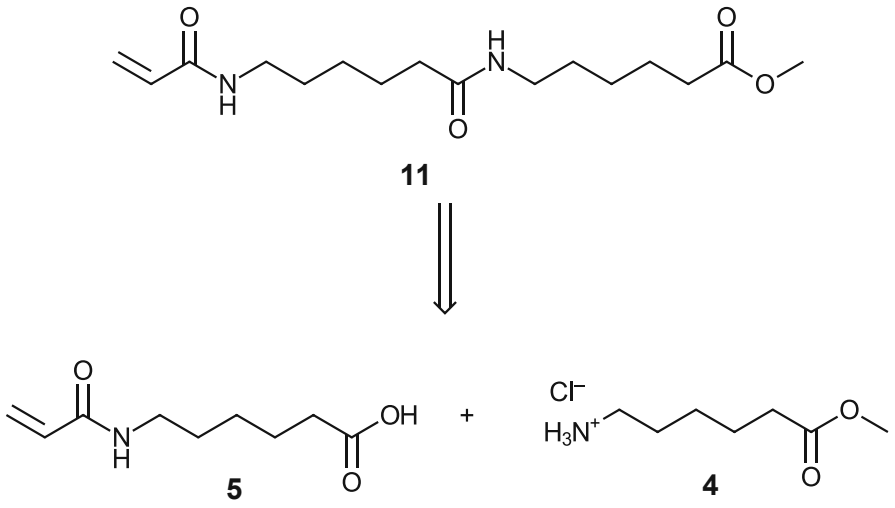

Figure 49: Retrosynthesis of 6-(6-acrylamidohexanamido)hexanoic acid (**11**).

The amide bond formation was the most important reaction during monomer synthesis. To form this bond, the carboxylic acid had to be activated. This can be done by making the more reactive acid chloride. Another possibility is linking the amide bond by using coupling agents. These two options are discussed in the following chapters.

3.1 Monomer synthesis

3.1.1 Synthesis of methyl 6-(6-acrylamidohexanamido) hexanoate (11)

3.1.1.1 Synthesis of methyl 6-(6-acrylamidohexanamido) hexanoate *via* the acid chloride route

Acid chlorides are usually prepared from the corresponding carboxylic acid using thionyl chloride [71]. Other popular possibilities for this synthesis would be, for example, the reaction with another chlorination reagent like oxalyl chloride (milder conditions in contrast to thionyl chloride) or *via* phosphorus chlorides [76].

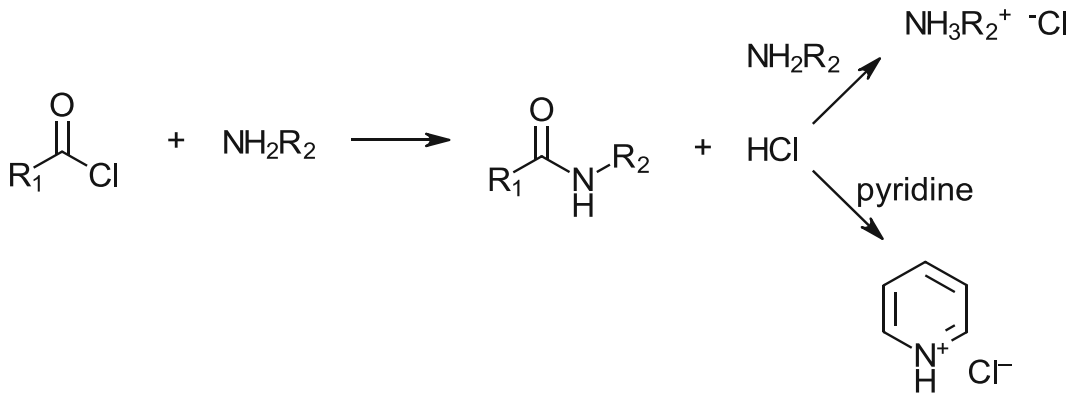

Figure 50: Synthesis of the amide bond with the help of acid chloride. The amine must either be added in excess or additional TEA or pyridine must be added to the reaction solution to ensure complete conversion. The HCl formed during the reaction is bound by pyridine (or TEA). Otherwise, HCl reacts with the amine, which is used as reactant.

For the amide bond formation the acid chloride must be reacted with twice the amount of amine since the resulting hydrochloric acid (HCl) will protonate the unreacted amine, which therefore can no longer react to the amide. Another possibility is to add pyridine (or TEA) to the reaction mixture. Then pyridine reacts with the HCl in place of the reactant (Figure 50) [71].

3.1.1.1.1 Stepwise synthesis of methyl 6-(6-acrylamidohexanamido) hexanoate (11)

The desired monomer **11** can be prepared by using 1 eq carboxylic acid **5** and 1 eq hydrochloride **4** (Figure 51). The synthesis was carried out *via* the intermediate acid chloride of **5** (Figure 52) as described in Bruice [71]. First 3 eq TEA is added to form the free amine of **4**. After formation of the acid chloride of **5** with 1 eq $SOCl_2$, which leads to an activation of the carboxylic acid, the amide bond can be formed.

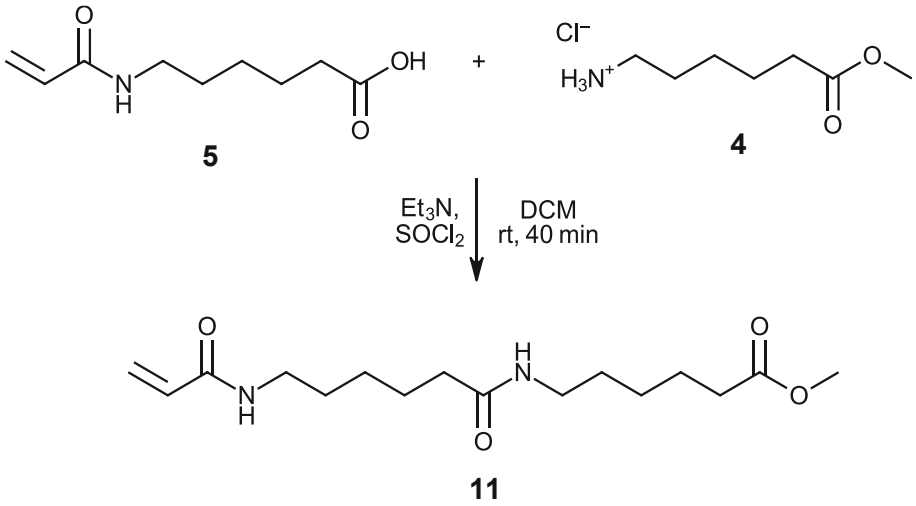

Figure 51: Reaction of **4** and **5** *via* the intermediate acid chloride to **11**. By using TEA, the free amine can be synthesized. Then the amine attacks the activated acid chloride and **11** is formed.

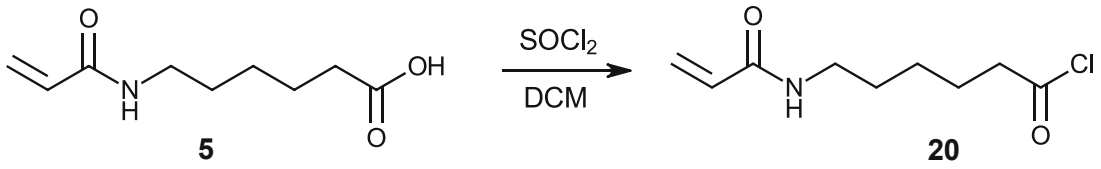

Figure 52: Carboxylic acid **5** reacts with thionyl chloride to form acid chloride **20**. Thus, the carboxylic acid is activated, allowing synthesis with hydrochloride **4** to form monomer **11**.

Since yields were always low, attempts were made to optimize the synthesis by varying the reaction parameters (Table 1). Different solvents and bases were used. In addition, the influence of a stabilizer and different amounts of thionyl chloride were tested. Et_3N and pyridine were used as bases. Better results were obtained with Et_3N. DCM, DCM/DMF, chloroform and pyridine were used as solvents. Since only reactant **4** and the product dissolve in DCM, a few drops of DMF were added to enhance the solubility of acrylamide **5**. However, only the experiments with DCM as solvent were successful. Furthermore, 4-methoxyphenol (MEHQ) was added as a stabilizer (No.4 and No.5), due to the rapid polymerization of such acrylamides. However, no significant difference could be observed compared to the synthesis without MEHQ. In addition, higher yields were obtained when using an excess of thionyl chloride during the synthesis (No.1).

Table 1: Varying synthesis parameters in the acid chloride activated formation of monomer **11**.

No.	$SoCl_2$ / eq	4 / eq	5 / eq	solvent	base	stabilizer	yield / %
1	1.5	1	1	DCM	Et_3N	-	24
2	1	1	1	DCM	Et_3N	-	16
3	1	1	1	DCM/DMF	Et_3N	-	-
4	1	1	1	DCM	Et_3N	MEHQ	16
5	1	1	1	DCM	pyridine	MEHQ	2
6	1	1	1	chloroform	Et_3N	-	-
7	1	1	1	pyridine	pyridine	-	-

The experiments described in No. 1, 2, 4 and 5 led to the desired product. However, only 2 % of product could be observed when using pyridine as base (No.5). The experiments described in No. 3, 6 and 7 were not successful. The best result was achieved when using Et_3N as base and DCM as solvent. No increase in yield could be observed after the addition of MEHQ. The yield could only be influenced by different amounts of thionyl chloride. Compared to No.2, there is an increase of 50 % in yield when using 1.5 eq $SOCl_2$ (No.1).

Product **11** was identified *via* ^{1}H-NMR (Figure 53).

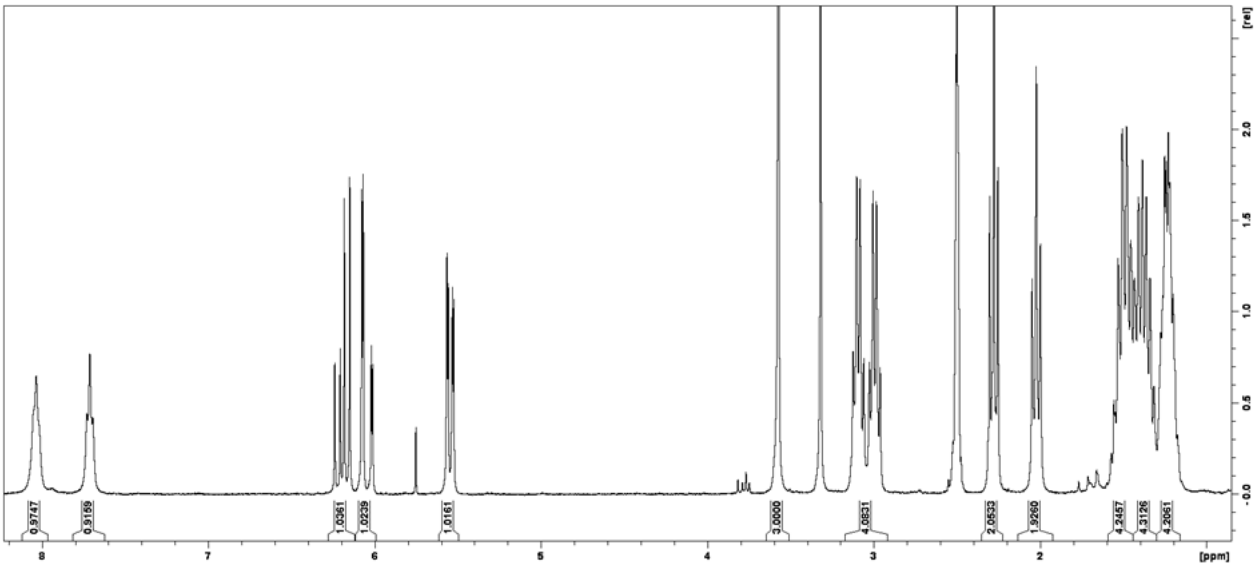

Figure 53: ^{1}H-NMR (300 MHz, DMSO-d_6 = 2.50 ppm, H_2O = 3.33 ppm) of **11**. The spectrum shows all characteristic signals of the compound.

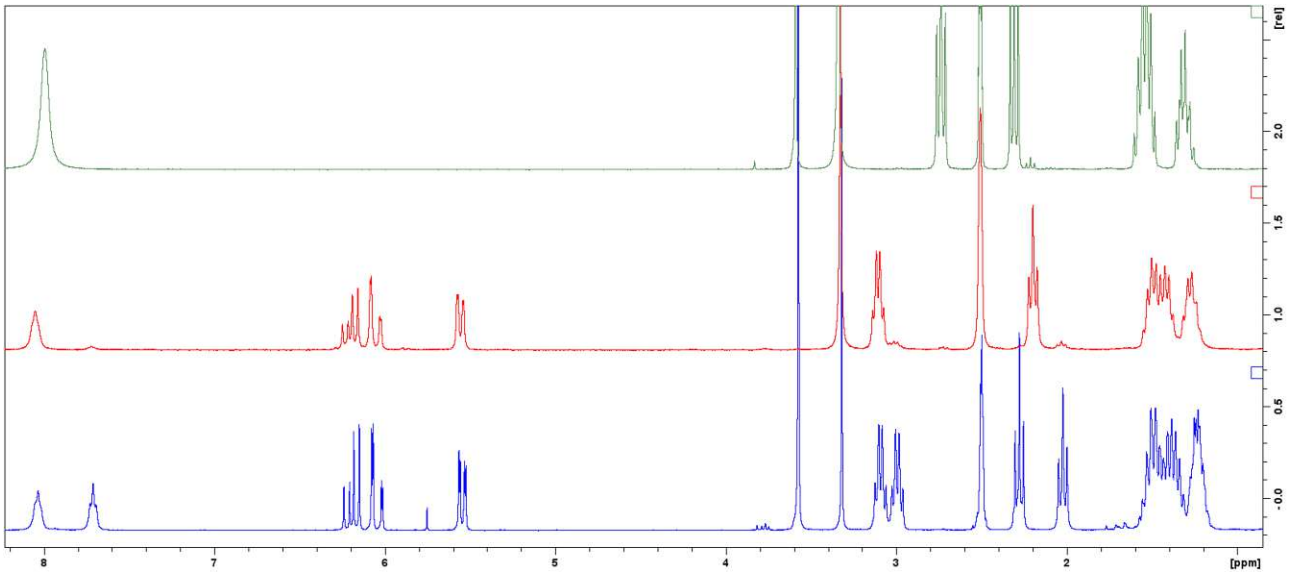

Figure 54: Comparison of the ^{1}H-NMR spectra (300 MHz, DMSO-d_6 = 2.50 ppm, H_2O = 3.33 ppm) of reactant **4** (green), **5** (red) and product **11** (blue). In the spectrum of the product all signals are assignable to the substance-specific groups. The two amide signals at 8.03 ppm and 7.71 ppm indicate the formation of **3**. The amide signal at 7.71 ppm corresponds to the newly formed amide bond during the synthesis.

The amide signal at 7.71 ppm corresponds to the new formed amide bond. Since there is an overlap of the amide peaks of product **11** and reactant **5**, the integrals can be used to determine whether residual reactant is still present (Figure 54). If the conversion is complete, the two amide signals of the product are present in a ratio of 1:1. If this is not the case (Figure 55), any reactant still present can be separated from the final product by additional extraction steps (Figure 56).

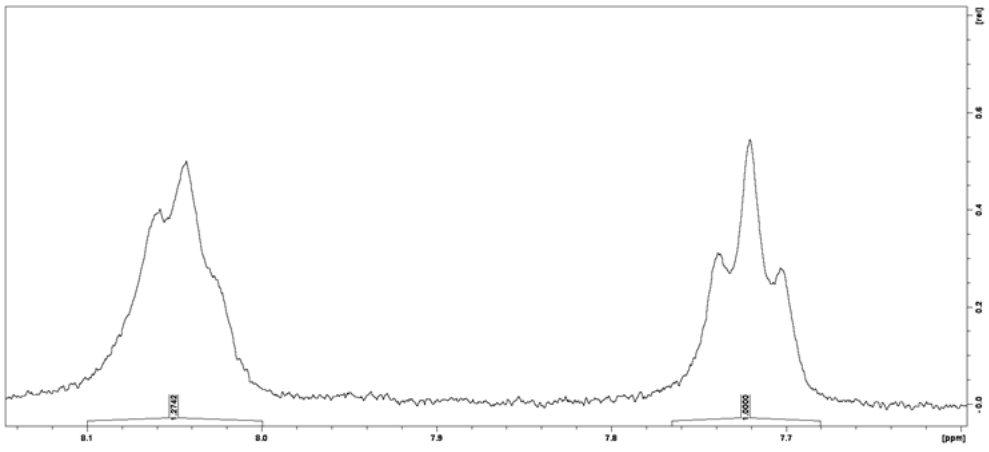

Figure 55: Section of the ^{1}H-NMR spectrum (300 MHz, DMSO-d_6 = 2.50 ppm) of **11** before further workup. The two amide signals are not in the same ratio. Therefore, it can be concluded that there is still residual reactant **5** in the final product.

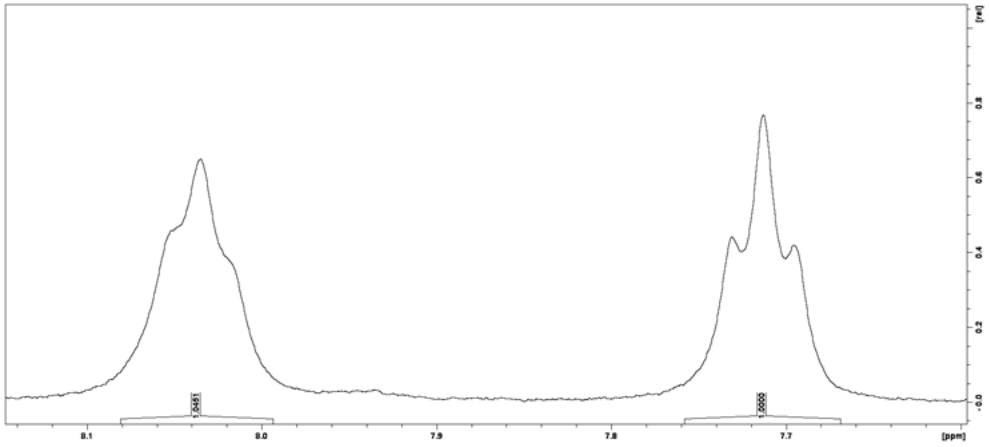

Figure 56: Section of the ^{1}H-NMR spectrum (300 MHz, DMSO-d_6 = 2.50 ppm) of **11**. After further extraction steps, the remaining reactant **5** was successfully separated. The two amide signals are now present in a ratio of about 1:1. It is assumed that there is no more reactant in the product.

The two NMR spectra from Figure 55 and Figure 56 differ due to different workup procedures of the product. After recording the NMR spectrum of the crude product **11** (Figure 55), the product was dissolved in DCM again. The solution was then extracted three times with Na_2CO_3 (20 g/L) and the remaining solvent was removed on the rotary evaporator. Then the NMR spectrum of the purified product was recorded (Figure 56). Due to the additional extraction, the ratio of the amide peaks is almost 1:1. Therefore it can be concluded that the residual reactant is completely separated.

3.1.1.1.2 One-pot synthesis of methyl 6-(6-acrylamidohexanamido) hexanoate (11)

According to Leggio *et al.* [77] secondary and tertiary amides can be prepared *via* one-pot synthesis (Figure 57). This type of synthesis was used in the reaction of **4** with **5**, whereby the acid chloride is also formed first before the amide bond can be formed.

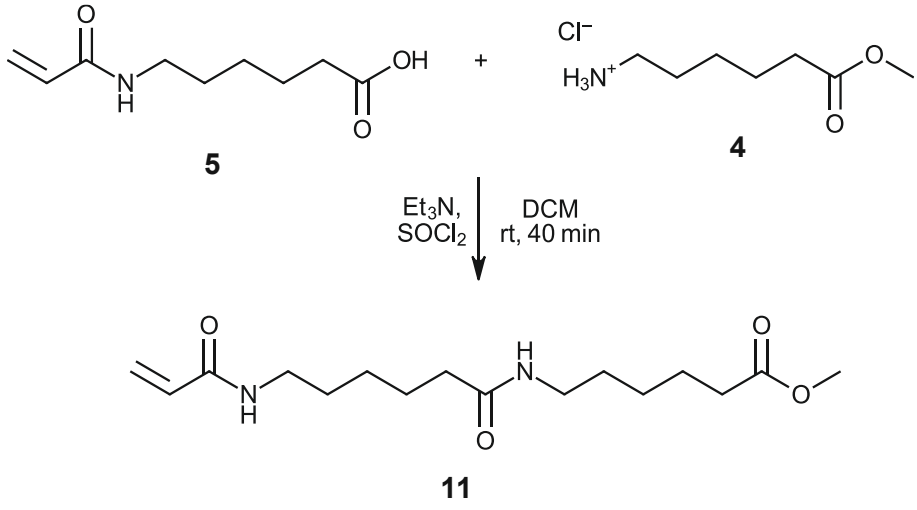

Figure 57: Reaction of **4** and **5** *via* a one-pot synthesis. Amide **4** and carboxylic acid **5** react to product **11** *via* the intermediate acid chloride.

The yield increased as expected in contrast to the yield obtained by the classical synthesis *via* the acid chloride. Due to the convenience of this one-pot synthesis, this procedure was chosen for the formation of monomer **11**. In contrast to reference [77], the reaction time was extended from 20 min to 40 min as this maximized the yield.

However, since maximum yields of 24 % were achieved *via* the acid chloride, another synthetic route was chosen for the monomer. Another possibility to synthesize monomer **11** is by the usage of coupling agents.

3.1.1.2 Synthesis of methyl 6-(6-acrylamidohexanamido) hexanoate (11) *via* coupling agent

The aim of this synthesis was to produce the same molecule as described before *via* the acid chloride route. However, the yield was desired to be drastically improved in order to be able to easily produce enough material for polymerization. *N*,*N*'-dicyclohexylcarbodiimide (DCC) is often used in peptide synthesis and is used as a carboxyl activating agent [71,78]. The resulting reactive ester then reacts with an amine to form the corresponding amide. DCC must be used in stoichiometric amounts and the reaction produces *N*,*N*''-dicyclohexylurea (DCU) as a by-product [71]. In addition, 4-(dimethylamino)pyridine (DMAP) is used in catalytic amounts [79]. By contact with water, DCC reacts to form the urea DCU [80]. With the help of DCC, the amide bond can be formed under milder conditions than *via* the acid chloride (Figure 58) [81].

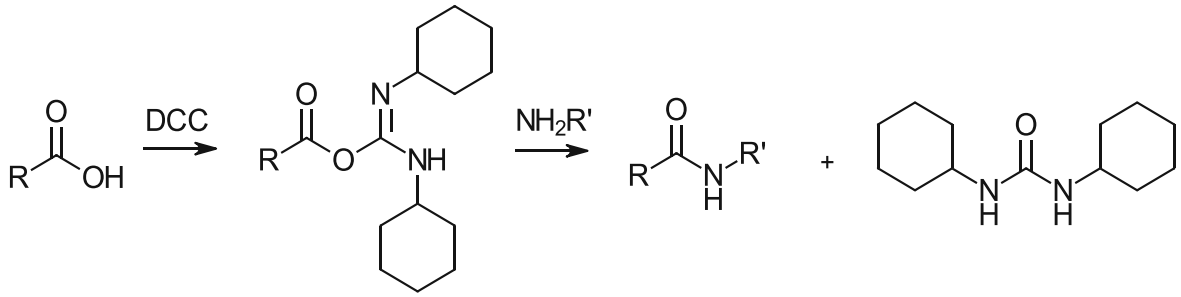

Figure 58: Preparation of the amide bond with the aid of the coupling agent DCC. First, the carboxylic acid reacts with DCC. The reaction with an amine results in the formation of the amide and the urea DCU is formed as a by-product.

As an alternative to DCC, benzotriazole-1-yloxytris(dimethylamino)phosphonium hexafluorophosphate (BOP) or the water-soluble 1-ethyl-3-(3-dimethylaminopropyl) carbodiimide (EDC) could also be used [80]. One of the main advantages of EDC is that the urea formed can be separated more easily [82].

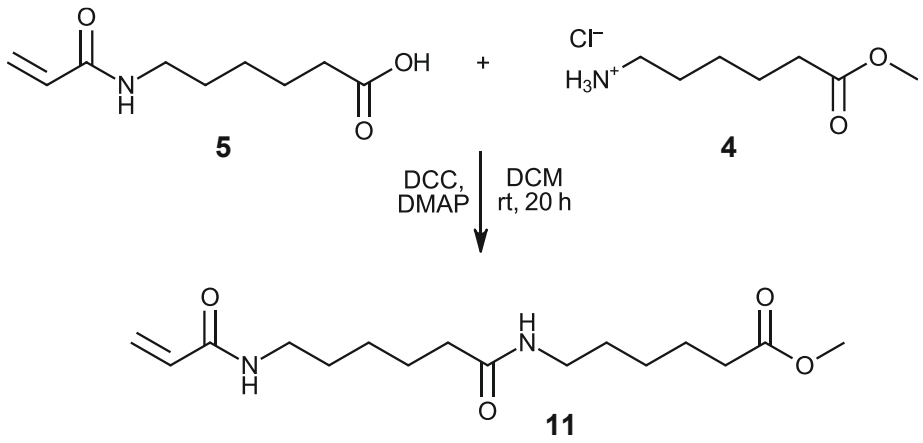

Figure 59: Synthesis of methyl 6-(6-acrylamidohexanamido) hexanoate (**11**) *via* DCC as coupling agent.

DCC activates the carboxylic acid, making it more reactive to form the desired amide with the amino group of **4** (Figure 59). The reaction was carried out in accordance with Neises and Steglich [79]. Therefore, 1 eq DCC was reacted with 1 eq acrylamide **5**. In addition, 1 eq of the hydrochloride **4** reacted with 3 eq of TEA. After the carboxylic acid, activated with DCC, and the free amine were obtained, the amide bond could be formed. The urea DCU formed during the reaction is mostly insoluble in DCM and can be separated by filtration after the reaction. Therefore, the product was purified by extraction with HCl and a Na_2CO_3 solution (20 g L^{-1}). A white solid was always formed at the phase interface. NMR analysis was used to determine if it was the product. The signals in the ^{1}H-NMR spectrum indicate that it is a mixture of product, reactants and DCU (Figure 60). The signals at 8.21 ppm and 1.81-1.56 ppm can be assigned to DCU. At 8.03 ppm the signals of the product and reactant **5** and at 5.56 ppm and 1.56-0.95 ppm the signals of DCU, product and reactant are superimposed. Therefore, increasing the solvent volume during the extraction step significantly reduced this interface and increased the overall yield of the purified product **11**.

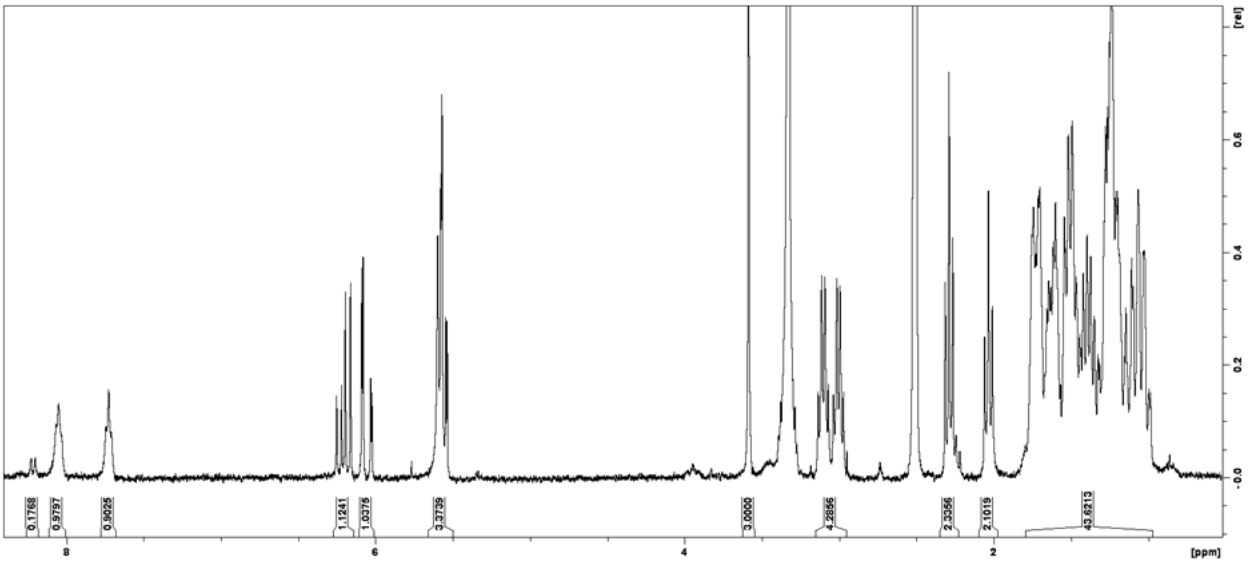

Figure 60: ^{1}H-NMR (300 MHz, DMSO-d_6 = 2.50 ppm, H_2O = 3.33 ppm) of the isolated solid between the organic and aqueous phase during extraction. This is a mixture of product, reactants and DCU (8.21 ppm, 1.81-1.56 ppm). The signal at 8.03 ppm is assigned to the product **11** and reactant **5** and the signals at 5.56 ppm and 1.56-0.95 ppm to DCU, product and reactant.

Usage of dry DCM showed an increase in yield by over 10 %. While using non-absolute DCM the yield was around 58 %, working completely anhydrous increased the yield to over 70 %. This is caused by the water sensitivity of DCC. Therefore, all experiments were conducted water-free by heating out the flasks and using dry solvents. The monomer **11** was fully characterized by ^{1}H-NMR, ^{13}C-NMR, COSY, HSQC, HMBC and IR spectroscopy.

Comparing the final products of the synthesis of monomer **11**, which was prepared on the one hand by using DCC and on the other hand, *via* the acid chloride, additional signals in the ^{1}H-NMR spectrum are found (Figure 61). The incomplete separation of the DCU results in additional signals in the range of 1.81-0.95 ppm and 8.21 ppm in the spectrum. Otherwise, the products do not differ either in spectra or in their appearance.

The by-product DCU, which is formed during the coupling reaction with DCC, can be separated by filtration. However, DCU is always a bit soluble in most organic solvents, therefore, residues of DCU can still be found in the final product and its NMR spectrum.

Instead of DCC, other coupling agents such as EDC could have been used for activation. One advantage of EDC over DCC is the easier separation of the by-product. The urea formed in the reaction with EDC is for example soluble in water and can therefore be completely removed from the product by dissolution. Regarding the high cost difference between DCC and EDC this thesis focused on the use of DCC.

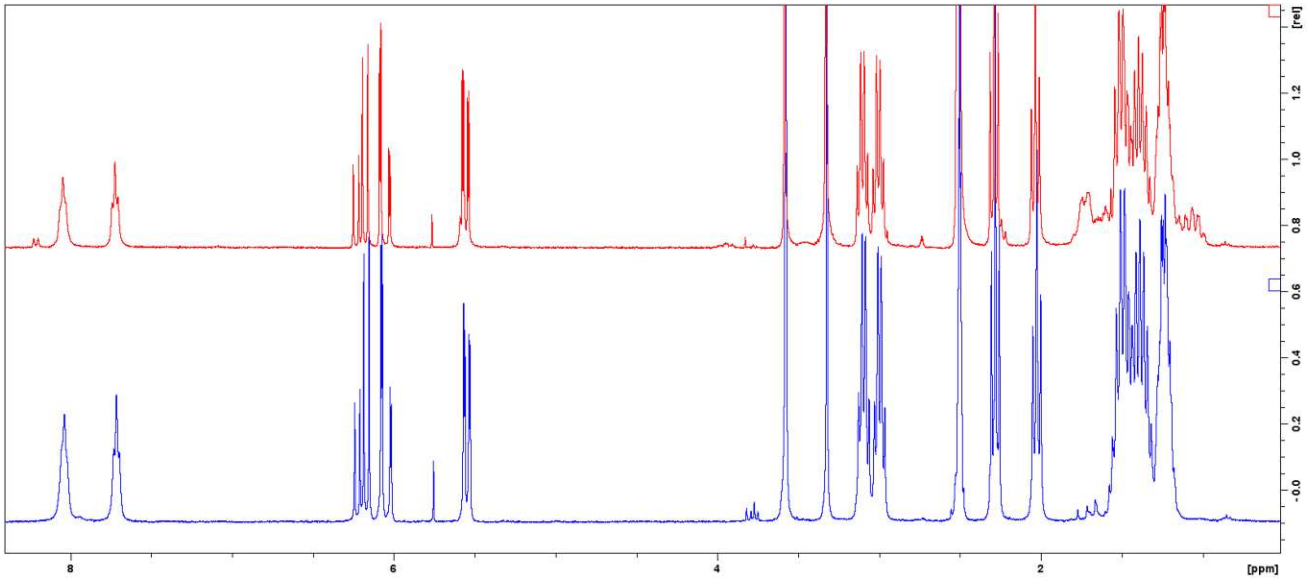

Figure 61: Comparison of the synthesized monomer **11** using DCC (red) and thionyl chloride (blue). The products do not differ in their appearance. The NMR spectrum shows additional signals in the range 1.81-0.95 ppm and at 8.21 ppm. These signals are caused by the DCU formed during the reaction. Most of the DCU can be separated by filtration, but residues of it still remain in the product.

The melting point of product **11** was measured on the Kofler hot stage microscope. Most of the sample melts at 55 °C, but there are small grains still visible in the melt (Figure 62).

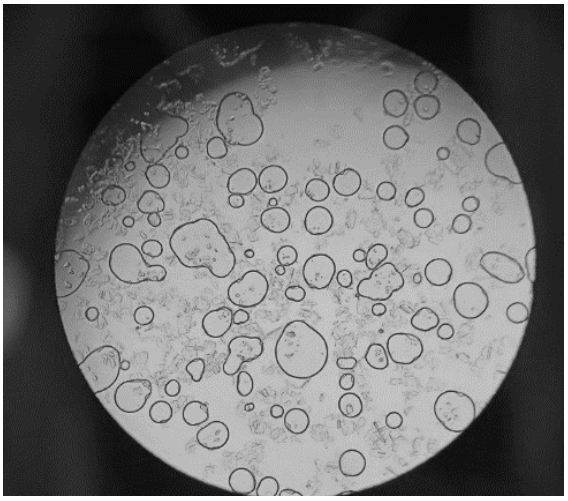

Figure 62: Image of the melt of product **11**. The sample was heated on the Kofler hot stage microscope. Most of the product melts at 55 °C. However, up to 150 °C small not melted particles still remained in the melt. Therefore, it was assumed that these were residues of DCU (melting point 232-233 °C).

It is assumed that these particles were residual DCU. The assumption is confirmed, since even at temperatures above 150 °C small not melted particles were still visible. The melting point of DCU is 232-233 °C [83]. However, the sample was not heated to such a high temperature as the remaining sample began to decompose and made a reliable measurement impossible.

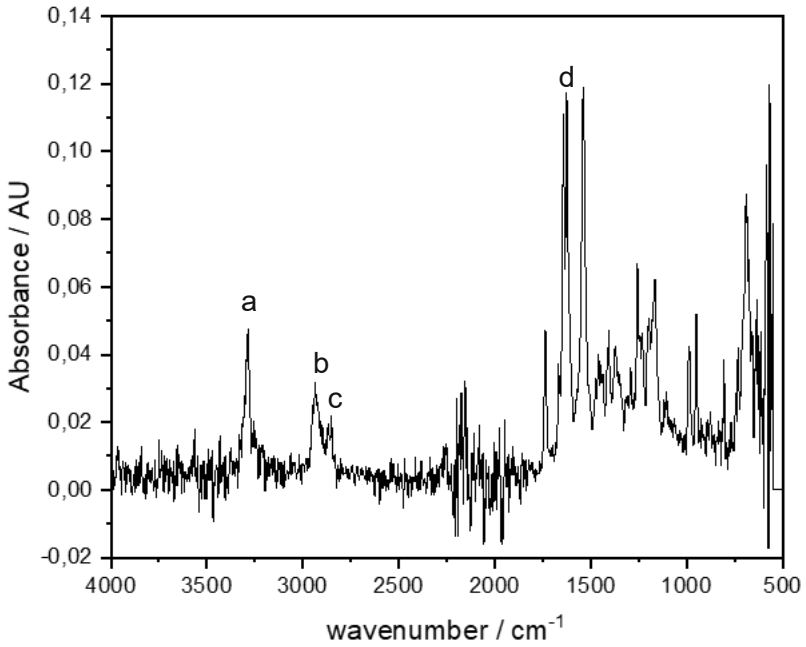

Figure 63: FTIR-ATR spectrum of monomer **11**. (a) 3288 cm^{-1} (amide), (b) 2939 cm^{-1} (CH_2-stretching), (c) 2852 cm^{-1} (CH-stretching, alkane), (d) 1736 cm^{-1} (C=O stretching, ester), 1643 cm^{-1} (secondary amide), 1626 cm^{-1} (monosubstituted alkene), 1164 cm^{-1} (C-O-stretching, ester).

In the IR spectrum, all signals are assignable to the substance-specific groups (Figure 63). The sharp signal at 3288 cm^{-1} is indicative of an amide. In addition, the CH_2 stretching vibration at 2939 cm^{-1} proofs the methylene-chains. The signal at 1736 cm^{-1} is caused by the C=O stretching vibration of the ester. In addition, the signal at 1643 cm^{-1} indicates a secondary amide.

Compound **11** was fully characterized with ^{1}H-NMR, ^{13}C-NMR (APT), HSQC, HMBC and COSY. Figure 64 shows the ^{13}C-NMR and Figure 65 the corresponding COSY.

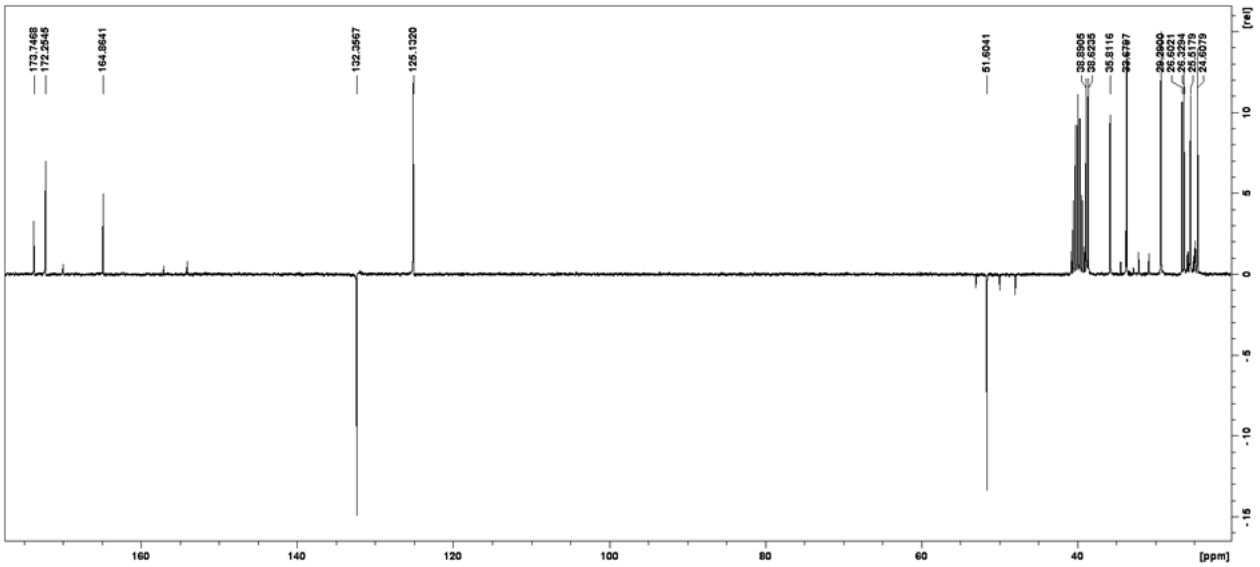

Figure 64: APT ^{13}C-NMR (75 MHz, DMSO d_6 = 40.0 ppm) spectrum of monomer **11**.

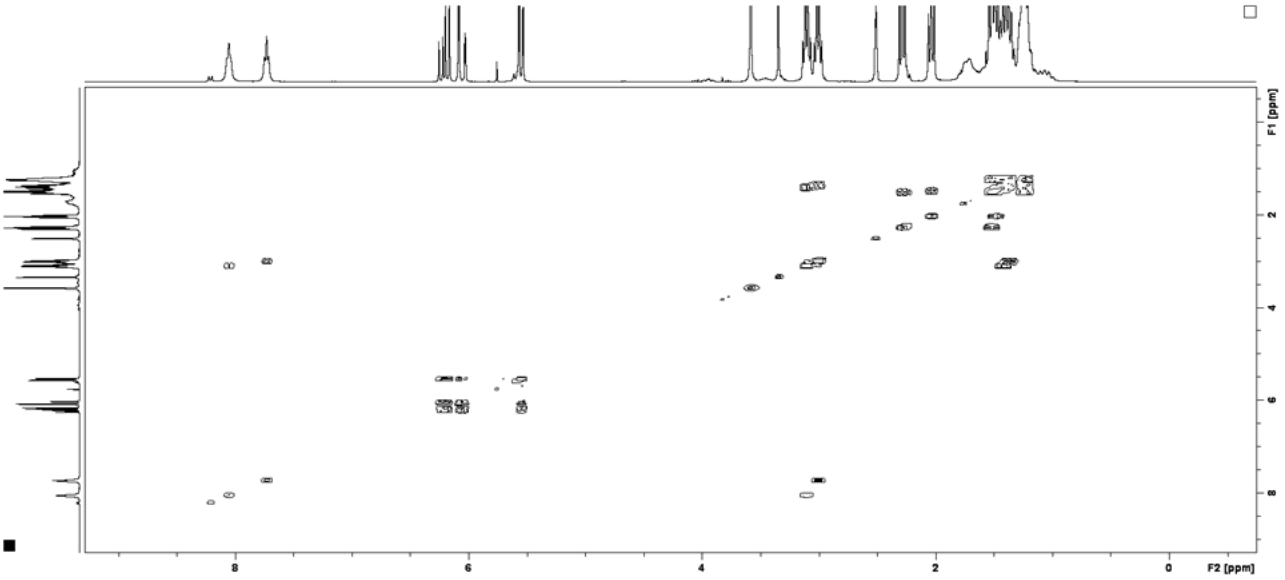

Figure 65: H,H COSY-spectrum of monomer **11**.

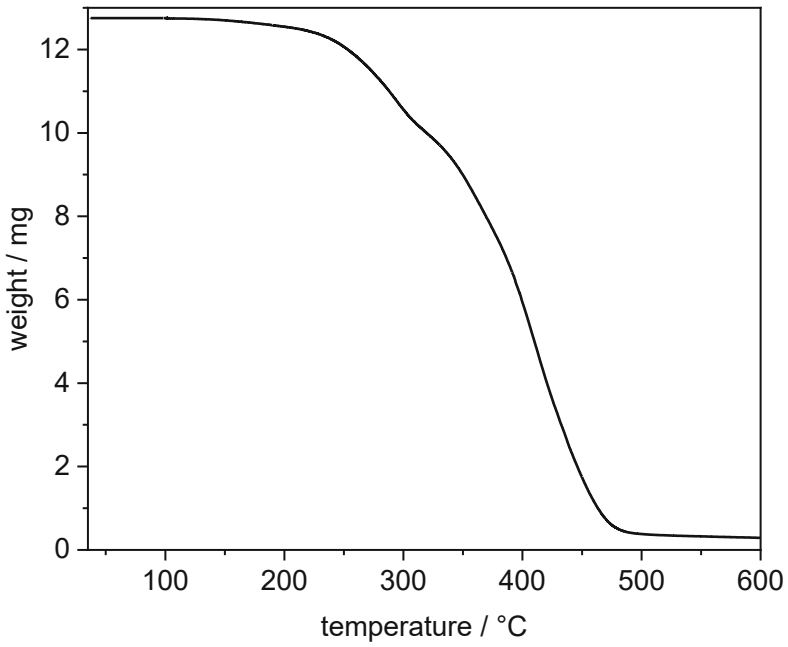

Figure 66: TGA of monomer **11**. The two-stage decomposition of the product takes place in the range of 160-475 °C.

The TGA thermogram shows that the product does not contain any water or volatile solvent residuals (Figure 66). Otherwise, there should be a decrease in the graph at about 100°C. Additionally, decomposition starts at about 160 °C and at 475 °C the sample has lost 95.3 % of its mass. Also visible is the step in the decomposition curve at 313 °C. This indicates that at this temperature, a part of the molecule splits off before decomposing further.

3.1.2 Synthesis of methyl 6-(11-acrylamidoundecanamido) hexanoate (21)

Instead of acrylamide **5**, an attempt was also made to link acrylamide **1** and hydrochloride **4** *via* an amide bond (Figure 67).

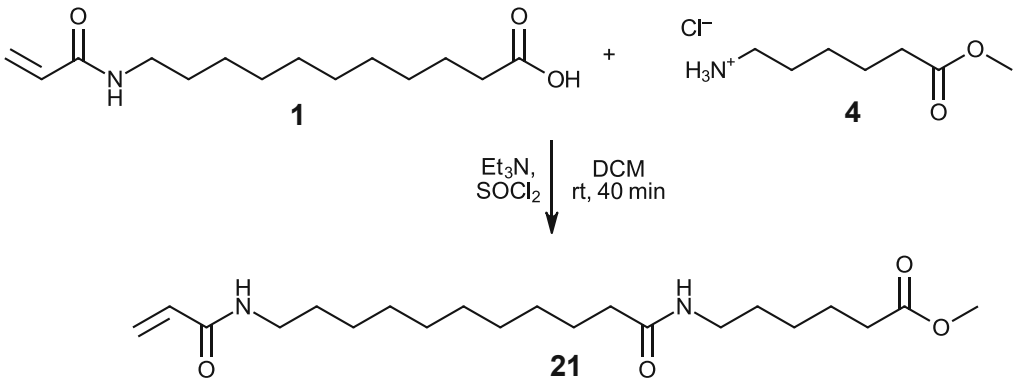

Figure 67: Synthesis of methyl 6-(11-acrylamidoundecanamido) hexanoate **21** *via* the acid chloride activation.

The procedure is identical to the one used for the synthesis of monomer **11** *via* the one-pot synthesis. 1 eq of acrylamide **1** and 1 eq of hydrochloride **4** were mixed. Then 3 eq of TEA were added and finally 1.5 eq of $SOCl_2$ were dropped to the reaction mixture. Noticeable was the obtained higher yield of 46 % under the same reaction conditions. However, the ratio of the amide signals in the NMR spectrum revealed that there is still about 50% reactant **1** in the product. Comparable to the workup of monomer **11**, the crude product **21** can be purified by additional extraction steps.

Nevertheless, yields higher than 46 % could not be achieved and no further optimization was performed on this synthesis pathway as the focus lay on the production of monomer **11** and its polymers.

3.2 Polymerization

3.2.1 Polymerization of methyl 6-(6-acrylamidohexanamido) hexanoate

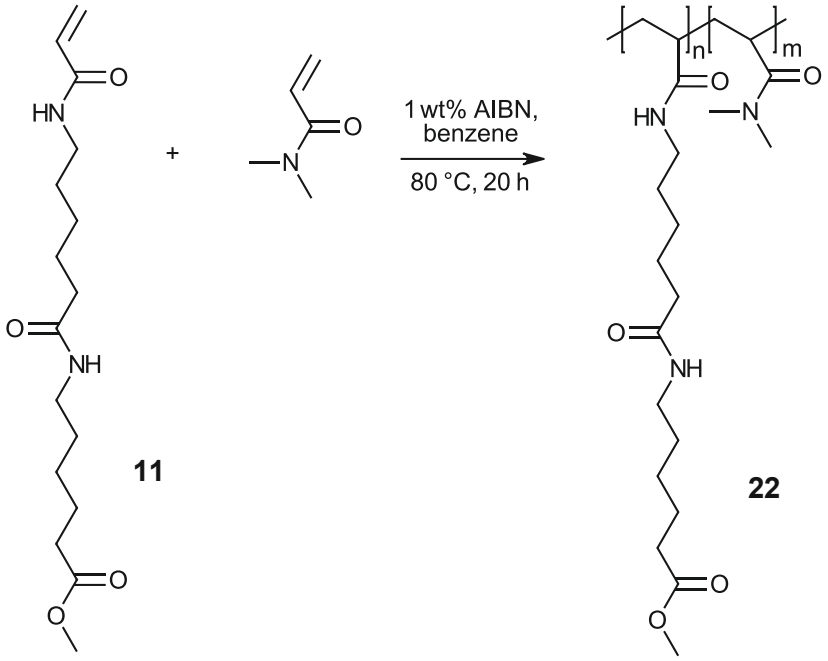

Figure 68: Synthesis of poly(DMAA-co-methyl 6-(6-acrylamidohexanamido)hexanoate) (**22**).

Polymerization experiments with acrylamide **1** are already described in a master´s thesis [58]. The polymerization of these materials works best in benzene. Therefore, benzene was chosen as the solvent for the synthesis of poly(DMAA-co-methyl 6-(6-acrylamidohexanamido)hexanoate) **22** (Figure 68). Attempts were also made to carry out the polymerization in water, methanol and DMF to avoid the harmful benzene.

During the polymerization of monomer **11**, various reaction parameters were varied. Different solvents, initiators, concentrations and reaction times were chosen (Table 2).

Table 2: Synthesis of polymer **22** with different reaction parameters.

No.	*n* 11 / mmol	*n* DMAA[1)] / mmol	solvent / 20 mL	Initiator / 1 wt%	time / h	temperature / °C	yield / %
1	1.6	1.5	DMF	AIBN	20	80	-[2)]
2	1.6	1.5	Methanol	AIBN	20	64	-
3	1.6	1.5	Water	3%APS 20 µL TEMED	20	75	78
4	1.6	1.5	Benzene	AIBN	2	80	59
5	1.6	1.5	Benzene	AIBN	20	80	81

[1)] DMAA: *N*,*N*-dimethylacryl amide

[2)] Yield was not determined

By varying the parameters, it was possible to determine what was best for the preparation of polymer **22**.

3.2.1.1 Polymerization in DMF

Polymer **21** was obtained by polymerization in DMF followed by precipitation in 0.5 N HCl. The yield was not determined in this experiment because only very small amounts of polymer were obtained. Polymerization with DMF as solvent is therefore not suitable for monomer **11**.

3.2.1.2 Polymerization in water

With water as solvent, a different initiator had to be used due to the insolubility of AIBN. Instead, 3 wt% ammonium persulfate (APS) and 20 µL tetramethylethylenediamine (TEMED) were used. The main problem with polymerization in water was the insolubility of monomer **11**. During polymerization, it could be seen that the polymer had trapped unreacted monomer. This prevented the remaining monomer particles from reacting to form the desired polymer. To solve this problem, the solubility of the monomer in water must be increased. Further research was conducted on this topic as part of a bachelor's thesis. The aim of this work was to optimize the polymerization of such monomers in water.

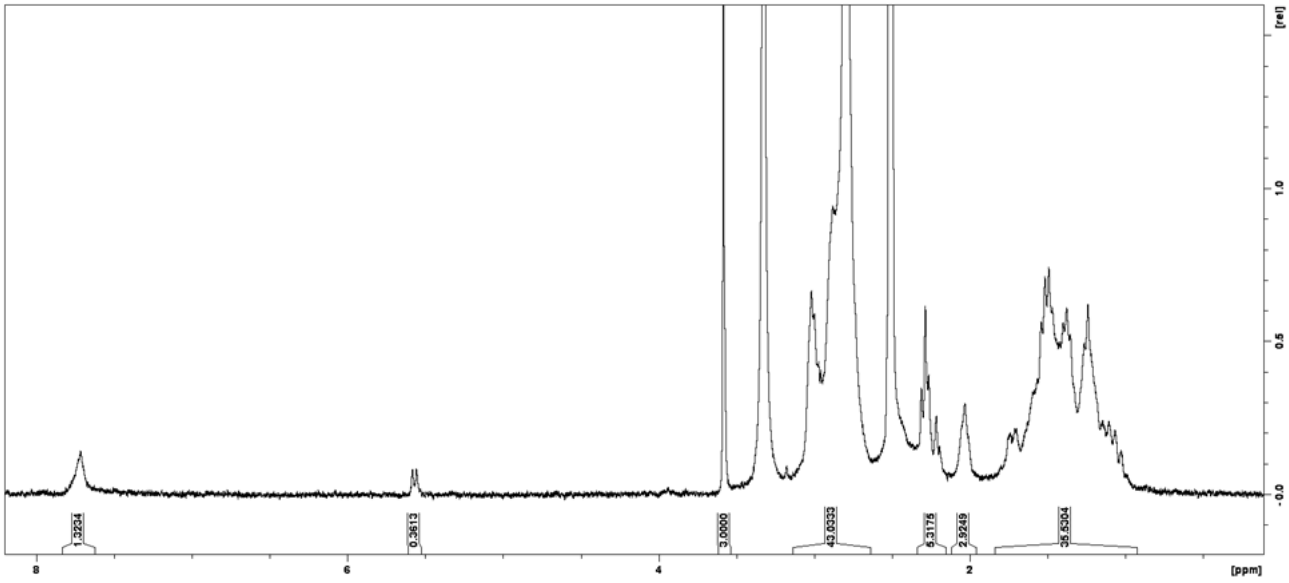

Figure 69: ^{1}H-NMR spectrum (300 MHz, DMSO-d_6 = 2.50 ppm, H_2O = 3.33 ppm) of **22** synthesized *via* polymerization in water. The spectrum shows that the DMAA concentration in the polymer is higher than the concentration of monomer **11**.

The ^{1}H-NMR spectrum (Figure 69) shows, that the intensities of the signals in the range of 3.17-2.63 ppm and 1.82-0.93 ppm are too high because more DMAA is present in the polymer. The DCU signals also overlap with these signals and DCU is additionally responsible for the signal at 5.57 ppm. In this thesis, the polymerization in water was not further investigated.

3.2.1.3 Polymerization in benzene

The highest yield was obtained with polymerization in benzene. Different concentrations of monomer and initiator were tested. The polymerization time was always around 20 h at 80 °C.
A special feature of polymer **22** was the different properties when using different monomer concentrations during polymerization. The polymerization was carried out as described in Table 2 No. 5. However, it was also attempted to perform the polymerization under the same conditions but with only 10 mL benzene, providing polymers with very special properties. In water they are insoluble and in most other solvents, such as DCM, tetrahydrofuran (THF), dimethyl sulfoxide (DMSO) or benzene, a reversible swelling behavior can be observed. After drying, the polymer was white, hard and brittle. In benzene, for example, it became transparent and increased significantly in size and weight. In addition, the polymer was now gel-like. Afterwards, the polymer could be completely dried again and the swelling process can be repeated. This special property allows these substances to be used, for example, as solvent-dependent actuators.

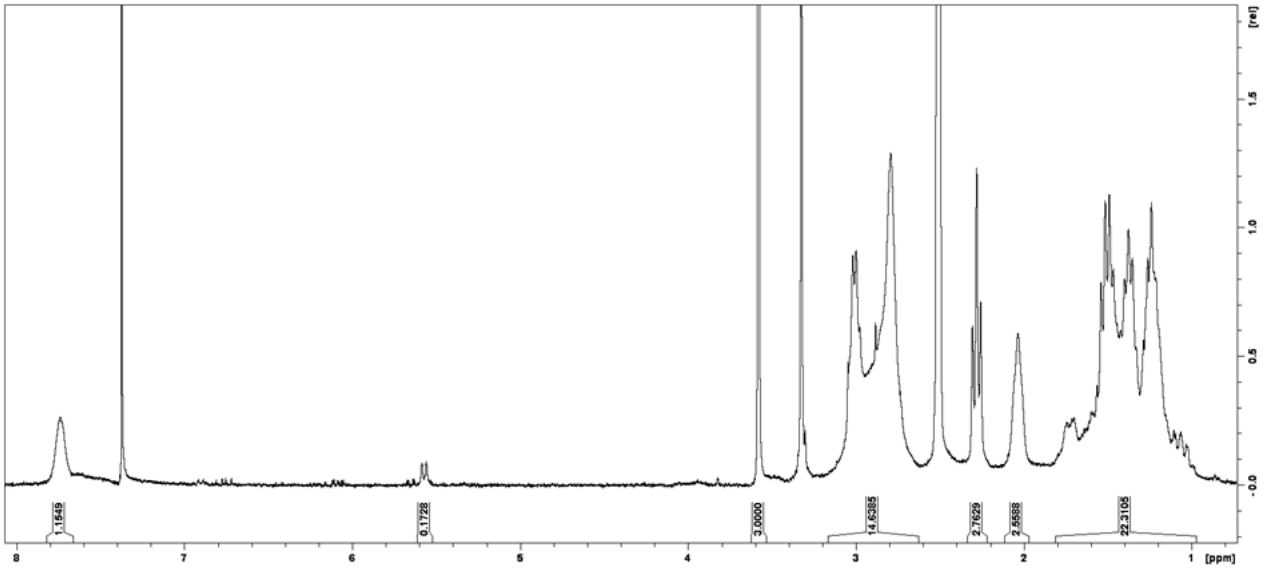

Figure 70: ^{1}H-NMR spectrum of (300 MHz, DMSO-d_6 = 2.50 ppm, H_2O = 3.33 ppm, benzene = 7.37 ppm) **21** synthesized *via* polymerization in benzene. The spectrum shows an additional peak at 7.37 ppm caused by benzene. The DMAA concentration in the polymer is not as high as after polymerization in water.

In the ^{1}H-NMR spectrum (Figure 70), the signals in the range of 3.17-2.63 ppm and 1.82-0.93 ppm can be assigned to DMAA. In the spectrum of the polymer prepared in benzene, the DMAA signals are not as intense as the DMAA signals in the spectrum of the polymer prepared in water. Therefore, it can be concluded that three times more DMAA is incorporated into the polymer during polymerization in water. In this spectrum also an additional peak can be detected at 7.37, which is caused by residual benzene.

With TGA, the thermal stability was investigated (Figure 71). Decomposition starts at 160°C. The two-stage decomposition is again clearly visible. At 320° the inflection point is reached, and the ester is split off.

In the IR spectrum, all signals are assignable to the substance-specific groups (Figure 72).

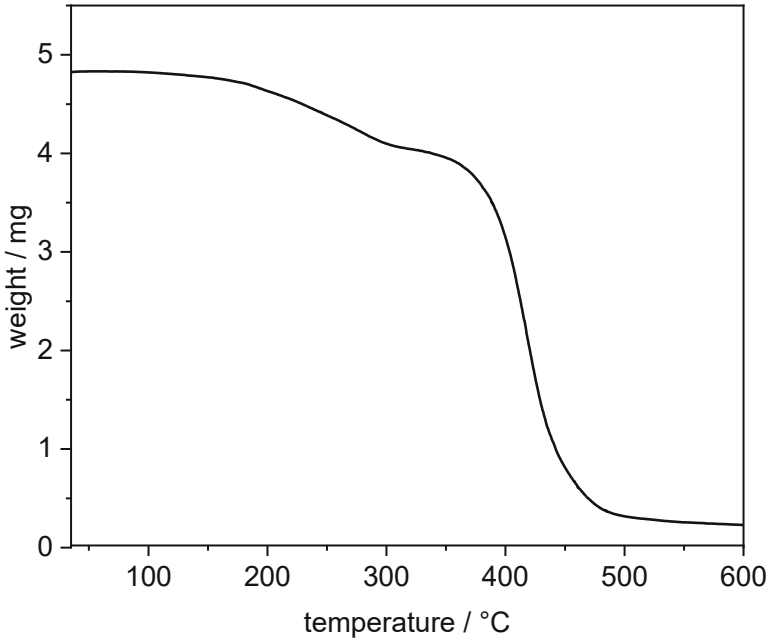

Figure 71: TGA thermogram of polymer **22**. Decomposition takes place in the temperature range of 160-490 °C.

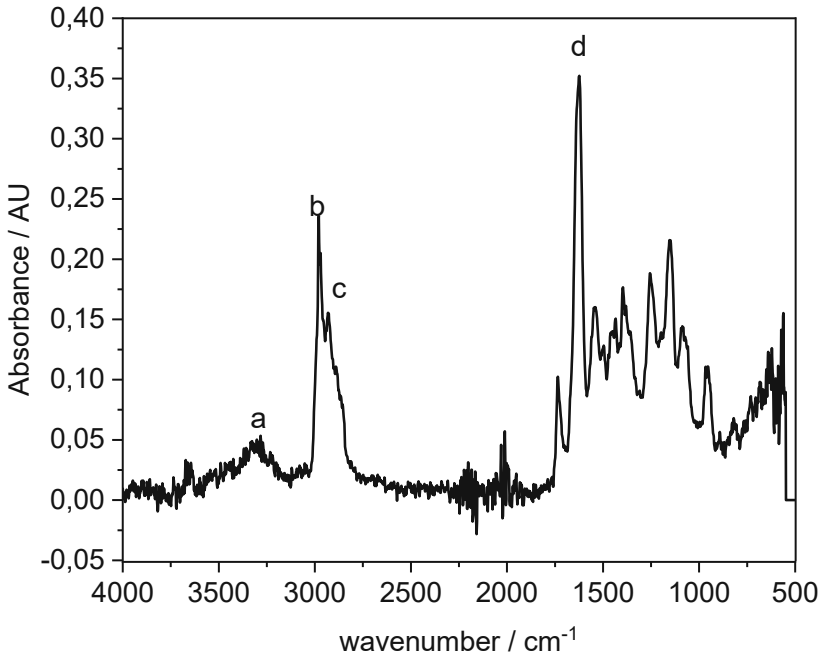

Figure 72: FTIR-ATR spectrum of Polymer **22**. (a) 3290 cm^{-1} (amide), (b) 2927 cm^{-1} (CH_2-stretching), (c) 2858 cm^{-1} (CH-stretching, alkane), (d) 1735 cm^{-1} (C=O-stretching, ester), 1626 cm^{-1} (secondary amide), 1437 cm^{-1} (CH-bending, methyl group), 1165 cm^{-1} (C-O-stretching, ester).

In summary, the desired polymer **22** could be synthesized with benzene, water and DMF as solvents,. For synthesis with DMF, the conversion was so low that no yield of the product was determined. The synthesis in methanol was not successful. However, the best yield was obtained with polymerization in benzene.

3.2.2 Saponification of poly(DMAA-co-methyl 6-(6-acrylamidohexanamido)hexanoate)

After polymerization, saponification of the methyl ester was carried out in accordance with Leibetseder [58].

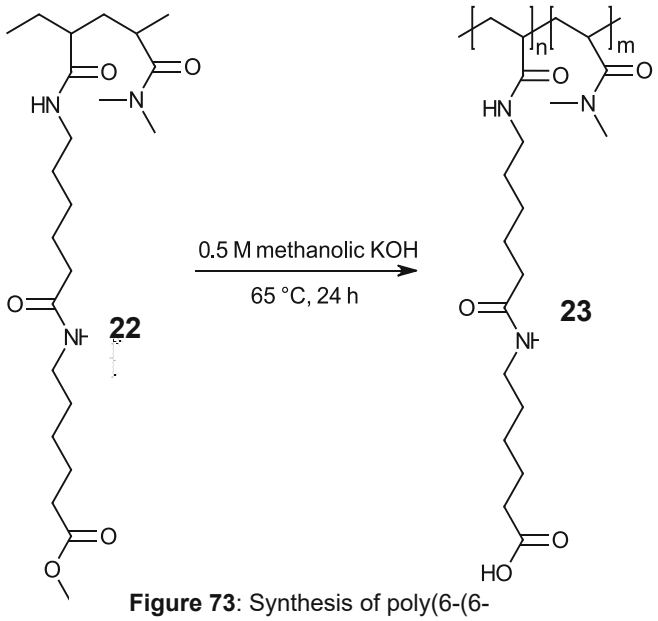

Figure 73: Synthesis of poly(6-(6-acrylamidohexanamido)hexanoic acid-co-DMAA) (**23**).

Therefore, methanolic KOH was used to produce poly(6-(6-acrylamidohexanamido)hexanoic acid-co-DMAA) (**23**) (Figure 73)**.** After basic deprotection, the polymer was protonated in HCl acidic water and precipitated. The carboxylic acid was obtained, which was verified by NMR. The attempt to saponify the monomer before polymerization was unsuccessful due to monomer decomposition. Therefore, saponification followed polymerization. Polymer **23** also showed interesting properties and swells in various solvents.

3.2.3 Synthesis of lithium- (24) and TBA-salts (25) of poly(6-(6-acrylamidohexanamido)hexanoic acid-co-DMAA)

In accordance with Leibetseder [58], finally, poly(DMAA-co-lithium 6-(6-acrylamidohexanamido)hexanoate) (**24**) and poly(DMAA-co-tetrabutylammonium 6-(6-acrylamidohexanamido)hexanoate) (**25**) were synthesized.

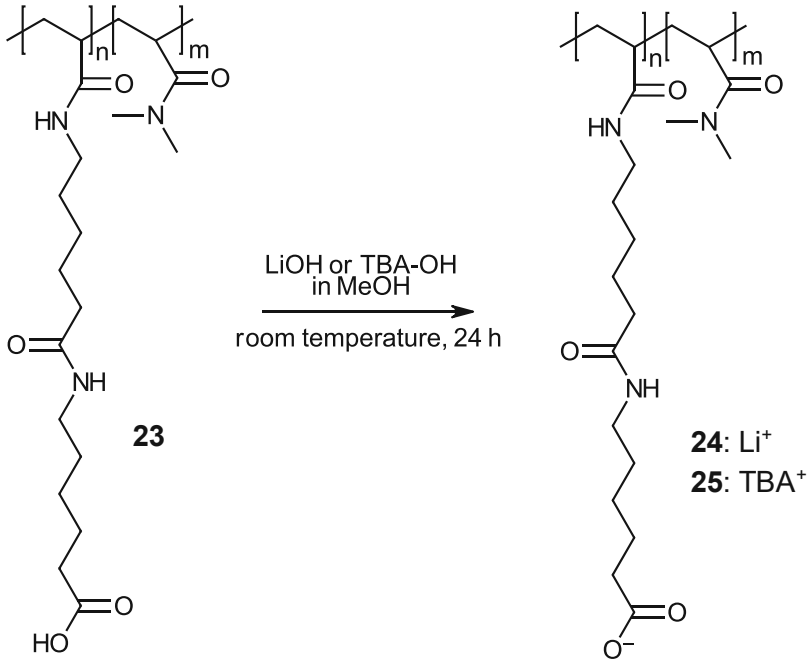

Figure 74: Structure of poly(DMAA-co-lithium 6-(6-acrylamidohexanamido)hexanoate) (**24**) and poly(DMAA-co-tetrabutylammonium 6-(6-acrylamidohexanamido)hexanoate) (**25**).

Therefore, carboxylic acid **23** reacts with a methanolic lithium hydroxide (or tetrabutylammonium hydroxide) solution (Figure 74). These two counterions were chosen because lithium is a small ion and tetrabutylammonium (TBA) is a much larger ion. These counterions therefore occupy different amounts of space in the polymer, which could lead to a different arrangement and thus to different properties. Again, the swelling behavior of both polymers **24** and **25** was noticeable. A difference between the lithium and TBA salt could be observed especially in the dry state. The lithium salt was white, hard and brittle after drying, whereas the TBA salt was still deformable and soft when dried. This property is due to the significantly larger TBA counterion.

Figure 75 shows the thermogram comparing the two-stage degradation process of the methyl ester **22** and the lithium salt **24**. The DSC thermogram shows the glass transition temperature of polymer **25** at -16 °C.

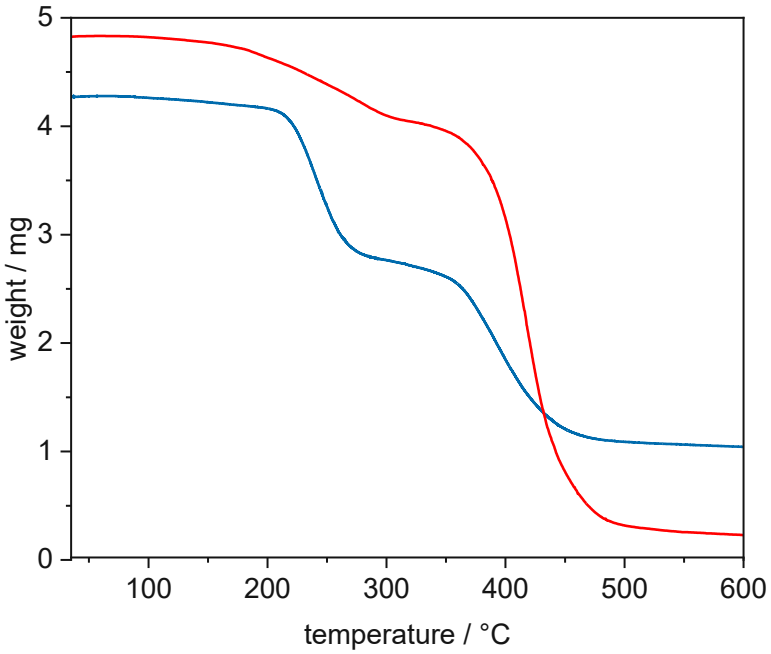

Figure 75: TGA thermogram of polymer **22** (free acid, red) and **24** (Li-salt, blue). Both polymers show a two-stage degradation process. In the case of **22**, decomposition starts earlier at about 160 °C. In the case of **24** (blue line), decomposition starts at 225 °C. It is possible that water is still present in the sample of polymer **22** (red), which could explain the early weight loss of the sample. From sample **24** (blue), 1.2 mg is left at the end of the measurement (carbon and lithium is left). In comparison, only carbon (and therefore less) is left from the other sample (0.2 mg, red).

4. Characterization

The synthesized polymers were characterized by IR, NMR, DSC and TGA and compared with each other. The aim was also to investigate the swelling behavior of the polymers. In the following chapter, the polymers **18** (C6 methyl ester) (Figure 76), **22** (C12 methyl ester) (Figure 77), **23** (C12 carboxylic acid) (Figure 78), **24** (C12 lithium salt) (Figure 79) and **25** (C12 tetrabutylammonium salt) (Figure 79) will be discussed in more detail.

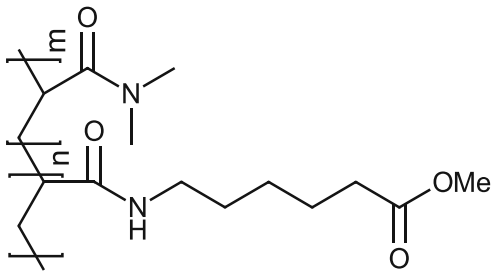

18

Figure 76: Structure of poly(DMAA-co-methyl-6-acrylamidohexanoate) (**18**).

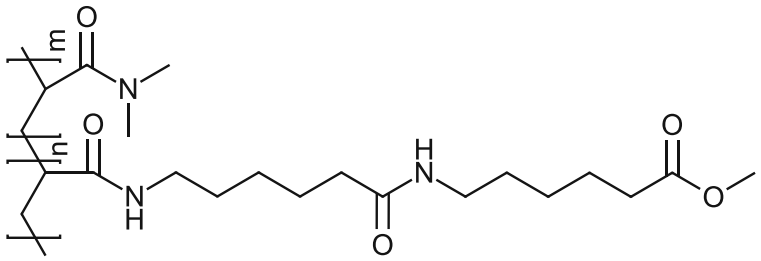

22

Figure 77: Structure of poly(DMAA-co-methyl 6-(6-acrylamidohexanamido)hexanoate) (**22**).

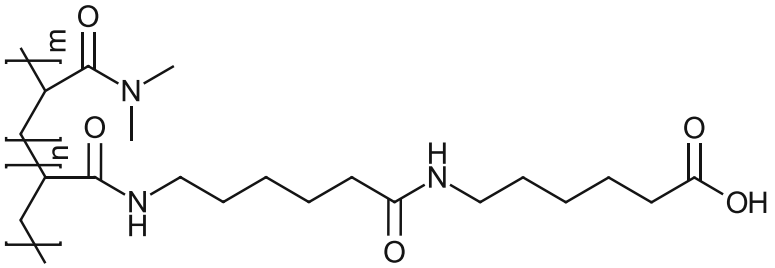

23

Figure 78: Structure of poly(6-(6-acrylamidohexanamido)hexanoic acid-co-DMAA) (**23**).

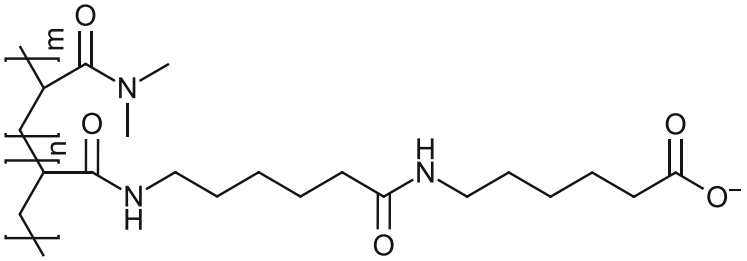

24: Li^+
25: TBA^+

Figure 79: Structure of poly(DMAA-co-lithium 6-(6-acrylamidohexanamido)hexanoate) (**24**) and poly(DMAA-co-tetrabutylammonium 6-(6-acrylamidohexanamido)hexanoate) (**25**)

4.1 Main differences of the synthesized brush polymers

In the following, the differences between comb polymers with C6 and C12 side chains will be discussed.

In contrast to C12 methyl ester **22**, C6 methyl ester **18** has a shorter side-chain length (6 aliphatic carbon atoms instead of 12) and a missing amide bond, therefore different properties were expected. Polymer **22** can form hydrogen bonds due to the additional amide bond and thus self-order. Swelling behavior could also only be observed with the polymers with 12 carbon atoms in the side chain (methyl ester **22**, carboxylic acid **23**, lithium-salt **24** and TBA-salt **25**).

Figure 80 shows the TGA thermogram of the C12 lithium-salt **24** compared to the C6 methyl ester **18**. The main difference is that polymer **24** decomposes in two steps due to the longer side chain. However, it should also be noted that the decomposition of polymer **18** is very similar to the second step of the decomposition of polymer **24**.

Figure 81 and Figure 82 show the different appearance of C12 methyl ester **22** and C6 methyl ester **18**. Figure 83 shows the swollen polymer **22**. Polymer **18** shows no swelling behavior. Therefore the swelling behavior should be investigated in more detail.

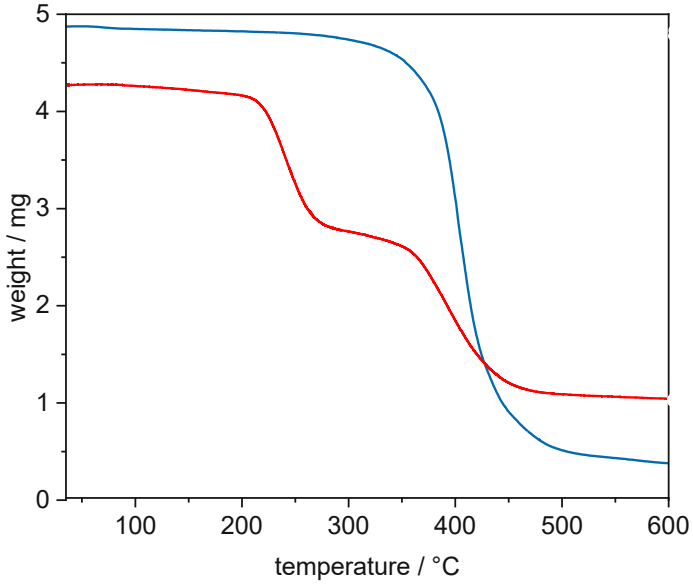

Figure 80: TGA of polymer **18** (blue) and **24** (red). The two-stage decomposition is clearly visible in polymer **24.** This indicates that the middle amide bond of polymer **24** is broken first during decomposition. Polymer **18** (shorter side-chain) is therefore also thermally more stable and decomposition starts at about 350 °C. Polymer **24** decomposes already at 210 °C.

Figure 81: Polymer **18** is a white powdery polymer.

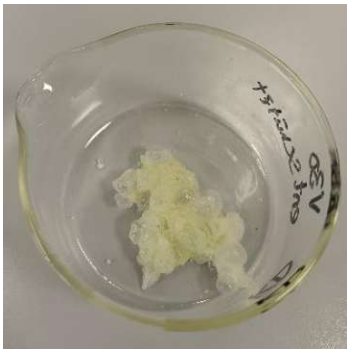

Figure 82: Polymer **22**. In the dry state, this polymer is very hard and brittle.

Figure 83: Polymer **22**. After the polymer is placed in DMF, it increases in size and becomes soft and malleable.

4.2 Swelling behavior tests

Swelling is the term used to describe the increase in the volume of a polymer after liquid absorption [51]. During the dissolving process of polymers, such polymer gels are always formed first. If the polymer is not dissolved, the solvent molecules are nevertheless present in the polymer matrix, resulting in a larger swollen polymer. This process occurs mainly in polymer networks. These are formed by inter- and intramolecular crosslinking. The polymer concentration has an important influence on crosslinking, with intramolecular reactions occurring at low concentrations and intermolecular reactions at high polymer concentrations [51].

During the synthesis of methyl ester **22**, carboxylic acid **23**, lithium-salt **24** and TBA-salt **25**, the swelling behavior of these polymers was observed. Therefore, an experiment was carried out for three different polymers to determine the degree of swelling (Table 3). The optical change, as well as the weight gain, was determined. Since all three polymers show good swelling behavior in DMF, the experiments were conducted in DMF. Polymers **22**, **23** and **24** were weighed and then submerged in DMF for 20 hours. Then excess DMF was wiped off and the weight of the polymer was determined. Likewise, it was determined how quickly the polymers released the solvent and thus returned to their original state.

Equation 1 describes the swelling ratio of the swollen polymer of mass a and the original non-swollen polymer of mass b [84].

$$Q = \frac{a - b}{b} \qquad (1)$$

Polymers **22** and **23** (ester and corresponding free carboxylic acid) exhibited very similar behavior and showed an almost identical degree of swelling. The swelling degrees of the polymers are shown in Table 3.

Table 3: Swelling behavior of different polymers.

No.	Polymer	Original weight / mg	Final weight / mg	Swelling degree Q
1	**22**	13.1	215.2	15.4
2	**23**	11.6	188.7	15.3
3	**24**	1.2	8.8	6.3

Lithium-salt **24** has a significantly lower degree of swelling. However, this may be because significantly less polymer was used for the test, which results in a measurement inaccuracy, making comparison with methyl ester **22** and carboxylic acid **23** erroneous.

Figure 84 shows the weight loss of swollen polymers **22**, **23** and **24**. During this experiment, the polymers were also photographed to record the visual change (Figure 85-88). The fully swollen polymer (Figure 85) is much larger, colorless and transparent.

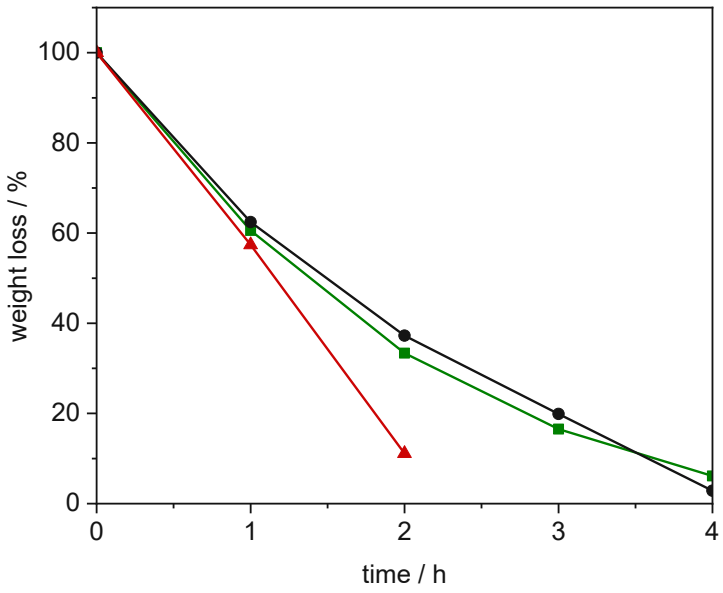

Figure 84: Polymers **22** (green), **23** (grey) and **24** (red) were submerged in DMF for 20 h. Starting point constitutes the fully swollen polymer. The polymers were then dried in air and the weight was determined once per hour. After about 4 h, almost all the solvent evaporated and the polymers showed their original weight before treatment with DMF. The ester **22** (green) and the correlated free acid **23** (grey) show similar behavior. The Li-salt **24** (red) is difficult to compare because less polymer was used. Nevertheless, it is also visible here that the polymer can swell in DMF.

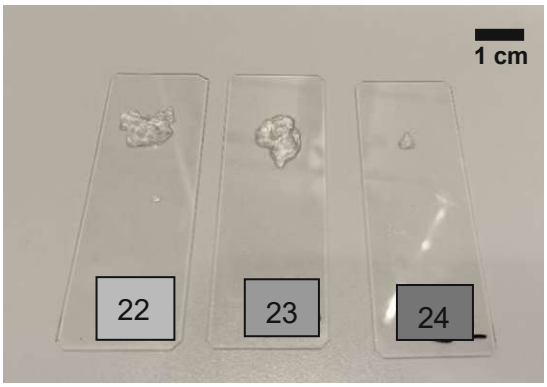

Figure 85: Polymers **22**, **23** and **24** swollen in DMF for 20 h. Significantly less polymer was used for polymer **24**. All 3 polymers are now colorless and deformable.

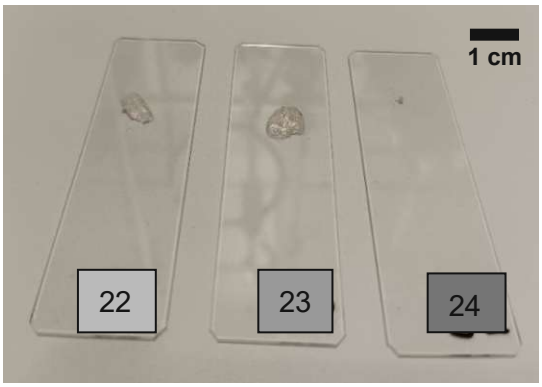

Figure 86: Polymers **22**, **23** and **24** swollen in DMF after 2 hours drying time. The polymers were left in air on a glass slide and the drying progress was then determined by weighing.

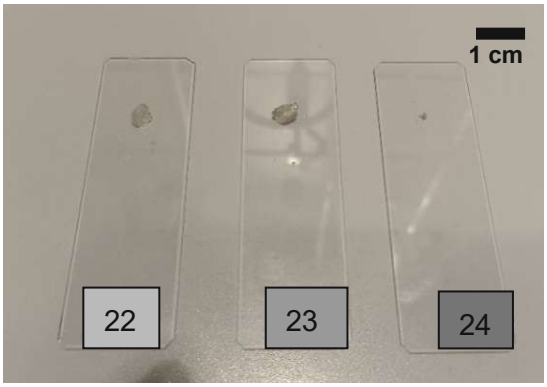

Figure 87: Polymers **22**, **23** and **24** swollen in DMF after 3 hours drying time. The polymers are already smaller and are no longer as soft and deformable as before.

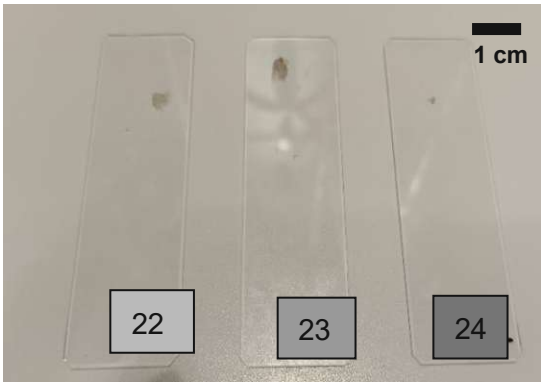

Figure 88: Polymers **22**, **23** and **24** swollen in DMF after 5 hours drying time. The polymers have reached the original weight and have thus released almost all of the DMF.

4.3 Compounding

The properties of TBA-salt **25** were special because it was rubbery, soft and formable without solvent. Nevertheless, the polymer showed after synthesis an inhomogeneous macroscopic morphology. Thus, the idea was to additionally introduce a high-boiling solvent and distribute it homogeneously in the polymer. The solvent should act as internal softener and should allow the polymer to self-order. Subsequently, the homogeneous polymer was to be formed into a strand by extrusion.

Pre-tests showed that the polymer also swells in tetraethylene glycol (TEG). Since the boiling point for this solvent is about 327 °C, the evaporation of the solvent from the polymer can be kept low. Therefore, polymer **25** was mixed with 20% TEG and then put into the twin-screw extruder (Figure 89).

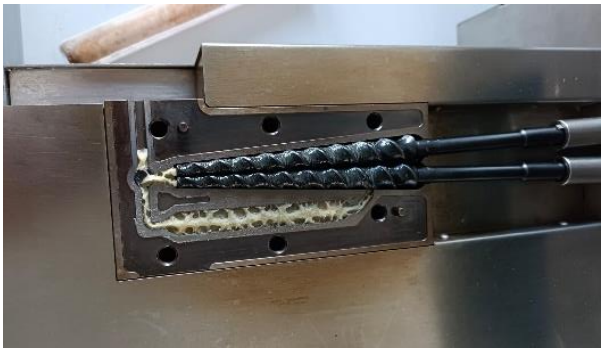

Figure 89: Extrusion of polymer **25** . The polymer was mixed with tetraethylene glycol at 60 °C for 40 min. However, extrusion could not take place because too little material was used. The polymer could be mixed well with TEG, but remained stuck in the extruder.

After a compounding time of 40 min at 60 °C, the polymer was extruded. However, no extrusion occurred but after the extruder was opened, it was evident that the polymer was well mixed. One reason for failed extrusion is that probably too little material was used. Another reason, however, are the properties of the polymer. It was very sticky and adhered strongly to the walls of the extruder, which also made extrusion difficult.

However, it was possible to produce a homogeneous polymer mixed with TEG, which is easily formable. The material was characterized visually and showed a very homogeneous structure. The inhomogeneous structure (as after synthesis) was no longer recognizable. In the future, material should be produced according to the synthesis routes in this thesis, so that different compounds can be produced and tested.

4.4 Influence of an electric field

The properties of TBA-salt **25** were also tested in terms of behavior in an electrical field. For this purpose, polymer **25**, which contains a carboxy group on the side chains, was swollen in DMF. A template was covered with aluminum foil, then a layer of polymer and DMF was placed on top, followed by another layer of aluminum foil (Figure 90). The polymer was then allowed to swell between the two aluminum layers which acted as electrical contact. The test strip was removed from the template and then cut as shown in Figure 91.

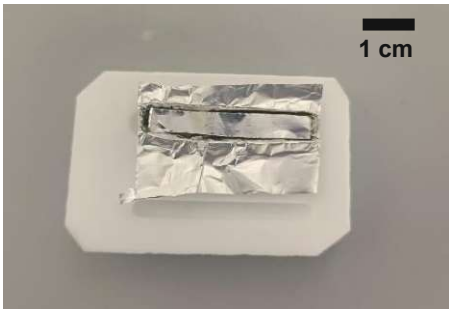

Figure 90: Polymer **25** was swollen in DMF between two aluminum foils in a mold.

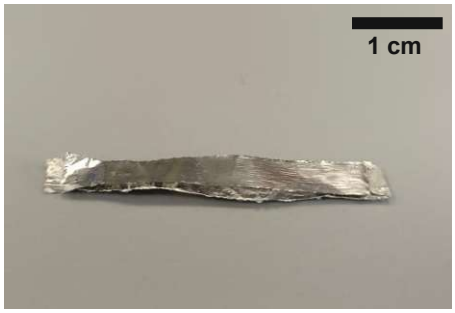

Figure 91: After the polymer has swollen, the test strip is removed from the mold and any excess aluminum foil is cut off.

The test setup can be seen in Figure 92. An electrical voltage between 5 V and 20 V was applied to the aluminum contacts with a laboratory power supply. As described in Browe *et al.* [28], the material was then to be bent (Figure 93).

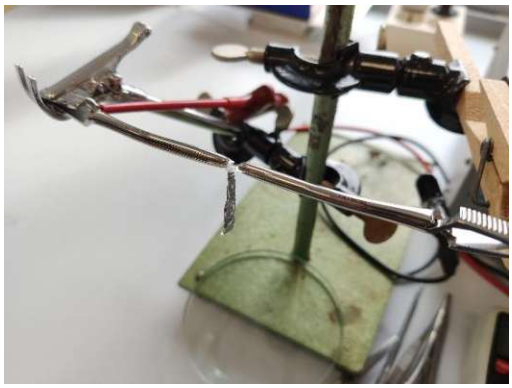

Figure 92: The test strip was fixed by two aluminum clamps and a voltage between 5-20 V was applied.

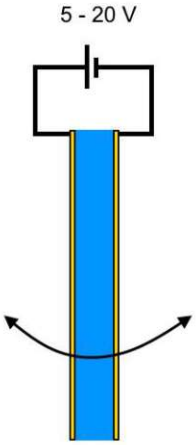

Figure 93: By applying the voltage, bending should be observed due to ionic motion in the polymer (blue).

This was a first attempt to investigate such materials in an electric field. Unfortunately, the experiment described in Browe *et al.* [28] could not be reconstructed and no bending of the material could be detected. This could be due to the fact that the aluminum foil, which adhered directly to the swollen polymer, was too heavy to move it. In addition, as shown in Figures 92 and Figure 93, the test strip was very small, which made handling difficult. Another problem was that the polymer layer was very thin and there was a risk of short circuits, especially on the edges of the test strip. Nevertheless, such tests to use these materials as an actuator should continue to be carried out in the future, with optimization of the test setup.

EXPERIMENTAL PART

1. Brush polymers with aromatic based C12 side chains

1.1 Monomer synthesis

1.1.1 Synthesis of methyl 6-aminohexanoate hydrochloride (4)

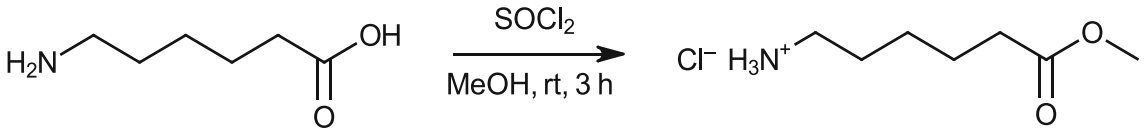

4

Target molecule **4** was synthesized according to Gurjar *et al.* [69]. Therefore, 29.81 g (250.6 mmol) thionyl chloride was added dropwise to 110 mL cooled methanol and the reaction mixture was stirred for 20 min. Afterwards, 16.43 g (125.3 mmol) of 6-aminohexanoic acid (**3)** was added and the ice bath was removed. The reaction mixture was stirred for 3.5 h at room temperature. Then the solvent was evaporated under reduced pressure. A white solid was obtained and the product was identified *via* ^{1}H-NMR.

Yield: 45.54 g, (90 % of theory, 94 % of lit. [69])

mp.: 121-123 °C (lit.: 117-124°C [70])

HPLC-FTMS + cAPCI (m/z): calc.: 146.1176 $[M+H]^+$, found: 146.1174 $[M+H]^+$

^{1}H NMR: (300 MHz, DMSO-d_6, 25 °C, *δ*): 8.01 (s_b, 3H, - N**H$_3$**+Cl-), 3.58 (s, 3H, -COOC**H$_3$**), 2.76-2.69 (m, 2H, Cl-H_3N^+-C**H$_2$**-), 2.30 (t, 2H, J=7.7 Hz, -C**H$_2$**-$COOCH_3$), 1.54 (m, 4H, $Cl^-H_3N^+$-CH_2-C**H$_2$**-CH_2-C**H$_2$**-CH_2-$COOCH_3$), 1.35-1.25 (m, 2H, $Cl^-H_3N^+$-CH_2-CH_2-C**H$_2$**-CH_2-CH_2-$COOCH_3$) ppm.

IR (ATR, *ν*): 2929, 1724, 1581, 1473, 1313, 1072, 885 cm^{-1}.

1.1.2 Synthesis of methyl 6-(4-aminobenzamido)hexanoate (7)

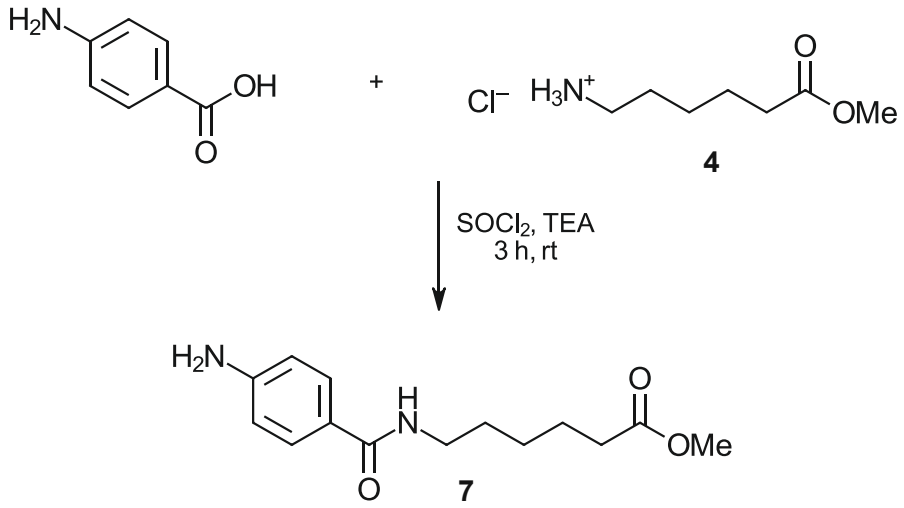

Target molecule **7** was synthesized as described in a general synthesis procedure in Bruice [71]. Therefore, a solution of 0.50 g (3.6 mmol) 4-aminobenzoic acid and 20 mL DCM was cooled with ice and then 0.86 g (7.2 mmol) $SOCl_2$ was added dropwise. The solution was stirred for 1 h and then the solvent was removed under reduced pressure and 4-aminobenzoyl chloride was obtained.

To a solution of 4-aminobenzoyl chloride in 20 mL DCM, a solution of 1.32 g hydrochloride **4** (7.2 mmol) and 0.73 g (7.2 mmol) TEA in 20 mL DCM was added at 0 °C. The solution was stirred for 2 h at room temperature and then the solution was extracted with 50 mL brine. The organic phase was dried with Na_2SO_4, filtered and afterwards the solvent was removed under reduced pressure. Methyl 6-(4-aminobenzamido)hexanoate (**7**) was obtained as white powder and identified *via* ^{1}H-NMR and IR.

Yield: 0.28 g (29 % of theory)

^{1}H NMR: (300 MHz, DMSO-d_6, 25 °C, *δ*): 7.94 (t, J = 5.6 Hz, 1H, C(O)-N**H**), 7.57 (dd, J=8.65 Hz, 19.22 Hz, 2H, Ar-**H**), 6.53 (dd, J= 5.39 Hz, 8.69 Hz, 2H, Ar-**H**), 5.55 (s, 2H, Ar-N**H2**), 3.57 (s, 3H, C(O)-O-C**H3**), 3.17 (q, J= 6.87 Hz, 12.81 Hz, 2H, -NH-C**H2-**), 2.30 (t, J=7.36 Hz, 2H, -C**H2**-COO-CH3), 1.59-1.42 (m, 4H, C**H2**-CH2-C=O, NH-CH2-C**H2**-), 1.33-1.24(m, 2H, -C**H2**-CH2-CH2-COO-CH3) ppm.

IR (ATR, *ν*): 3344, 3224, 2942, 2867, 1720, 1309, 1106, 769 cm^{-1}.

1.1.3 Synthesis of 4-(2,2,2- trifluoro-acetylamino) benzoic acid (8)

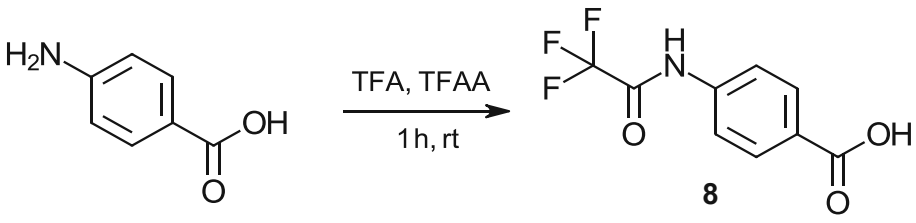

Target molecule **8** was synthesized according to Steiner *et al.* [72]. Therefore, 1.01 g (7.3 mmol) 4-aminobenzoic acid was dissolved in 9 mL TFA and cooled with an ice bath. Then, 1.80 g (8.6 mmol) of TFAA was added with a syringe. The milky white solution is stirred for 1 h at room temperature. The reaction solution is poured into cold water to thus precipitate the desired product. The product was filtered off and washed with water and n-hexane. 4-(2,2,2- trifluoro-acetylamino)-benzoic acid (**8**) was obtained as a powdery white solid, dried under high vacuum and characterized by ^{1}H-NMR.

Yield: 1.25 g (62.19 % of theory)

^{1}H NMR: (300 MHz, DMSO-d_6, 25 °C, *δ*): 12.96 (s, 1H, -O**H**), 11.53 (s, 1H, -N**H**), 7.98 (d, 2H, J= 8.56 Hz, -C**H**-), 7.81 (d, 2H, J=8.56 Hz, -C**H**-)ppm.

1.1.4 Synthesis of methyl 6-((2,2,2- trifluoro-acetylamino)benzylamino) hexanoate (9)

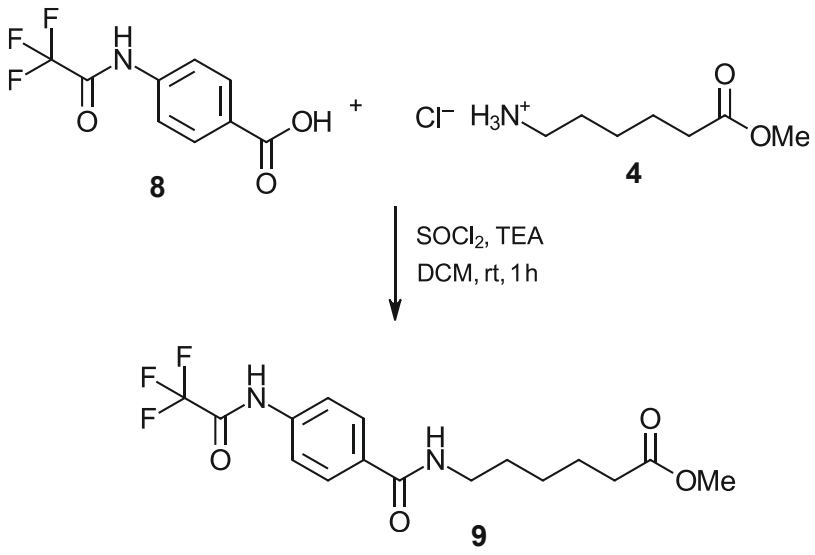

Target molecule **9** was synthesized in accordance with Bruice [71]. Therefore, a solution of 0.96 g (4.2 mmol) benzoic acid **8** and 20 mL DCM was cooled with ice and then 0.72 g (6.1 mmol) $SOCl_2$ was added dropwise. The solution was stirred for 1 h and then the solvent was removed under reduced pressure and 4-(2,2,2- trifluoro-acetylamino)-benzoyl chloride (**10**) was obtained.
Acyl chloride **10** was dissolved in 20 mL DCM and cooled with an ice bath. Then a solution of 0.78 g (4.3 mmol) hydrochloride **4** and 1.33 g (13.1 mmol) TEA in 20 mL DCM was added and the mixture was stirred for 2 h at room temperature. The solvent was removed under reduced pressure and afterwards dissolved in DCM again. The solution was extracted with 1 N HCl for three times, then dried over Na_2SO_4 and the solvent was removed under reduced pressure. A white powder was obtained and characterized *via* ^{1}H-NMR.

Yield: 0.69 g (45.95 % of theory)
^{1}H NMR: (300 MHz, DMSO-d_6, 25 °C, *δ*): 11.54 (s, 1H, -NH), 11.44 (s, 1H, -NH), 7.87 (d, 2H, J= 8.60 Hz, -Ar**H**-), 7.75 (d, 2H, J=8.60 Hz, -Ar**H**-), 3.57 (s, 3H, -CH3), 3.24 (m, 2H, J=8.8Hz, -C**H$_2$**-CH_2-CH_2-CH_2-CH_2-$COOCH_3$), 2.31 (t, 2H, J=8.8 Hz, -C**H$_2$**-$COOCH_3$)1.62-1.45 (m, 4H, -C**H$_2$**-CH_2-C**H$_2$**-CH_2-$COOCH_3$), 1.37-1.20 m, 2H, -C**H$_2$**-CH_2-CH_2-$COOCH_3$) ppm.

2. Brush polymers with amide based C6 side chains

2.1 Monomer synthesis

2.1.1 Synthesis of 6-acrylamidohexanoic acid (5)

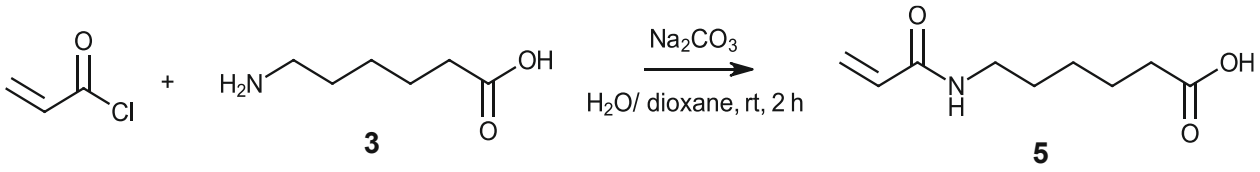

Target molecule **5** was synthesized according to D'Souza *et al.* [73]. Therefore, 13.13 g (100.1 mmol) of amino acid **3** and 21.25 g (200.5 mmol) sodium carbonate were dissolved in 150 mL water and the solution was cooled with ice/NaCl. Then 9.88 g (109.2 mmol) acryloyl chloride was dissolved in 25 mL dioxane and dropwise added to the reaction mixture. After removing the cooling bath, the mixture was stirred at room temperature for 2 h. Afterwards, the reaction mixture was cooled again and conc. HCl was added to achieve a pH of 2. The solution was extracted with ethyl acetate three times. The combined organic layers were dried over Na_2SO_4 and the solvent was evaporated. To remove the remaining acryloyl chloride, the product was dried at 45 °C under vacuum overnight. A white powder was obtained and identified *via* ^{1}H-NMR.

Yield: 13.54 g (73 % of theory, 73 % of lit. [73])

mp.: 89-90 °C (lit.: 89 °C [87])

HPLC-FTMS + cAPCI (m/z): calc.: 186.1125 $[M+H]^+$, found.: 186.1122 $[M+H]^+$

^{1}H NMR: (300 MHz, DMSO-d_6, 25 °C, *δ*): 12.00 (s_b, 1H, COO**H**), 8.04 (t, 1H, J=4.7 Hz, -N**H**), 6.20 (dd, 1H, J_1=17.1, J_2=9.9, CH_2=C**H**-CO-NR), 6.05 (dd, 1H, J_1=17.1 Hz, J_2=2.5 Hz, C**H**$_2$=CH-), 5.55 (dd, 1H, J_1=9.9 Hz, J_2=2.5 Hz, C**H**$_2$=CH-), 3.15-3.05 (m, 2H, -NH-C**H**$_2$-), 2.19 (t, 2H, J=7.3 Hz, -C**H**$_2$-COOH), 1.56-1.45 (m, 2H, -NH-CH_2-C**H**$_2$-), 1.45-1.35 (m, 2H, -C**H**$_2$-CH_2-COOH), 1.31-1.23 (m, 2H, -NH-$(CH_2)_2$-C**H**$_2$-) ppm.

IR (ATR, *ν*): 3460-2280, 3286, 3062, 2945, 1691, 1651, 1623 cm^{-1}.

2.1.2 Synthesis of methyl 6-acrylamidohexanoate (12)

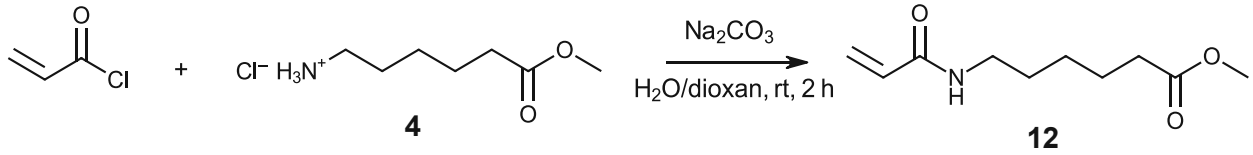

Target molecule **12** was synthesized according to D'Souza *et al.* [73]. Therefore, 2.01 g (11.1 mmol) of hydrochloride **4** and 2.33 g (21.9 mmol) sodium carbonate were dissolved in 25 mL water and the solution was cooled with ice/NaCl. Then 1.11 g (12.3 mmol) acryloyl chloride was dissolved in 2.75 mL dioxane and dropwise added to the reaction mixture. After removing the cooling bath, the mixture was stirred at room temperature for 2 h. Afterwards, the reaction mixture was cooled again and conc. HCl was added to achieve a pH of 2. The solution was extracted with ethyl acetate three times. The combined organic layers were dried over Na_2SO_4 and the solvent was evaporated. To remove the remaining acrylic acid, the product was dried at 45 °C under vacuum overnight. A white powder was obtained and identified *via* ^{1}H-NMR.

Yield: 1.53 g (69 % of theory, 75 % of lit. [73])

^{1}H NMR (300 MHz, DMSO-d_6, 25 °C, *δ*): 8.07 (t, 1H, J=4.5 Hz, -N**H**-), 6.20 (dd, 1H, J_1=17.1 Hz, J_2=9.7, CH_2=C**H**-CO-), 6.06 (dd, 1H, J_1=17.2 Hz, J_2=2.4 Hz, trans C**H$_2$**=CH-CO-), 5.56 (dd, 1H, J_1=9.9 Hz, J_2=2.4 Hz, cis C**H$_2$**=CH-CO-), 3.57 (s, 3H, -COOC**H$_3$**), 3.10 (m, 2H, acryloyl-CONH-C**H$_2$**-), 2.29 (t, 2H, J=7.6 Hz, -$(CH_2)_4$-C**H$_2$**-$COOCH_3$), 1.59-1.19 (m, 6H, -CO-NH-CH_2-(C**H$_2$**)$_3$- ppm.

2.2 Polymerization

2.2.1 Synthesis of poly(6-acrylamidohexanoic acid) (13)

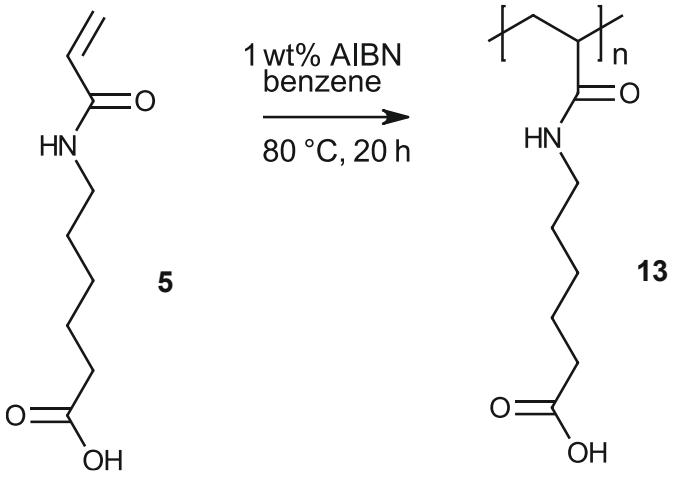

For the synthesis of polymer **13** 5.01 g (26.9 mmol) of acryl amide **5** was dissolved in 30 mL benzene and purged with argon. Then 1 wt% AIBN was added and the solution was stirred under reflux overnight. The solvent was removed under reduced pressure and the final polymer was dried in vacuum.

Decomposition (TGA): 402 °C

^{1}H NMR (300 MHz, DMSO, 25 °C, *δ*): 11.99 (s, 1H, -O**H**-), 8.04 (s, 1H, -N**H**-), 3.02 (m, 2H, -NH-C**H$_2$**-), 2.22 (m, 2H, -C**H$_2$**-COO-), 1.67-1.08 (m, 6H, -NH-CH$_2$-(C**H$_2$**)$_3$-) ppm.

IR (ATR, *ν*): 3617-3033, 2919, 2859, 1701, 1637, 1390, 1172 cm^{-1} .

2.2.2 Synthesis of poly(6-acrylamidohexanoic acid) copolymers (14, 15)

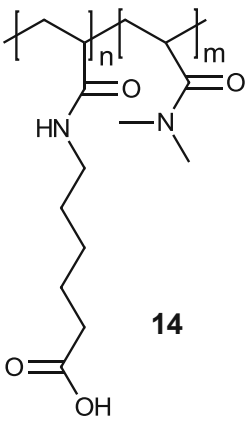

14

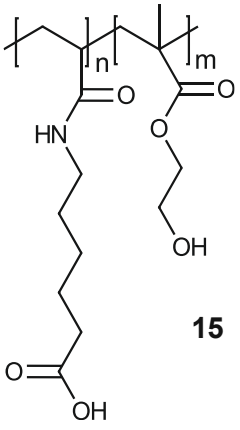

15

For the synthesis of copolymer **14**, 3.56 g (19.1 mmol) of acryl amide **5** and 1.93 g (19.4 mmol) of DMAA were weighed in and 30 mL benzene was added. The mixture was purged with argon and 1 wt% AIBN (related to **5**) was added. Then the reaction mixture was stirred under reflux overnight and the solvent was removed under reduced pressure. The final polymer was dried at 40 °C in vacuum overnight. Polymer **15** with HEMA as comonomer was synthesized *via* the same route.

Analytical Data for **14**:

Decomposition (TGA): 403 °C

^{1}H NMR (300 MHz, D_2O, 25 °C, *δ*): 3.25-2.81 (m, 8H, -CO-N(CH_3)$_2$ and -NH-CH_2-), 2.18 (t, 2H, J=7.1 Hz, -CH_2-COO-), 1.65-1.41 (m, 4H, -CH_2-CH_2-COO- and -NH-CH_2-CH_2-), 1.40-1.24 (m, 2H, -NH-(CH_2)$_2$-CH_2-) ppm.

IR (ATR, *ν*): 3617-3033, 2919, 2859, 1637, 1400, 1141 cm^{-1} .

Analytical Data for **15**:

Decomposition (TGA): 424 °C

2.2.3 Synthesis of the lithium salts of poly(6-acrylamidohexanoic acid) copolymers (16, 17)

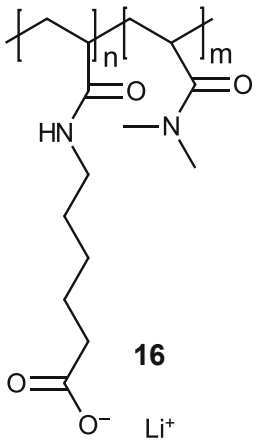

16

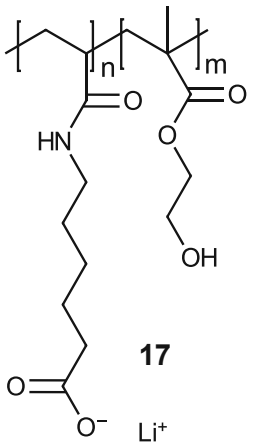

17

The synthesis of the lithium salts **16** and **17** was carried out as described in Leibetseder [58]. Therefore, 0.49 g (1.7 mmol) of the deprotected polymer **14** was weighed in and 0.07 g (1.7 mmol) $LiOH*H_2O$ was added. Then 15 mL MeOH was added and the solution was stirred at room temperature overnight. The solvent was removed under reduced pressure and the polymer was dried at 40 °C in vacuum overnight. Polymer **17** with HEMA as comonomer was synthesized *via* the same route.

Analytical data for **16**:

Decomposition (TGA): 398 °C

^{1}H NMR (300 MHz, D_2O, 25 °C, *δ*): 3.25-2.81 (m, 8H, -CO-N($C\mathbf{H_3}$)$_2$ and -NH-$C\mathbf{H_2}$-), 2.18 (t, 2H, J=7.1 Hz, -$C\mathbf{H_2}$-COO-), 1.65-1.41 (m, 4H, -$C\mathbf{H_2}$-CH_2-COO- and -NH-CH_2-$C\mathbf{H_2}$-), 1.40-1.24 (m, 2H, -NH-$(CH_2)_2$-$C\mathbf{H_2}$-) ppm.

IR (ATR, *ν*): 3617-3033, 2919, 2859, 1637, 1400, 1141 cm^{-1} .

Analytical data for **17**:

Decomposition (TGA): 438 °C

^{1}H NMR (300 MHz, CD_3OD, 25 °C, *δ*): 4.06 (m, 2H, -CO-O-$C\mathbf{H_2}$-), 3.80 (m, 2H, -CO-O-CH_2-$C\mathbf{H_2}$-), 3.25-3.00 (m, 2H, -NH-$C\mathbf{H_2}$-), 2.18 (t, 2H, -$C\mathbf{H_2}$-COO-), 1.72-0.85 (m, 9H, -$C\mathbf{H_2}$-CH_2-COO-, -NH-CH_2-$C\mathbf{H_2}$-, -NH-$(CH_2)_2$-$C\mathbf{H_2}$- and -CO-C-$C\mathbf{H_3}$) ppm.

2.2.4 Synthesis of methyl 6-acrylamidohexanoate copolymers (18, 19)

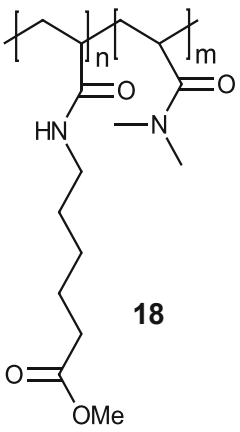

18

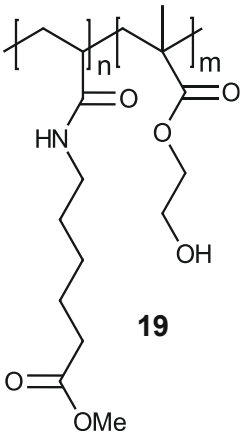

19

For the synthesis of copolymer **18** 1.41 g (7.1 mmol) of **12** and 0.71 g (7.1 mmol) of DMAA were weighed in and 30 mL benzene was added. The mixture was purged with argon and 1 wt% AIBN (related to **12**) was added. Then the reaction mixture was stirred under reflux overnight and the solvent was removed under reduced pressure. The final polymer was dried at 40 °C in vacuum overnight. Polymer **19** was synthesized *via* the same route but with the same molar amount HEMA as comonomer instead of DMAA.

Analytical Data for **18**:

Decomposition (TGA): 401 °C

^{1}H NMR (300 MHz, DMSO, 25 °C, *δ*): 7.59 (s, 1H, -N**H**-), 3.57 (s, 3H, -O-C**H$_3$**), 3.10-2.66 (m, 8H, -CO-N(C**H$_3$**)$_2$ and -NH-C**H$_2$**-), 2.28 (t, 2H, -C**H$_2$**-COO-), 1.61-1.15 (m, 4H, -C**H$_2$**-CH$_2$-COO- and -NH-CH$_2$-C**H$_2$**-), 1.40-1.24 (m, 2H, -NH-(CH$_2$)$_2$-C**H$_2$**-) ppm.

IR (ATR, *ν*): 3288, 2916, 2837, 1740, 1637, 1450, cm^{-1}.

Analytical Data for **19**:

Decomposition (TGA): 444 °C

^{1}H NMR (300 MHz, DMSO, 25 °C, *δ*): 7.62 (s, 1H, -N**H**-), 4.87 (m, 2H, -CO-O-C**H$_2$**-), 3.90 (m, 2H, -CO-O-CH$_2$-C**H$_2$**-), 3.57 (s, 3H, -O-C**H$_3$**), 3.18-2.70 (m, 2H, -NH-C**H$_2$**-), 2.28 (m, 2H, -C**H$_2$**-COO-), 2.11-0.64 (m, 9H, -C**H$_2$**-CH$_2$-COO-, -NH-CH$_2$-C**H$_2$**-, -NH-(CH$_2$)$_2$-C**H$_2$**- and -CO-C-C**H$_3$**) ppm.

3. Brush polymers with amide based C12 side chain

3.1 Monomer synthesis

3.1.1 Synthesis of methyl 6-(6-acrylamidohexanamido) hexanoate (11)

3.1.1.1 Synthesis of methyl 6-(6-acrylamidohexanamido) hexanoate (11) *via* the acid chloride route

3.1.1.1.1 Stepwise synthesis of methyl 6-(6-acrylamidohexanamido) hexanoate (11)

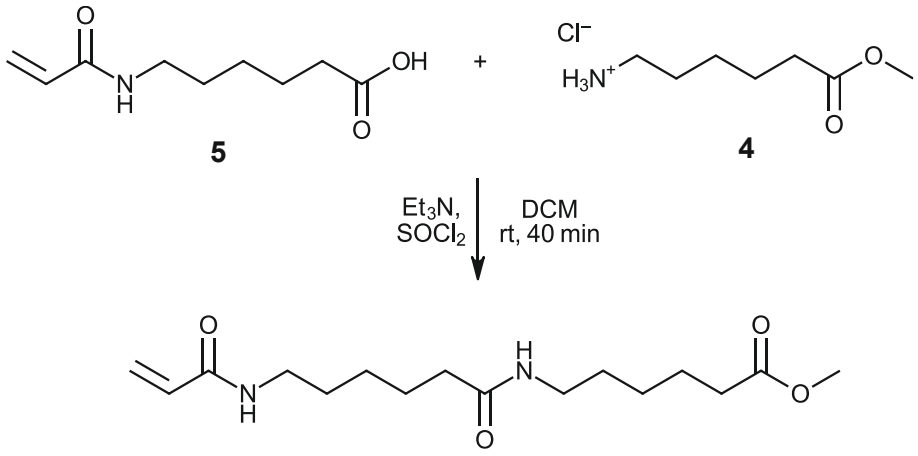

Target molecule **11** was synthesized according to Bruice [71]. Therefore, 0.49 g (2.6 mmol) of acrylamide **5** was mixed with 15 mL DCM. Then the reaction mixture was cooled with an ice bath and 0.35 g (2.9 mmol) $SOCl_2$ in 8 mL DCM was added dropwise. The solution was stirred for 1.5 h at room temperature. In a second flask 0.49 g (2.7 mmol) of hydrochloride **4** were mixed with 20 mL DCM. Then 0.92 g (9.1 mmol) Et_3N was added and the solution was stirred for 1.5 h at room temperature. Afterwards, both reaction solutions were combined and stirred for 2 h at room temperature. Finally, the residue was filtered, and the solvent was evaporated under reduced pressure. The residues were dissolved in 50 mL DCM and the solution was extracted with 1 N HCl and a 20 g/L Na_2CO_3 solution. The organic phase was dried over Na_2SO_4 and the solvent was removed under reduced pressure. A white powder was obtained.

Yield: 0.16 g (20 % of theory)

The analytical data are summarized in chapter 3.1.1.3

3.1.1.1.2 One-pot synthesis of methyl 6-(6-acrylamidohexanamido) hexanoate (11)

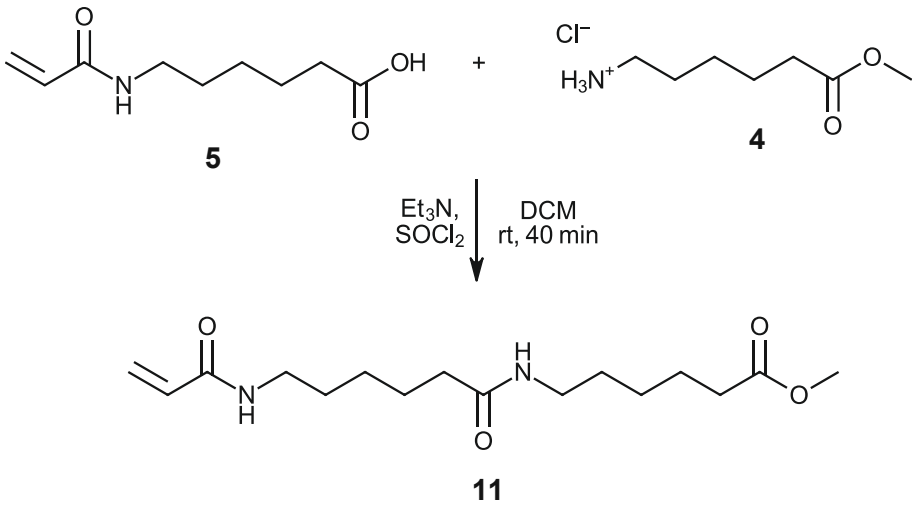

Target molecule **11** was synthesized according to Leggio *et al.* [77]. Therefore, 0.25 g (1.3 mmol) of acrylamide **5** and 0.19 g (1.1 mmol) of hydrochloride **4** were mixed with 20 mL DCM. Then 0.31 g (3.1 mmol) Et_3N was added and the reaction mixture was stirred at room temperature. Afterwards, 0.18 g (1.5 mmol) $SOCl_2$ was dropped into the solution and the mixture was stirred for 40 min at room temperature. Then the residue was filtered, and the solvent was evaporated under reduced pressure. The residues were dissolved in 10 mL DCM and the solution was extracted with 1 N HCl and a 20 g/L Na_2CO_3 solution. The organic phase was dried over Na_2SO_4 and the solvent was removed under reduced pressure. The final product was a white powder, soluble in chloroform, DCM and pyridine.

Yield: 0.083 g (24 % of theory)

The analytical data are summarized in chapter 3.1.1.3

3.1.1.2 Synthesis of methyl 6-(6-acrylamidohexanamido) hexanoate (11) *via* coupling agent

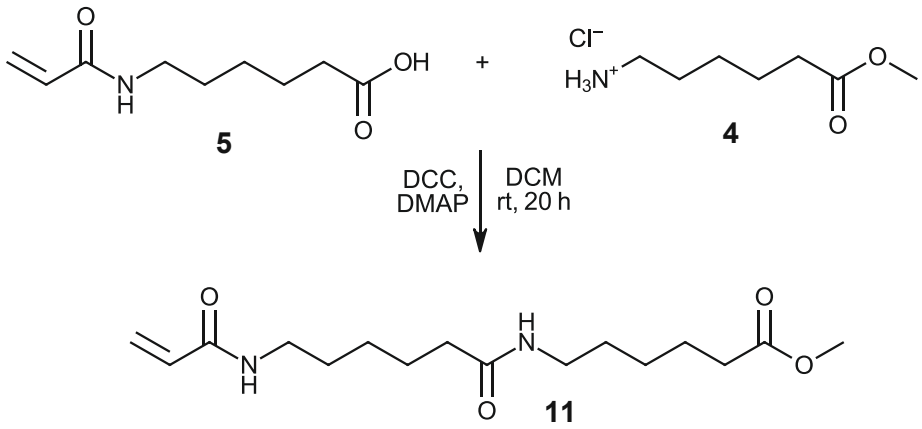

The synthesis of monomer **11** was carried out in accordance with Neises and Steglich [79]. Therefore, 4.00 g (21.6 mmol) of acrylamide **5**, 4.55 g (22.1 mmol) DCC and 0.45 g (3.7 mmol) DMAP were weighed in and 100 mL dry DCM was added. In a second flask, 3.98 g (21.9 mmol) of hydrochloride **4** and 6.53 g (64.5 mmol) Et_3N were mixed with 50 mL dry DCM. Both flasks were stirred for 2 h at room temperature. Then the two reaction mixtures were combined and stirred for 20 h at room temperature. Afterwards, the solution was filtered and the solvent was evaporated under reduced pressure. The residue was solved in DCM and extracted with 1N HCl twice. Then the organic phase was extracted twice with a 20 g/L Na_2CO_3 solution. The organic phase was dried over $MgSO_4$ and the solvent was evaporated under reduced pressure. The final product was a white powder and was identified *via* ^{1}H-NMR.

Yield: 4.72 g (70 % of theory, 94 % of lit. [79])

mp.: 55-57 °C

HPLC-FTMS + cAPCI (m/z): calc.: 313.2122 $[M+H]^+$, found: 313.21191 $[M+H]^+$

^{1}H NMR: (300 MHz, DMSO-d_6, 25 °C, *δ*): 8.04 (t, 1H, J=4.8 Hz, CH_2=CH-CO-N**H**-), 7.72 (t, 1H, J=5.4 Hz, -CH_2-CO-N**H**-), 6.19 (dd, 1H, J_1=17.1 Hz, J_2=9.9, CH_2=C**H**-CO-), 6.04 (dd, 1H, J_1=17.1 Hz, J_2=2.5 Hz, trans C**H_2**=CH-CO-), 5.54 (dd, 1H, J_1=9.9 Hz, J_2=2.4 Hz, cis C**H_2**=CH-CO-), 3.57 (s, 3H, -COOC**H_3**), 3.09 (m, 2H, acryloyl-CONH-C**H_2**-), 2.99 (m, 2H, -CH_2-CO-NH-C**H_2**-), 2.28 (t, 2H, J=7.4 Hz, -CH_2-CO-NH-$(CH_2)_4$-C**H_2**-$COOCH_3$), 2.03 (t, 2H J=7.3 Hz, acryloyl-CO-NH-$(CH_2)_4$-C**H_2**-CO-NH-), 1.56-1.43 (m, 4H, acryloyl-CO-NH-CH_2-C**H_2**- and -CH_2- CO-NH-CH_2-C**H_2**-), 1.43-1.30 (m, 4H, acryloyl-CO-NH-$(CH_2)_3$-C**H_2**- and -CH_2-CO-NH-$(CH_2)_3$- C**H_2**-), 1.30-1.20 (m, 4H, acryloyl-CO-NH-$(CH_2)_2$-CH_2- and -CH_2-CO-NH-$(CH_2)_2$-C**H_2**-) ppm.

APT ^{13}C NMR (75 MHz, DMSO-d_6, 25 °C, δ): 173.3 (C15), 171.8 (C9), 164.4 (C3), 131.9 (C2), 124.7 (C1), 51.14 (C16), 38.43 (C4), 38.16 (C10), 35.35 (C8), 33.22 (C14), 28.85 (C5), 28.83 (C11),26.12 (C6), 25.87 (C7), 25.06 (C12), 24.15 (C13) ppm.

IR (ATR, *ν*): 3288, 2939, 2852, 1736, 1643, 1626, 1164 cm^{-1}.

3.1.2 Synthesis of methyl 6-(11-acrylamidohexanamido)hexanoate (21)

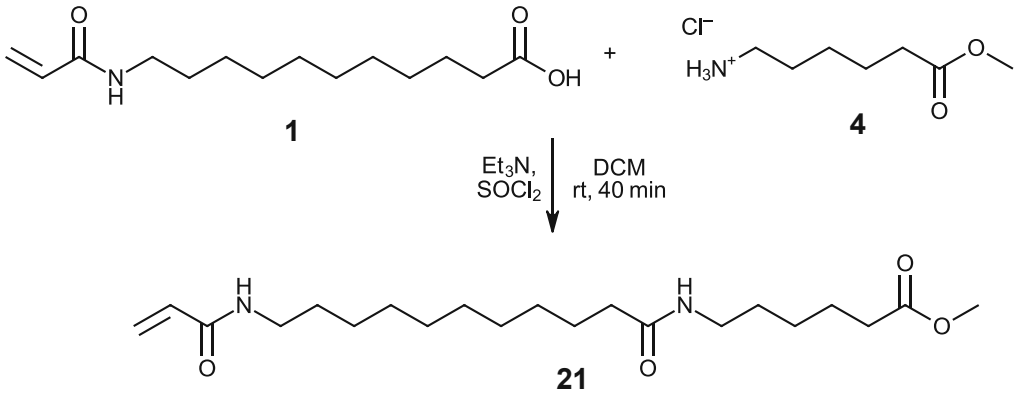

The synthesis of 21 was carried out in accordance with Leggio *et al*. [77]. Therefore, 0.25 g (0.9 mmol) of acrylamide **1** and 0.19 g (1.1 mmol) of hydrochloride **4** were mixed with 20 mL DCM. Then 0.31 g (3.1 mmol) Et_3N was added and the reaction mixture was stirred at room temperature. Afterwards, 0.17 g (1.5 mmol) $SOCl_2$ was dropped into the solution and the mixture was stirred 40 min at room temperature. Then the residue was filtered and the solvent was evaporated under reduced pressure. The residues were dissolved in 10 mL DCM and the solution was extracted with 1 N HCl and 1 N NaOH. The organic phase was dried over Na_2SO_4 and the solvent was removed under reduced pressure. Monomer **21** was obtained as a white powder.

Yield: 0.16 g (46 % of theory)

^{1}H NMR (300 MHz, DMSO-d_6, 25 °C, *δ*): 8.03 (t, 1H, J=5.2 Hz, CH_2=CH-CO-N**H**-), 7.71 (t, 1H, J=4.9 Hz, -CH_2-CO-N**H**-), 6.19 (dd, 1H, J_1=16.9 Hz, J_2=9.5, CH_2=C**H**-CO-), 6.04 (dd, 1H, J_1=16.7 Hz, J_2=2.2 Hz, trans C**H$_2$**=CH-CO-), 5.55 (dd, 1H, J_1=9.9 Hz, J_2=2.4 Hz, cis C**H$_2$**=CH-CO-), 3.57 (s, 3H, -COOC**H$_3$**), 3.09 (m, 2H, acryloyl-CONH-C**H$_2$**-), 2.99 (m, 2H, -CH_2-CO-NH-C**H$_2$**-), 2.28 (t, 2H, J=7.7 Hz, -CH_2-CO-NH-$(CH_2)_4$-C**H$_2$**-$COOCH_3$), 2.02 (t, 2H J=6.5 Hz, acryloyl-CO-NH-$(CH_2)_9$-C**H$_2$**-CO-NH-), 1.60-1.13 (m, 24H, acryloyl-CO-NH-$(CH_2)_9$- and -CH_2-CO-NH-CH_2 $(CH_2)_3$-) ppm.

3.2 Polymerization

3.2.1 Polymerization of methyl 6-(6-acrylamidohexanamido) hexanoate (22)

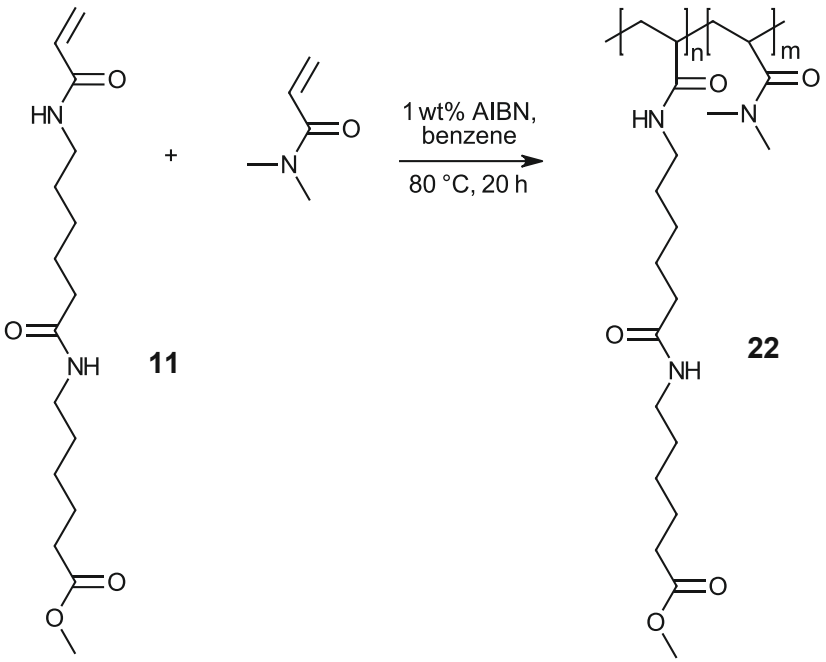

For the synthesis of polymer **22** 4.50 g (14.4 mmol) of monomer **11** and 1.34 g (13.5 mmol) of DMAA were weighed in a 250 mL round-bottom flask and 100 mL benzene was added. The reaction mixture was purged with argon and 1 wt% AIBN (related to **11**) was added. The mixture was stirred for 20 h under reflux. Afterwards, the solvent was evaporated under reduced pressure and the polymer was dried at 40 °C in vacuum overnight. Polymer **22** was obtained as a white, brittle solid and analyzed *via* ^{1}H-NMR and ATR IR. The crude product was used in the following step without purification. The polymer was purified in the saponification step by precipitation.

Decomposition (TGA): 244 °C

^{1}H NMR (300 MHz, DMSO-d_6, 25 °C, *δ*): 7.73 (s_b, 1H, -$(CH_2)_5$-CO-N**H**-), 3.57 (s, 3H, -COOC**H$_3$**), 3.13-2.70 (m, 10H, -N**$(CH_3)_2$**, R_2-CH-CO-NH-C**H$_2$**- and -$(CH_2)_5$-CO-NH-C**H$_2$**-), 2.27 (t, 2H, J=7.3 Hz, -C**H$_2$**-$COOCH_3$), 2.03 (t, 2H, J=6.3 Hz, R_2-CH-CO-NH-$(CH_2)_4$-C**H$_2$**-), 1.55-1.45 (m, 4H, R_2-CH-CH_2-CO-NH-CH_2-C**H$_2$**- and -$(CH_2)_5$-CO-NH-CH_2-C**H$_2$**-), 1.45-1.31 (m, 4H, R_2-CH-CO-NH- $(CH_2)_3$-C**H$_2$**- and -C**H$_2$**-CH_2-$COOCH_3$), 1.31-1.15 (m, 4H, R_2-CH-CO-NH-$(CH_2)_2$-C**H$_2$**-$(CH_2)_2$-COand -NH-$(CH_2)_2$-C**H$_2$**-$(CH_2)_2$-$COOCH_3$) ppm.

IR (ATR, *ν*): 3290, 2927, 2858, 1735, 1626, 1437, 1165 cm^{-1}.

3.2.2 Saponification of poly(DMAA-co-methyl 6-(6-acrylamidohexanamido) hexanoate)

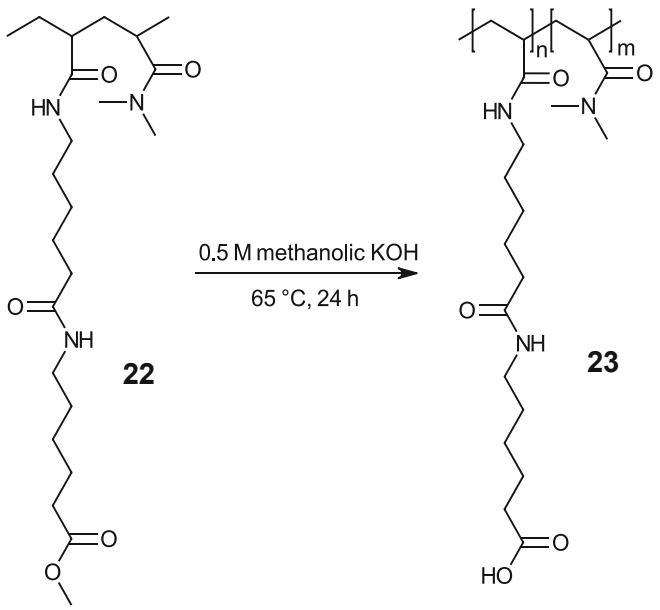

The saponification was carried out in accordance with Leibetseder [58]. Therefore, 6.81 g (15.7 mmol) of polymer **22** was added to 200 mL of a 0.5 M methanolic KOH and the solution was stirred under reflux overnight. Then the polymer was precipitated in 6 N HCl, filtered off with a Büchner funnel and washed with water. Finally, the polymer was dried at 40 °C in vacuum overnight.

Decomposition (TGA): 239°C

^{1}H NMR (300 MHz, DMSO-d_6, 25 °C, *δ*): 7.79 (s, 1H, -$(CH_2)_5$-CO-N**H**-), 3.13-2.70 (m, 10H, -N(C**H$_3$**)$_2$, R_2-CH-CO-NH-C**H$_2$**- and -$(CH_2)_5$-CO-NH-C**H$_2$**-), 2.18 (t, 2H, J=7.3 Hz, -C**H$_2$**-COO-), 2.03 (s, 2H, R_2-CH-CO-NH-$(CH_2)_4$-C**H$_2$**-), 1.56-1.43 (m, 4H, R_2-CH--CO-NH-CH_2-C**H$_2$**- and -$(CH_2)_5$-CO-NH-CH_2-C**H$_2$**-), 1.43-1.30 (m, 4H, R_2-CH-CO-NH-$(CH_2)_3$-C**H$_2$**- and -C**H$_2$**-CH_2-COO-), 1.30-1.15 (m, 4H, R_2-CH-CO-NH-$(CH_2)_2$-C**H$_2$**-$(CH_2)_2$-CO- and -NH-$(CH_2)_2$-C**H$_2$**-$(CH_2)_2$-COO-) ppm.

IR (ATR, *ν*): 3608-2362, 2935, 2814, 1631, 1402, 1041 cm^{-1} .

3.2.3 Synthesis of lithium- (24) and TBA- (25) salts of poly(6-(6-acrylamidohexanamido) hexanoic acid-co-DMAA)

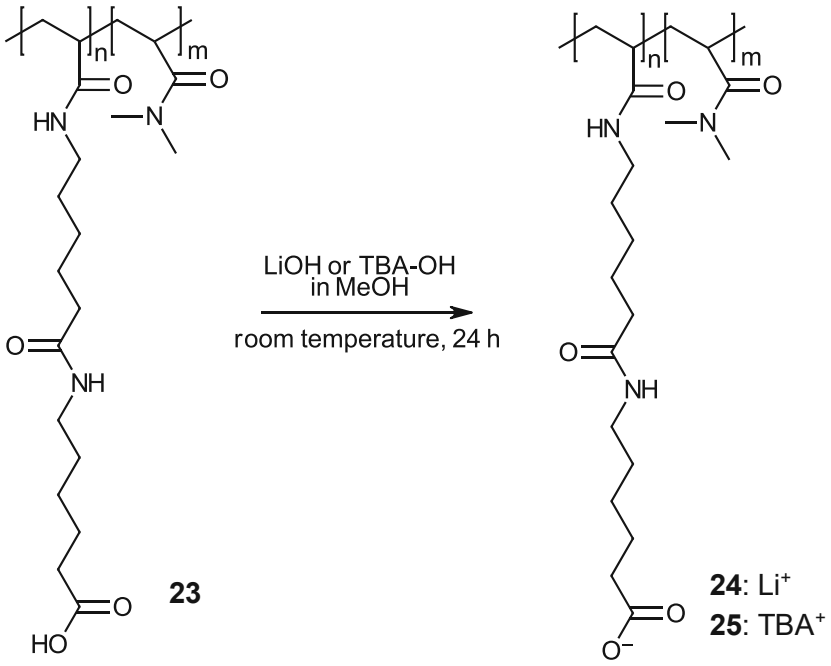

The lithium- and TBA- salts were synthesized in accordance with Leibetseder [58]. Therefore, 2.02 g (4.8 mmol) of polymer **23** and 0.21 g (5.0 mmol) of LiOH*H_2O were stirred in 65 mL MeOH at room temperature overnight. Afterwards, the solvent was removed under reduced pressure and the polymer was dried at 40 °C in vacuum overnight. Polymer **25** was synthesized *via* the same route but with tetrabutylammonium hydroxide instead of LiOH.

Analytical Data for **24**:

Decomposition (TGA): 264 °C

^{1}H NMR (300 MHz, DMSO-d_6, 25 °C, *δ*): 7.79 (s, 1H, -$(CH_2)_5$-CO-N**H**-), 3.13-2.70 (m, 10H, -N(C**H$_3$**)$_2$, R_2-CH-CO-NH-C**H$_2$**- and -$(CH_2)_5$-CO-NH-C**H$_2$**-), 2.18 (t, 2H, J=7.3 Hz, -C**H$_2$**-COO-), 2.03 (s, 2H, R_2-CH-CO-NH-$(CH_2)_4$-C**H$_2$**-), 1.56-1.43 (m, 4H, R_2-CH--CO-NH-CH_2-C**H$_2$**- and -$(CH_2)_5$-CO-NH-CH_2-C**H$_2$**-), 1.43-1.30 (m, 4H, R_2-CH-CO-NH-$(CH_2)_3$-C**H$_2$**- and -C**H$_2$**-CH_2-COO-), 1.30-1.15 (m, 4H, R_2-CH-CO-NH-$(CH_2)_2$-C**H$_2$**-$(CH_2)_2$-CO- and -NH-$(CH_2)_2$-C**H$_2$**-$(CH_2)_2$-COO-) ppm.

IR (ATR, *ν*): 3608-2362, 2935, 2814, 1631, 1402, 1041 cm^{-1} .

Analytical Data for **25**:

T_g: -15 °C

Decomposition (TGA): 246 °C

SUMMARY AND CONCLUSION

Electric cars represent the future in the automotive industry. Therefore, a lot of research is being done in the field of battery development, since batteries are the biggest problem in this area. So-called solid-state batteries are very promising. Therefore, polyelectrolytes are used. Polyelectrolytes are also used in many other areas such as actuators and sensors, in lab-on-a-chip systems or as so-called self-healing hydrogels.
The aim of this work was the synthesis of 6-aminohexanoic acid based monomers as precursor for polyelectrolytes. Two units were to be linked by different functional groups in order to obtain different properties of the molecules. In addition, the monomers should contain an acrylic group to enable free-radical polymerization of the monomers. In this master´s thesis, the monomers methyl 6-(4-(6-acrylamidohexanamido)benzamido)hexanoate **2** (Figure 94) and methyl 6-(6-acrylamidohexanamido)hexanoate **11** (Figure 95) were synthesized and subsequently polymerized and tested.

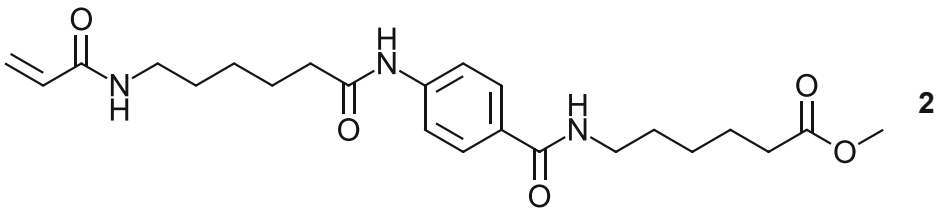

2

Figure 94: Structure of methyl 6-(4-(6-acrylamidohexanamido)benzamido)hexanoate (**2**).

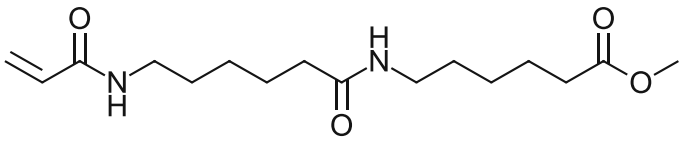

11

Figure 95: Structure of methyl 6-(6-acrylamidohexanamido)hexanoate (**11**).

The synthesis of acrylamide **2** (Figure 94) soon proved unsuccessful in the course of this work, so the focus was on the synthesis of acrylamide **11** (Figure 95). The monomer synthesis of monomer **11** was initially carried out *via* the corresponding acid chloride, resulting in a yield of 24 %. Since the monomer synthesis *via* the acid chloride could not be further optimized in terms of yield, the amide bond was prepared using a coupling agent. For this purpose, DCC with DMAP as catalyst was used and a yield of 70 % could be achieved.
After monomer synthesis, (co-)polymerization followed. In the polymerization of acrylamide **11** , the best results were obtained with benzene as the solvent and 1 wt% AIBN as the initiator. Polymerization in DMF and methanol did not work. For polymerization in water, APS/TEMED was used as initiator. Polymerization in water resulted in an increased incorporation of the co-monomer

DMAA, due to the insolubility of methyl 6-(6-acrylamidohexanamido) hexanoate . As a result, three times more DMAA was incorporated than during polymerization in benzene.

By using different monomer concentrations of acrylamide **11** during polymerization in benzene, different properties were achieved. At higher monomer concentrations, the swelling behavior of the resulting polymers was observed. As a result, the polymers became very poorly soluble and swell in various solvents such as DMF.

After the saponification of poly(DMAA-co-methyl 6-(6-acrylamidohexanamido)hexanoate) (**22**) , different counterions were used to study their influence. On the one hand, lithium was used, resulting in a rather hard, brittle polymer - on the other hand, tetrabutylammonium (TBA) was used, making the polymer very flexible.

Compounded with tetraethylene glycol, poly(DMAA-co-TBA 6-(6-acrylamidohexanamido) hexanoate) (**25**) was to be extruded into a strand. Although too little material was used for extrusion, the polymer could still be obtained well homogenized. The idea behind this was to produce a deformable strand based on polyelectrolytes and to increase the order of the molecules. Finally, the behavior of TBA salt **25** in an electric field was to be tested. However, only preliminary tests were carried out and no positive results could yet be obtained.

For comparison with poly(DMAA-co-lithium 6-(6-acrylamidohexanamido)hexanoate (**24**) (Figure 96) , poly(DMAA-co-lithium 6-acrylamidohexanoate) (**16**) (Figure 97) was also prepared.

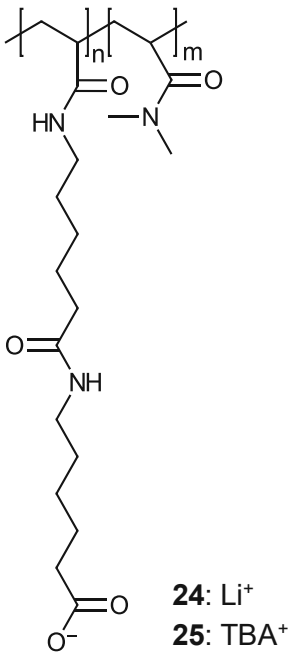

Figure 96: Structure of poly(DMAA-co-lithium 6-(6-acrylamidohexanamido)hexanoate) (**24**) and poly(DMAA-co-TBA 6-(6-acrylamidohexanamido)hexanoate) (**25**).

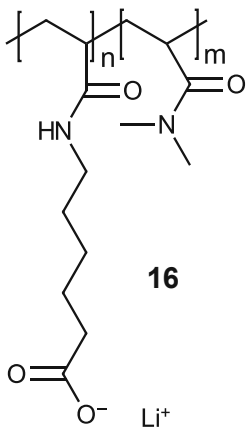

Figure 97: Structure of poly(DMAA-co-lithium 6-acrylamidohexanoate) (**16**).

Due to the missing amide bond and the shorter aliphatic chain, no swelling behavior was observed here. These polymers are hard, brittle polymers that are poorly soluble in DCM, benzene and DMSO. The influence of DMAA as a comonomer was also investigated here. Comparing poly(6-acrylamidohexanoic acid) (**13**) with copolymer poly(6-acrylamidohexanoic acid-co-DMAA) (**14**), the copolymer is no longer as brittle as the homopolymer due to the incorporation of DMAA. In addition, HEMA was also used as a comonomer.

Various polyelectrolytes were synthesized and exciting properties such as swelling behavior were observed. This results in the desired properties of the final polyelectrolyte and enables the use in e.g. battery development or as self-healing hydrogels. However, polymerization in water can still be improved by overcoming the poor solubility of methyl 6-(6-acrylamidohexanamido)hexanoate (**11**), because waterwould probably be the better choice due to the more environmentally friendly solvent. In addition, the behavior of such materials in an electric field should be investigated in more detail.

CHEMICALS

All chemicals used in this Master thesis were purchased from standard chemical suppliers in reagent quality or better and used as received, unless specified otherwise.

AIBN was purchased from Sigma-Aldrich and recrystallized in EtOH before use. The crystals were dried under vacuum and then stored at 4 °C.

INSTRUMENTS

Dry solvents were received from the MB-SPS-7 solvent purifier by MBRAUN. The solvents were filled into dry flasks under N_2 atmosphere. They were always used immediately.

The solvents were evaporated using a Büchi Rotavapor RII with a water jet pump.

Melting points were determined with OptiMelt from SRS Stanford Research Systems at a heating rate of 1 °C min^{-1}.

Dialysis was carried out by dissolving 2 g of the crude polymer in 25 mL acetone and filling it into Spectra Por 3 dialysis membranes with a MWCO of 3.5 kDA. The membrane was closed and placed in a tall large beaker also filled with acetone (500 mL). The acetone from the beaker was changed after 1h, 2h, 3h and after 24h. Finally, the membrane could be opened and the acetone contained therein was removed under reduced pressure. Thus, the purified polymer could finally be obtained.

A vacuum drying cabinet by Heraeus with an AEG AMEB high vacuum oil pump was used to completely dry the samples and prepare them for further analytical methods.

Extrusion was performed with Haake Minilab Rheomex CTW5 by Thermo Scientific with a twin-screw compounder. 2.5 g of the polymer was mixed with 20% TEG and then added to the extruder through a funnel. The compounding time was 40 min at 60 °C.

All NMR spectra were recorded on a Bruker Avance spectrometer at 300 MHz for ^{1}H and 75 MHz for ^{13}C using standard pulse programs as provided by the manufacturer. Deuterated chloroform $CDCl_3$, deuterated D_2O or deuterated d_6-DMSO were used as NMR- solvents. Signals were referenced to the solvent signal at 7.26 ppm (^{1}H, $CDCl_3$), 4.79 ppm (^{1}H, D_2O), 2.50 ppm (^{1}H, DMSO) and 40.0 ppm (^{13}C, DMSO). For the ^{1}H spectra, about 10-15 mg of dried sample was

weighed and dissolved in the desired solvent; for the ^{13}C spectra, about 15-30 mg was used. All spectra were analyzed using the software TopSpin 3.6.3 by Bruker.

Fourier-transform infrared spectroscopy was performed on a Thermo Fisher Nicolet 5700 spectrometer with a Specac Golden Gate Attenuated Total Refectance (ATR) sampling unit. The samples were dried before measurement. Data were analyzed by the operational software supplied by the manufacturer and using the software OriginPro 2022 by OriginLab.

TGA was performed with TGA 4000 by Perkin Elmer for thermal analysis. About 5-10 mg of dry sample was weighed in and the sample temperature was held at 30 °C for 4 min. Then, the temperature program started at 30 °C and the sample was heated at 20 °C/min up to 800 °C under nitrogen flow. Data were analyzed by the operational software supplied by the manufacturer and using the software OriginPro 2022 by OriginLab.

DSC was performed with DSC 8000 by Perkin Elmer for thermal analysis. About 30 mg sample was weighed in a pan and heat-cool-heat cycles between −50 °C and 100 °C under nitrogen (20 mL min^{-1}) were performed with a heating rate of 10 °C min^{-1}. Data were analyzed by the operational software supplied by the manufacturer and using the software OriginPro 2022 by OriginLab.

Purity and MS analysis from the monomer samples were obtained from HPLC-MS analyses using a Finnigan Surveyor HPLC by Thermo Fisher with a Zorbax SB-C18 column (2.1*150 mm). The sample was dissolved in a mixture of acetonitrile and water (4:1, 1 mg mL^{-1}). Mass spectra were recorded on a LTQ Orbitrap Velos by Thermo Fisher with atmospheric pressure chemical ionization (APCI).

With a Laboratory Power supply PS-302A an electrical voltage between 5 V and 20 V was applied to the aluminum contacts, between which the swollen polymer sample was located. By visual inspection it was checked if there is any movement or bending of the polymeric material.

LIST OF COMPOUNDS

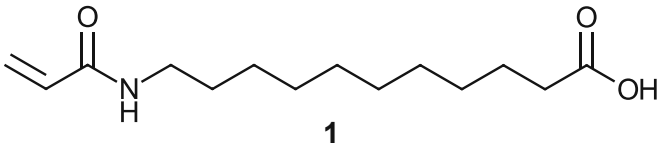

1

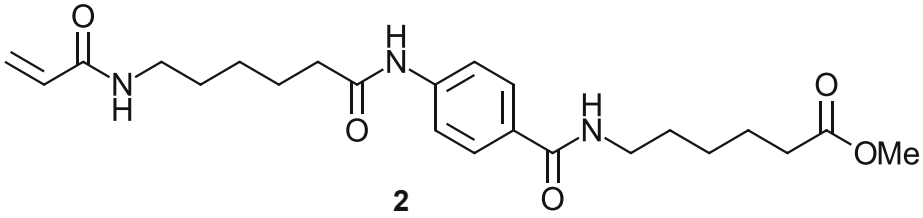

2

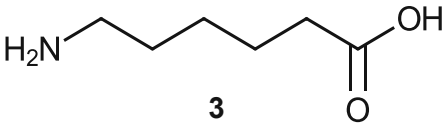

3

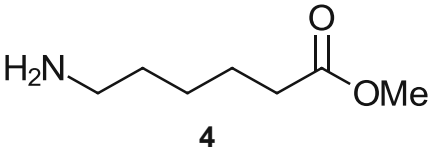

4

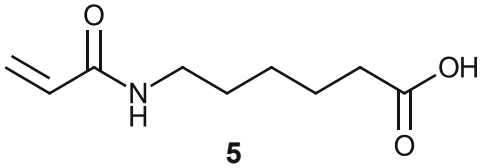

5

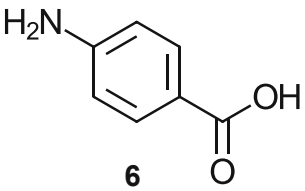

6

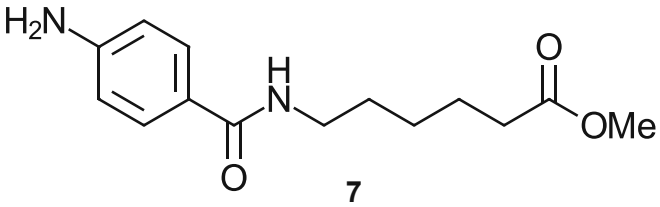

7

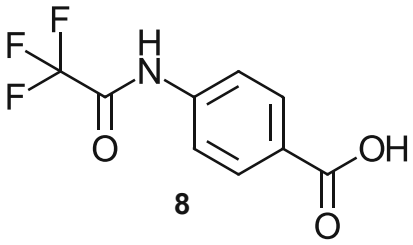

8

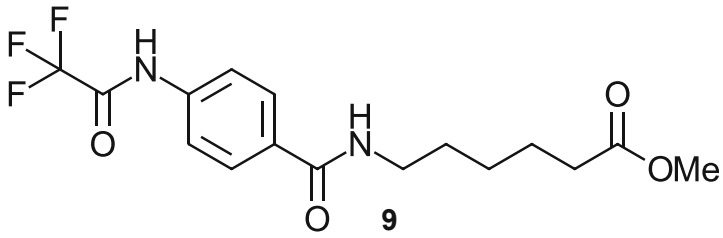

9

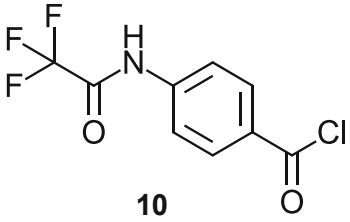

10

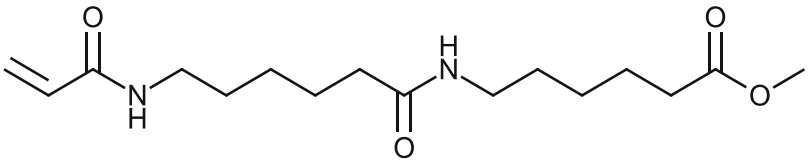

11

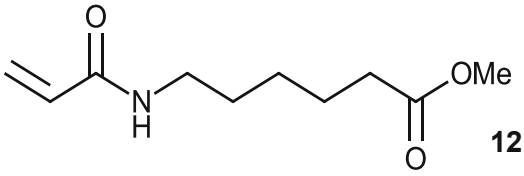

12

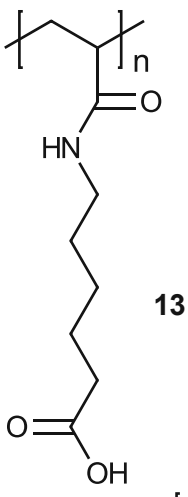

13

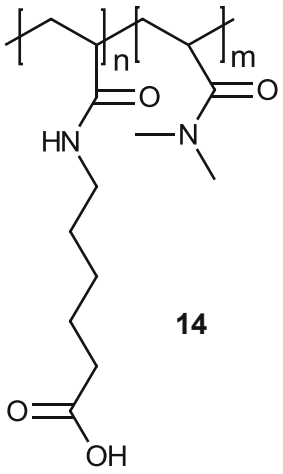

14

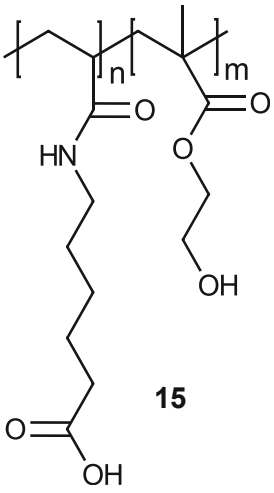

15

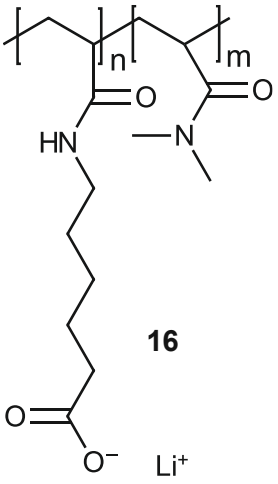

16

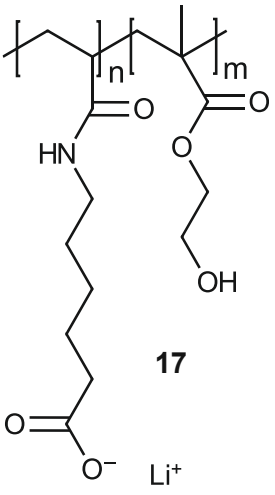

17

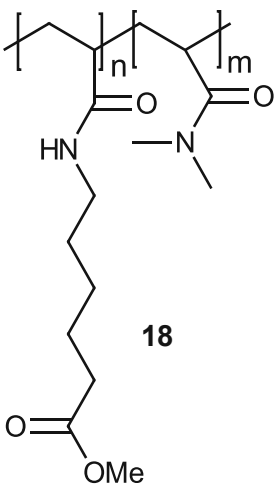

18

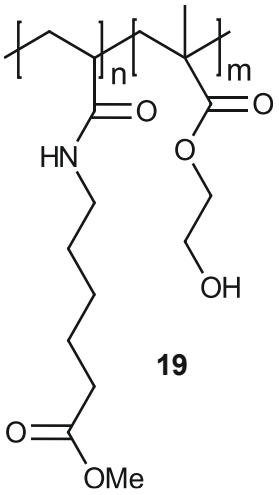

19

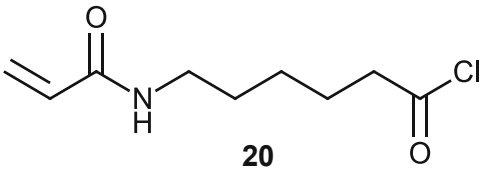

20

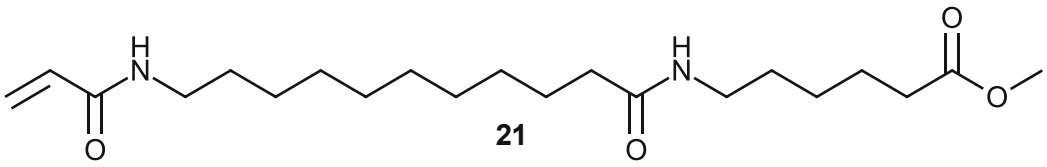

21

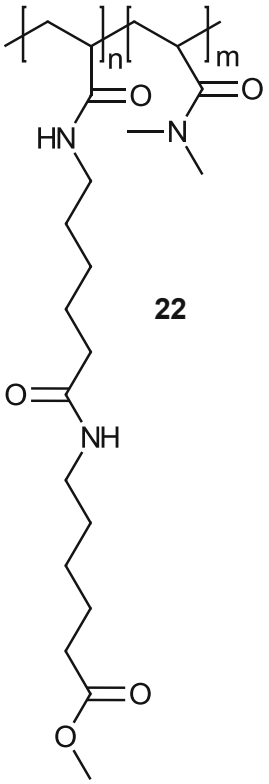

22

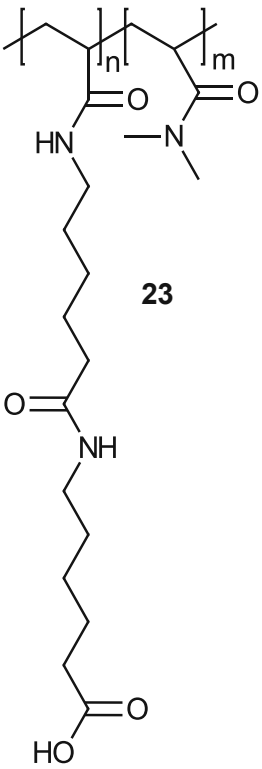

23

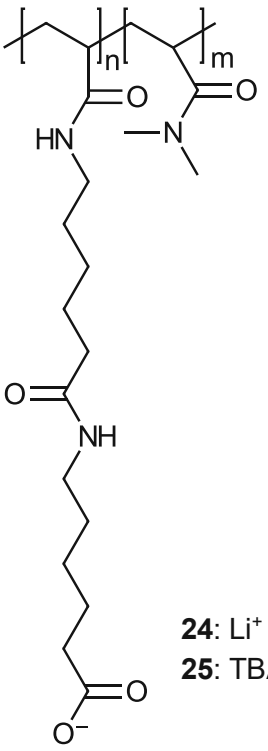

24: Li^+
25: TBA^+

NOTATION

6-AHS	6- aminohexanoic acid
AIBN	azo-bis-(isobutylonitril)
APCI	atmospheric pressure chemical ionization
APS	ammonium persulfate
APT	attached proton test
BOP	benzotriazole-1-yloxytris(dimethylamino)phosphonium hexafluorophosphate
calc.	calculated
conc.	concentrated
COSY	correlated spectroscopy
DCC	*N*,*N*'-dicyclohexylcarbodiimid
DCM	dichloromethane
DCU	*N*,*N*''-dicyclohexylurea
DMAA	*N*,*N*-dimethylacrylamide
DMAP	4-(dimethylamino)pyridine
DMF	dimethylformamide
DMSO	dimethyl sulfoxide
DNA	deoxyribonucleic acid
DSC	differential scanning calorimetry
EAP	electroactive polymer
EDC	1-ethyl-3-(3-dimethylaminopropyl) carbodiimide
Exp.	experimental part
FMOC	9-fluorenylmethoxycarbonyl
FTMS	fourier transform mass spectrometry
HCl	hydrochloric acid
HEMA	hydroxyethylmethacrylat
HMBC	heteronuclear multiple bond correlation

HPLC	high performance liquid chromatography
HSQC	heteronuclear single quantum correlation
IR	infrared spectroscopy
Li	lithium
lit	literature
MEHQ	4-methoxyphenol
MS	mass spectrometry
NMR	nuclear magnetic resonance
PAA	poly(acrylic acid)
PBS	phosphate buffer saline
PEGA	poly(ethylene glycol) diacrylate
Res.	results and discussion
rt	room temperature
SEI	solid electrolyte interphase
TBA	tetrabutylammonium
TEA	triethylamine
TEG	tetraethylene glycol
TEMED	tetramethylethylenediamine
TFA	trifluoroacetic acid
TFAA	trifluoroacetic anhydride
T_g	glass-transition temperature
TGA	thermogravimetric analysis
THF	tetrahydrofuran

REFERENCES

[1] S. Wilke, Erneuerbare Energien – Vermiedene Treibhausgase, Umweltbundesamt. (2016). https://www.umweltbundesamt.de/daten/energie/erneuerbare-energien-vermiedene-treibhausgase (accessed July 24, 2023).

[2] S. Wilke, Emissionen des Verkehrs, Umweltbundesamt. (2023). https://www.umweltbundesamt.de/daten/verkehr/emissionen-des-verkehrs (accessed June 14, 2023).

[3] EU-Parlament stimmt für Verbot neuer Autos mit Verbrennermotoren ab 2035, Bmvit INFOTHEK. (n.d.). https://infothek.bmk.gv.at/eu-parlament-stimmt-fuer-verbot-neuer-autos-mit-verbrennermotoren-ab-2035/ (accessed June 14, 2023).

[4] Überall sind Elektromotoren im Einsatz, (n.d.). https://karriere.vogel-hemer.de/schueler/ausbildung/elektromotor_was_ist_das.html (accessed July 21, 2023).

[5] Elektroantrieb: So funktioniert ein Elektroauto, (2023). https://www.adac.de/verkehr/tanken-kraftstoff-antrieb/alternative-antriebe/elektroantrieb/ (accessed July 21, 2023).

[6] Geschichte der E-Mobilität » von 1821 bis heute | Porsche Bank, Porsche Bank Austria. (n.d.). https://www.porschebank.at/news/die-geschichte-der-e-mobilitaet/ (accessed July 21, 2023).

[7] X.-B. Cheng, R. Zhang, C.-Z. Zhao, Q. Zhang, Toward Safe Lithium Metal Anode in Rechargeable Batteries: A Review, Chem. Rev. 117 (2017) 10403–10473. https://doi.org/10.1021/acs.chemrev.7b00115.

[8] D. Welle (www.dw.com), Elektroauto: Neue Batterietechnologie verzweifelt gesucht | DW | 16.02.2023, DW.COM. (n.d.). https://www.dw.com/de/elektroauto-neue-batterietechnologie-verzweifelt-gesucht/a-64708090 (accessed March 27, 2023).

[9] Bobby, What are Li-On Batteries?, News Energy Storage Batter. Clim. Change Environ. (2014). https://www.upsbatterycenter.com/blog/li-batteries/ (accessed March 27, 2023).

[10] M. Ghiji, V. Novozhilov, K. Moinuddin, P. Joseph, I. Burch, B. Suendermann, G. Gamble, A Review of Lithium-Ion Battery Fire Suppression, Energies. 13 (2020) 5117. https://doi.org/10.3390/en13195117.

[11] Bobby, What is a Lithium-ion polymer battery?, News Energy Storage Batter. Clim. Change Environ. (2014). https://www.upsbatterycenter.com/blog/lithium-ion-polymer-battery/ (accessed March 27, 2023).

[12] Bobby, The Global Battery Market – an Industry Report Review, News Energy Storage Batter. Clim. Change Environ. (2014). https://www.upsbatterycenter.com/blog/global-battery-market-industry-report-review/ (accessed March 27, 2023).

[13] R. Zhu, J. Feng, Z. Guo, In Situ Observation of Dendrite Behavior of Electrode in Half and Full Cells, J. Electrochem. Soc. 166 (2019) A1107–A1113. https://doi.org/10.1149/2.0921906jes.

[14] Richard, Solid State Lithium Batteries Without Dendrites, News Energy Storage Batter. Clim. Change Environ. (2022). https://www.upsbatterycenter.com/blog/solid-state-lithium-batteries-without-dendrites/ (accessed April 8, 2023).

[15] L. Bernstein, Polymere Elektrolyte für Lithium-Batterien, (n.d.).

[16] Z. Li, J. Huang, B. Yann Liaw, V. Metzler, J. Zhang, A review of lithium deposition in lithium-ion and lithium metal secondary batteries, J. Power Sources. 254 (2014) 168–182. https://doi.org/10.1016/j.jpowsour.2013.12.099.

[17] M.R. Aguilar, J. San Román, eds., Smart polymers and their applications, Woodhead Publishing, is an imprint of Elsevier, Cambridge, UK, 2014.

[18] L. Sutton, H. Moein, A. Rafiee, J.D.W. Madden, C. Menon, Design of an assistive wrist orthosis using conductive nylon actuators, in: 2016 6th IEEE Int. Conf. Biomed. Robot. Biomechatronics BioRob, IEEE, Singapore, Singapore, 2016: pp. 1074–1079. https://doi.org/10.1109/BIOROB.2016.7523774.

[19] C.A. custódio, R.L. Reis, J.F. Mano, A. Del Campo, Smart instructive polymer substrates for tissue engineering, in: Smart Polym. Their Appl., Elsevier, 2014: pp. 301–326. https://doi.org/10.1533/9780857097026.2.301.

[20] A. George, P.A. Shah, P.S. Shrivastav, Natural biodegradable polymers based nano-formulations for drug delivery: A review, Int. J. Pharm. 561 (2019) 244–264. https://doi.org/10.1016/j.ijpharm.2019.03.011.

[21] A.M. Grancarić, I. Jerković, V. Koncar, C. Cochrane, F.M. Kelly, D. Soulat, X. Legrand, Conductive polymers for smart textile applications, J. Ind. Text. 48 (2018) 612–642. https://doi.org/10.1177/1528083717699368.
[22] Q. Shi, H. Liu, D. Tang, Y. Li, X. Li, F. Xu, Bioactuators based on stimulus-responsive hydrogels and their emerging biomedical applications, NPG Asia Mater. 11 (2019) 1–21. https://doi.org/10.1038/s41427-019-0165-3.
[23] E. Hering, R. Martin, J. Gutekunst, J. Kempkes, K. Bressler, A. Vogt, Sensoren und Aktoren, in: Elektrotechnik Elektron. Für Maschinenbauer, Springer Berlin Heidelberg, Berlin, Heidelberg, 2012: pp. 433–469. https://doi.org/10.1007/978-3-642-12881-3_7.
[24] K.J. Kim, S. Tadokoro, eds., Electroactive polymers for robotic applications: artificial muscles and sensors, Springer, London, 2007.
[25] P. Martins, D.M. Correia, V. Correia, S. Lanceros-Mendez, Polymer-based actuators: back to the future, Phys. Chem. Chem. Phys. 22 (2020) 15163–15182. https://doi.org/10.1039/D0CP02436H.
[26] M. Shahinpoor, Y. Bar-Cohen, J.O. Simpson, J. Smith, Ionic polymer-metal composites (IPMCs) as biomimetic sensors, actuators and artificial muscles - a review, Smart Mater. Struct. 7 (1998) R15–R30. https://doi.org/10.1088/0964-1726/7/6/001.
[27] Y. Bar-Cohen, Electroactive polymers as artificial muscles, in: C.H.M. Jenkins (Ed.), WIT Trans. State Art Sci. Eng., 1st ed., WIT Press, 2005: pp. 69–81. https://doi.org/10.2495/978-1-85312-941-4/04.
[28] D.P. Browe, C. Wood, M.T. Sze, K.A. White, T. Scott, R.M. Olabisi, J.W. Freeman, Characterization and optimization of actuating poly(ethylene glycol) diacrylate/acrylic acid hydrogels as artificial muscles, Polymer. 117 (2017) 331–341. https://doi.org/10.1016/j.polymer.2017.04.044.
[29] A.K. Price, K.M. Anderson, C.T. Culbertson, Demonstration of an integrated electroactive polymer actuator on a microfluidic electrophoresis device, Lab. Chip. 9 (2009) 2076. https://doi.org/10.1039/b823465e.
[30] T. Wang, M. Farajollahi, Y.S. Choi, I.-T. Lin, J.E. Marshall, N.M. Thompson, S. Kar-Narayan, J.D.W. Madden, S.K. Smoukov, Electroactive polymers for sensing, Interface Focus. 6 (2016) 20160026. https://doi.org/10.1098/rsfs.2016.0026.
[31] E. Biddiss, T. Chau, Electroactive polymeric sensors in hand prostheses: Bending response of an ionic polymer metal composite, Med. Eng. Phys. 28 (2006) 568–578. https://doi.org/10.1016/j.medengphy.2005.09.009.
[32] A. Keshavarzi, M. Shahinpoor, K.J. Kim, J.W. Lantz, Blood pressure, pulse rate, and rhythm measurement using ionic polymer-metal composite sensors, in: Y. Bar-Cohen (Ed.), Newport Beach, CA, 1999: pp. 369–376. https://doi.org/10.1117/12.349695.
[33] Hydrogele - Fraunhofer IGB, Fraunhofer-Inst. Für Grenzflächen- Bioverfahrenstechnik IGB. (n.d.). https://www.igb.fraunhofer.de/de/forschung/funktionale-oberflaechen-und-materialien/materialien/hydrogele.html (accessed July 21, 2023).
[34] S.Y. Chin, Y.C. Poh, A.-C. Kohler, J.T. Compton, L.L. Hsu, K.M. Lau, S. Kim, B.W. Lee, F.Y. Lee, S.K. Sia, Additive manufacturing of hydrogel-based materials for next-generation implantable medical devices, Sci. Robot. 2 (2017) eaah6451. https://doi.org/10.1126/scirobotics.aah6451.
[35] L. Li, Y. Shi, L. Pan, Y. Shi, G. Yu, Rational design and applications of conducting polymer hydrogels as electrochemical biosensors, J. Mater. Chem. B. 3 (2015) 2920–2930. https://doi.org/10.1039/C5TB00090D.
[36] A. Phadke, C. Zhang, B. Arman, C.-C. Hsu, R.A. Mashelkar, A.K. Lele, M.J. Tauber, G. Arya, S. Varghese, Rapid self-healing hydrogels, Proc. Natl. Acad. Sci. 109 (2012) 4383–4388. https://doi.org/10.1073/pnas.1201122109.
[37] M.A. Kuzina, D.D. Kartsev, A.V. Stratonovich, P.A. Levkin, Organogels versus Hydrogels: Advantages, Challenges, and Applications, Adv. Funct. Mater. 33 (2023) 2301421. https://doi.org/10.1002/adfm.202301421.
[38] M. Bercea, Bioinspired Hydrogels as Platforms for Life-Science Applications: Challenges and Opportunities, Polymers. 14 (2022) 2365. https://doi.org/10.3390/polym14122365.
[39] M. Hess, R.G. Jones, J. Kahovec, T. Kitayama, P. Kratochvíl, P. Kubisa, W. Mormann, R.F.T. Stepto, D. Tabak, J. Vohlídal, E.S. Wilks, Terminology of polymers containing ionizable or ionic groups and of polymers containing ions (IUPAC Recommendations 2006), Pure Appl. Chem. 78 (2006) 2067–2074. https://doi.org/10.1351/pac200678112067.

[40] J. Koetz, S. Kosmella, Polyelectrolytes and nanoparticles, Springer, Berlin ; New York, 2007.
[41] M. Elżbieciak, S. Zapotoczny, P. Nowak, R. Krastev, M. Nowakowska, P. Warszyński, Influence of pH on the Structure of Multilayer Films Composed of Strong and Weak Polyelectrolytes, Langmuir. 25 (2009) 3255–3259. https://doi.org/10.1021/la803988k.
[42] B. Bolto, J. Gregory, Organic polyelectrolytes in water treatment, Water Res. 41 (2007) 2301–2324. https://doi.org/10.1016/j.watres.2007.03.012.
[43] N. Joseph, P. Ahmadiannamini, R. Hoogenboom, Ivo.F.J. Vankelecom, Layer-by-layer preparation of polyelectrolyte multilayer membranes for separation, Polym Chem. 5 (2014) 1817–1831. https://doi.org/10.1039/C3PY01262J.
[44] N.Y. Abu-Thabit, A.S. Hamdy, Stimuli-responsive Polyelectrolyte Multilayers for fabrication of self-healing coatings – A review, Surf. Coat. Technol. 303 (2016) 406–424. https://doi.org/10.1016/j.surfcoat.2015.11.020.
[45] S.T. Milner, Polymer Brushes, Science. 251 (1991) 905–914. https://doi.org/10.1126/science.251.4996.905.
[46] G. Moad, D.H. Solomon, G. Moad, The chemistry of radical polymerization, 2nd fully rev. ed, Elsevier, Amsterdam ; Boston, 2006.
[47] H.-G. Elias, Makromoleküle. 1: Chemische Struktur und Synthesen, 6., vollst. überarb. Aufl, Wiley-VCH, Weinheim, 1999.
[48] D.M. Ilgach, T.K. Meleshko, A.V. Yakimansky, Methods of controlled radical polymerization for the synthesis of polymer brushes, Polym. Sci. Ser. C. 57 (2015) 3–19. https://doi.org/10.1134/S181123821501004X.
[49] P.Y. Bruice, Synthetic Polymers, in: Org. Chem., Eighth edition, Pearson, Upper Saddle River, NJ, 2016.
[50] S. Koltzenburg, M. Maskos, O. Nuyken, Polymere: Synthese, Eigenschaften und Anwendungen, Springer Berlin Heidelberg, Berlin, Heidelberg, 2014. https://doi.org/10.1007/978-3-642-34773-3.
[51] E. Saldívar-Guerra, E. Vivaldo-Lima, Handbook of polymer synthesis, characterization, and processing, John Wiley & Sons, Inc, Hoboken, New Jersey, 2013.
[52] H. Ritter, Makromoleküle I: von einfachen Chemierohstoffen zu Hochleistungspolymeren, Springer Spektrum, Berlin [Heidelberg], 2018.
[53] Half-Life of Initiators, (n.d.). https://polymerdatabase.com/polymer%20chemistry/t-half2.html (accessed February 10, 2023).
[54] N.S. Simpkins, H. Zhang, H. Huang, Azobisisobutyronitrile (AIBN), in: Encycl. Reag. Org. Synth., 1st ed., Wiley, 2021: pp. 1–8. https://doi.org/10.1002/047084289X.ra121.pub2.
[55] K. Si, X.Q. Guo, K.Y. Qiu, Initiation Mechanism of Radical Polymerization Using Ammonium Persulfate and Polymerizable Amine Redox Initiators, J. Macromol. Sci. Part A. 32 (1995) 1149–1159. https://doi.org/10.1080/10601329508020336.
[56] B. Tieke, Makromolekulare Chemie: eine Einführung, 3. Aufl, Wiley-VCH, Weinheim, 2014.
[57] Basic Polymer Structure | MATSE 81: Materials In Today's World, (n.d.). https://www.e-education.psu.edu/matse81/node/2210 (accessed July 24, 2023).
[58] F. Leibetseder, Synthesis and characterization of acrylamide based polyacids, (2021).
[59] M. Zhang, H. Wang, B. Peng, D. Ma, M. Bai, X. Tang, S. Li, W. Zhao, S. Liu, Z. Wang, K. Zhou, C. Sun, Y. Ma, Macromolecular-level polymer brush layer enabling geometric customization of lithium deposits, Cell Rep. Phys. Sci. 2 (2021) 100324. https://doi.org/10.1016/j.xcrp.2021.100324.
[60] J. Zeng, Q. Liu, D. Jia, R. Liu, S. Liu, B. Zheng, Y. Zhu, R. Fu, D. Wu, A polymer brush-based robust and flexible single-ion conducting artificial SEI film for fast charging lithium metal batteries, Energy Storage Mater. 41 (2021) 697–702. https://doi.org/10.1016/j.ensm.2021.07.002.
[61] Z. Li, M. Tang, S. Liang, M. Zhang, G.M. Biesold, Y. He, S.-M. Hao, W. Choi, Y. Liu, J. Peng, Z. Lin, Bottlebrush polymers: From controlled synthesis, self-assembly, properties to applications, Prog. Polym. Sci. 116 (2021) 101387. https://doi.org/10.1016/j.progpolymsci.2021.101387.
[62] K. Kruusamäe, A. Punning, A. Aabloo, K. Asaka, Self-Sensing Ionic Polymer Actuators: A Review, Actuators. 4 (2015) 17–38. https://doi.org/10.3390/act4010017.
[63] S. Zhang, A.M. Bellinger, D.L. Glettig, R. Barman, Y.-A.L. Lee, J. Zhu, C. Cleveland, V.A. Montgomery, L. Gu, L.D. Nash, D.J. Maitland, R. Langer, G. Traverso, A pH-responsive

supramolecular polymer gel as an enteric elastomer for use in gastric devices, Nat. Mater. 14 (2015) 1065–1071. https://doi.org/10.1038/nmat4355.
[64] B.L. Deopura, Polyamide fibers, in: Polyest. Polyam., Elsevier, 2008: pp. 41–61. https://doi.org/10.1533/9781845694609.1.41.
[65] P.G.M. Wuts, T.W. Greene, T.W. Greene, Greene's protective groups in organic synthesis, 4th ed, Wiley-Interscience, Hoboken, N.J, 2007.
[66] P.J. Kocienski, Protecting groups, G. Thieme, Stuttgart ; New York, 1994.
[67] D.D. Wirth, S. Vikas, P. Jagadish, Thionyl Chloride, in: Encycl. Reag. Org. Synth., John Wiley & Sons, Ltd, Chichester, UK, 2017: pp. 1–6. https://doi.org/10.1002/047084289X.rt099.pub2.
[68] R. Salmon, I.V. Efremov, Oxalyl Chloride, in: John Wiley & Sons, Ltd (Ed.), Encycl. Reag. Org. Synth., John Wiley & Sons, Ltd, Chichester, UK, 2008: p. ro015.pub2. https://doi.org/10.1002/047084289X.ro015.pub2.
[69] M.K. Gurjar, A.M.S. Murugaiah, D.S. Reddy, M.S. Chorghade, A New Route to Prepare 6-Chloro-5-(2-chloroethyl)oxindole, Org. Process Res. Dev. 7 (2003) 309–312. https://doi.org/10.1021/op020095k.
[70] 6-Amino-hexansäure-methylester -hydrochlorid ≥99.0% (AT) | Sigma-Aldrich, (n.d.). http://www.sigmaaldrich.com/ (accessed March 23, 2023).
[71] P.Y. Bruice, Organic chemistry, Eighth edition, Pearson, Upper Saddle River, NJ, 2016.
[72] S. Steiner, J. Li, R.C. Schoenfeld, F.X. Talamas, Heterocyclic antiviral compounds, US20100158860, n.d.
[73] S. D'Souza, H. Murata, M.V. Jose, S. Askarova, Y. Yantsen, J.D. Andersen, C.D.J. Edington, W.P. Clafshenkel, R.R. Koepsel, A.J. Russell, Engineering of cell membranes with a bisphosphonate-containing polymer using ATRP synthesis for bone targeting, Biomaterials. 35 (2014) 9447–9458. https://doi.org/10.1016/j.biomaterials.2014.07.041.
[74] N,N Dimethylacrylamide | DMMA | CAS 2680-03-7 | Connect Chemicals, (n.d.). https://connectchemicals.com/en/product-finder/nn-dimethylacrylamide (accessed August 15, 2023).
[75] J. Zimmermann, Polyol- und Azlacton-Makromonomere für Netzwerksysteme, neue Werkstoffe und biomedizinische Anwendungen., Freiburg, 2001.
[76] M.F. Ansell, Preparation of acyl halides, in: S. Patai (Ed.), Acyl Halides 1972, John Wiley & Sons, Ltd., Chichester, UK, 1972: pp. 35–68. https://doi.org/10.1002/9780470771273.ch2.
[77] A. Leggio, E.L. Belsito, G. De Luca, M.L. Di Gioia, V. Leotta, E. Romio, C. Siciliano, A. Liguori, One-pot synthesis of amides from carboxylic acids activated using thionyl chloride, RSC Adv. 6 (2016) 34468–34475. https://doi.org/10.1039/C5RA24527C.
[78] E. Valeur, M. Bradley, Amide bond formation: beyond the myth of coupling reagents, Chem Soc Rev. 38 (2009) 606–631. https://doi.org/10.1039/B701677H.
[79] B. Neises, W. Steglich, Simple Method for the Esterification of Carboxylic Acids, Angew. Chem. Int. Ed. Engl. 17 (1978) 522–524. https://doi.org/10.1002/anie.197805221.
[80] J.S. Albert, A.D. Hamilton, A.C. Hart, X. Feng, L. Lin, Z. Wang, 1,3-Dicyclohexylcarbodiimide, in: Encycl. Reag. Org. Synth., John Wiley & Sons, Ltd, Chichester, UK, 2017: pp. 1–9. https://doi.org/10.1002/047084289X.rd146.pub3.
[81] P.H.M. Delanghe, M. Lautens, S. Marimganti, J.-M. Ahn, Acrylic Acid, in: John Wiley & Sons, Ltd (Ed.), Encycl. Reag. Org. Synth., John Wiley & Sons, Ltd, Chichester, UK, 2008: p. ra035.pub2. https://doi.org/10.1002/047084289X.ra035.pub2.
[82] R.S. Pottorf, P. Szeto, M. Srinivasarao, 1-Ethyl-3-(3′-dimethylaminopropyl)carbodiimide Hydrochloride, in: Encycl. Reag. Org. Synth., John Wiley & Sons, Ltd, Chichester, UK, 2017: pp. 1–5. https://doi.org/10.1002/047084289X.re062.pub2.
[83] N,N′-Dicyclohexylharnstoff 98% | Sigma-Aldrich, (n.d.). http://www.sigmaaldrich.com/ (accessed January 3, 2023).
[84] J.-H. Fang, Polyimide Proton Exchange Membranes, in: Adv. Polyim. Mater., Elsevier, 2018: pp. 323–383. https://doi.org/10.1016/B978-0-12-812640-0.00007-X.
[85] Y. Li, X. Luo, Q. Guo, Y. Nie, T. Wang, C. Zhang, Z. Huang, X. Wang, Y. Liu, Y. Chen, J. Zheng, S. Yang, Y. Fan, R. Xiang, Discovery of *N* 1-(4-((7-Cyclopentyl-6-(dimethylcarbamoyl)-7 *H* -pyrrolo[2,3- *d*]pyrimidin-2-yl)amino)phenyl)- *N* 8-hydroxyoctanediamide as a Novel Inhibitor Targeting Cyclin-dependent Kinase 4/9 (CDK4/9) and Histone Deacetlyase1 (HDAC1) against Malignant Cancer, J. Med. Chem. 61 (2018) 3166–3192. https://doi.org/10.1021/acs.jmedchem.8b00209.

[86] F. Weygand, *N* -Trifluoracetylamino-säuren. II. Mitteil., Chem. Ber. 87 (1954) 248–256. https://doi.org/10.1002/cber.19540870219.
[87] 6-Acrylamidohexanoic Acid 98.0 %, TCI America, Quantity: Each of 1 | Fisher Scientific, (n.d.). https://www.fishersci.com/shop/products/6-acrylamidohexanoic-acid-tci-america-3/A18961G (accessed June 20, 2023).